PhD Dissertation

NMR studies on the regulation of glucose and fatty acid oxidation in liver, heart and skeletal muscle in awake rats

by

Tiago Cardoso Alves

Department of Life Sciences, FCTUC
University of Coimbra

School of Medicine
Yale University

February, 2010

Supervision:

Prof. Rui de Carvalho and Prof. Carlos Palmeira

Department of Life Sciences, Faculty of Sciences and Technology, University of Coimbra, Portugal

Prof. Gerald I Shulman

Yale University School of Medicine, New Haven, USA

Table of Contents

Acknowledgments

Even though this might sound *cliché,* this thesis and all the work behind it would definitively not be possible without the help and support of certain people that I would like *immortalize* here. First and foremost I would like to thank Dr. Rui de Carvalho and Dr. Carlos Palmeira for accepting me as their PhD student. In particular, Dr. Rui certainly had an important role in my formation providing the bases of my knowledge by training me in the art of NMR and by giving me the possibility to continue my studies abroad. I would also like to thank Dr. Gerald Shulman for accepting me in his lab and to allow me to work in a project that was exactly what I had envisioned as a PhD work. I should also not forget Dr. Douglas Befroy who helped me to learn more and more about NMR and Dr. Richard Kibbey who introduced to mass spectrometry. Thank you for all the valuable advices and guidance. I'm also grateful to Roberto Codella, Andreas Birkenfield, Michael Jurczak, Rasmus Rabøl, Mario Kahn, Sara Beddow and Sachin Majumdar for the strong friendship created that helped me get through my three years at Yale. And the last but not the least I want to express my eternal gratitude to: my family - for the love, support and for understanding when I said: "I'm planning to go to USA" – and my good friends that I left in Lisbon - in particular Nuno lages, Filipe Freire, Irina Alho and Magda Atilano - for their constant presence and friendship even with an entire ocean in the middle. Thank you all!

Abbreviations

ACC	Acetyl-CoA Carboxylase
AFP	Adiabatic Full Passage
Akt/PKB	Akt/Protein Kinase B
ASO	Antisense Oligonucleotide
APE	Atom Percent Excess
AS160	Akt substrate of 160KDa
BMI	Body Mass Index
CDC	Center for Disease Control and Prevention
CPT-1	Carnitine Palmitoyl Transferase-1
CVD	Cardiovascular Disease
DAG	Diacylglycerol
FAT/CD36	Fatty Acid Translocase CD36
FAS	Fatty Acid Synthase
FFA	Free Fatty Acid
FID	Free Induction Decay
FoxO	Forkhead Factor O
G6P	Glucose-6-Phosphate
G6Pase	Glucose-6-Phosphatase
GIR	Glucose Infusion Rate
GK	Glucokinase
GKRP	Glucokinase Regulatory Protein
GLUT	Glucose Transporter
GSK	Glycogen Synthase Kinase
GSV	GLUT4 Storage Vesicles
HMG-CoA	3-Hydroxy-3-Methylglutaryl-CoA
HK	Hexokinase
HSL	Hormone-Sensitive Lipase
IR	Insulin Receptor
IRS	Insulin Receptor Substrate
LCFA	Long Chain Fatty Acids
LPL	Lipoprotein Lipase
MCD	Malonyl-CoA Decarboxylase
PDH	Pyruvate Dehydrogenase
PDK-1	3-Phosphoinositide-dependent Kinase-1

PDK(1-4)	Pyruvate Dehydrogenase Kinase (1-4)
PDP	Pyruvate Dehydrogenase Phosphatase
PEPCK	Phosphoenolpyruvate Carboxykinase
PFK-1	6-Phosphofructo-1-Kinase
PI3K	Phosphatidylinositol 3-Kinase
PI(4,5)P_2	Phosphatidylinositol 4,5-Diphosphate
PI(3,4,5)P_3	Phosphatidylinositol 3,4,5-Trisphosphate
PK	Pyruvate Kinase
PKA	Protein Kinase A
PKB	Protein Kinase B
PKC	Protein Kinase C
POCE-NMR	Proton Observed Carbon Edited-Nuclear Magnetic Resonance
PP-1	Protein Phosphatase 1
PPARα	Peroxisome Proliferator-Activated Receptor α
RQ	Respiration Quotient
siRNA	Small Interference RNA
SH2	*Src* Homology 2
SREBP-1c	Sterol Regulatory Element Binding Protein 1c
T2D	Type 2 Diabetes
TCA	Tricarboxylic Acid Cycle
TE	Echo Time
TG	Triglycerides
VLDL	Very-Low-Density Lipoprotein
V_{PDH}	PDH Flux
V_{TCA}	TCA Flux
WHO	World Health Organization

Abstract

Little is known about the *in vivo* contributions of mitochondrial glucose and fat oxidation to energy metabolism in liver, heart, and skeletal muscle in the transition from fasting to an insulin-stimulated state. In this study we employed a novel Proton-Observed Carbon-Edited Nuclear Magnetic Resonance (POCE-NMR) method to directly assess the relative contribution of mitochondrial glucose and fat oxidation to TCA cycle flux (V_{PDH}/V_{TCA}) in liver, heart and skeletal muscle in awake rats during fasting and insulin stimulation. The influence of insulin resistance and substrate availability on this pattern was also assessed.

Rats were fed a standard or a high-fat diet to induce insulin resistance. Chronically catheterized awake rats (6-8 *per* group) were infused with [1-^{13}C]glucose under either fasting [1 mg glucose/Kg/min)] or hyperinsulinemic (4mU/kg/min)-euglycemic clamp conditions. During the manipulation of plasma substrate levels, animals were subjected to a hyperinsulinemic-hyperglycemic clamp, to increase the availability of glucose, or to a hyperinsulinemic-euglycemic clamp with a concomitant infusion of a triglyceride (TG)/heparin emulsion to maintain fasting plasma levels of free fatty acids (FFA). At the end of each experiment the animals were euthanized and their liver, heart and soleus muscle were rapidly excised and freeze-clamped. Tissue extracts were analyzed by POCE-NMR at 500 MHz. V_{PDH}/V_{TCA} was calculated as the ratio between the ^{13}C enrichment of C4-glutamate *versus* C3-alanine.

Using this approach we found that fasting V_{PDH}/V_{TCA} flux in liver was ~17% and did not change during the hyperinsulinemic-euglycemic clamp. In contrast, fasting V_{PDH}/V_{TCA} flux was ~30% and increased to ~80% ($P<0.00005$) and ~60% ($P<0.01$) during the hyperinsulinemic-euglycemic clamp in heart and soleus muscle, respectively. High-fat diet decreased fasting V_{PDH}/V_{TCA} in liver by 95% ($P<0.00001$) and had no effect on fasting V_{PDH}/V_{TCA} in heart or soleus muscle. Finally, high-fat diet decreased insulin stimulated V_{PDH}/V_{TCA} flux in all tissues by 50-70% ($P<0.05$). The higher availability of fatty acids during the TG/heparin infusion had no effect on the insulin-stimulated values of V_{PDH}/V_{TCA} in liver and heart but completely abolished it in soleus ($P<0.001$). During the hyperinsulinemic-

hyperglycemic clamp, the higher availability of glucose, both in low-fat and high-fat fed animals, increased V_{PDH}/V_{TCA} in all tissues by ~50%-100% ($P<0.05$).

These studies demonstrate important tissue specific differences in basal and insulin stimulated V_{PDH}/V_{TCA} flux and have important implications for understanding the pathogenesis of fat-induced insulin resistance in heart, liver and skeletal muscle.

Resumo

A insulina é uma hormona reconhecida pela sua capacidade de inibição da oxidação de ácidos gordos e estímulo da oxidação de glucose nos tecidos sujeitos à sua acção. Contudo, o conhecimento quantitativo da transição de uma dependência elevada relativamente à oxidação de ácidos gordos (em jejum) para uma situção em que a oxidação de glucose é dominante (por estimulação com insulina) é surprendentememnte limitado. No trabalho aqui apresentado, o efeito da insulina na alteração da contribuição da oxidação de glucose e de ácidos gordos para o ciclo dos ácidos tricarboxílicos (V_{PDH}/V_{TCA}) foi quantificado nos tecidos hepático, cardíaco e no músculo *soleus* usando um método de ressonância magnética nuclear de detecção indirecta de enriquecimento em ^{13}C (Proton-Observed Carbon-Edited Nuclear Magnetic Resonance – POCE-NMR). A influência de um estado de insulino-resistência assim como o efeito da manipulação das concentracões de glucose e ácidos gordos no plasma sanguíneo na regulação da V_{PDH}/V_{TCA} foram também determinados.

Os objectivos acima propostos foram levados a cabo em ratos sujeitos a uma dieta controlo ou rica em lípidos de modo a induzir um estado de insulino-resistência. Os animais sujeitos a ambas as dietas foram divididos por grupos (6-8 animais por grupo) e sujeitos a uma infusão de [1-^{13}C]glucose durante jejum [1mg glucose/Kg/min)] ou durante 2h de hiperinsulinémia (4mU/Kg/min)-euglicémia. A manipulação da concentração de glucose no plasma foi conseguida durante 2h de hiperinsulinémia-hyperglicémia enquanto as concentrações de ácidos gordos livres foram mantidas constantes durante o período de hiperinsulinémia-euglicémia devido a uma co-infusão de uma emulsão the triglicéridos com heparina. No final de cada experiência os animais foram sacrificados e os seus tecidos (fígado, coração e *soleus*) removidos e armazenados para extracção futura. Os extractos resultantes foram analisados por POCE-NMR usando um magnete vertical de 500MHz. V_{PDH}/V_{TCA} foi calculada pela razão entre [4-$^{13}C_4$]glutamato e [3-$^{13}C_3$]alanina.

Utilizando esta abordagem determinou-se que, em animais sujeitos à dieta controlo, a V_{PDH}/V_{TCA} no fígado, em jejum, representava cerca 17% enquanto que nenhuma alteração foi verificada durante estimulação com insulina. Em contraste, a V_{PDH}/V_{TCA} em coração e

soleus foi de cerca de 30% em jejum aumentando para cerca de 80% ($P<0.00005$) e 60% ($P<0.01$), respectivamente, durante o período de hiperinsulinémia-euglicémia. A dieta rica em lípidos, por seu lado, promoveu, no tecido hepático, uma diminuíção da V_{PDH}/V_{TCA} em 95% ($P<0.00001$) durante jejum. Nenhuma alteração foi registada na V_{PDH}/V_{TCA} do tecido cardíaco e *soleus* nas mesmas condições. Contudo, durante o período de hiperinsulinémia-euglicémia, esta dieta levou a uma redução da resposta à insulina em 50-70% nos três tecidos estudados ($P<0.05$).

A maior disponibilidade de ácidos gordos livres durante a co-infusão de triglicéridos/heparina não teve efeito nos valores de V_{PDH}/V_{TCA} em fígado e coração suprimindo, contudo, o efeito da insulina verificado anteriormente no músculo *soleus*. Por outro lado, a maior disponibilidade de glucose aumentou os valores de V_{PDH}/V_{TCA} em 50%-100% em todos os tecidos analisados ($P<0.05$).

Estes resultados determinados *in vivo* revelam diferenças, em termos de selecção de substratos oxidativos na ausência e presença de insulina, que são específicas de cada tecido e que permitem uma melhor compreensão do mecanismo de desenvolvimento de resistência à acção de insulina nos tecido hepático e muscular.

“For the first time in the history of our planet, the number of people who are overfed has overtaken the number of the underfed” (1)

1. Introduction

Over the past 5 decades, a complex combination of increased access to highly-caloric foods and a sedentary lifestyle, has promoted a rising of the prevalence of obesity (1). Associated with this is a tendency for increased incidence of type 2 diabetes mellitus (T2D) and cardiovascular disease (CVD) (2-4). The development of insulin resistance, which precedes T2D, carries profound metabolic alterations in tissues. In particular, it can affect the ability of tissues to switch between oxidative substrates in response to the insulin stimulus. *In vivo* experiments performed by Kelley *et al* demonstrated that insulin-sensitive skeletal muscle is characterized by a switch of oxidative preferences from fatty acids, during fasting, to glucose, during insulin stimulation. In insulin-resistant skeletal muscle, however, this transition was absent (5). The capacity to measure the insulin-stimulated substrate preferences of tissues is particularly relevant since it provides important information about the regulation of the oxidative metabolism and mechanisms that lead to insulin resistance.

In the next sections of this chapter the general mechanisms of insulin action will be overviewed as well as the intracellular events that lead to the development of insulin resistance and impaired substrate selection.

1.1. Definitions and trends of obesity

The definition of overweight/obesity is based on the calculation of the body mass index (BMI), i.e., the quotient of weight in kilograms and height in meters squared. This measurement has been used to define four classes of body weight in adults: *underweight* (BMI < 18.5), *normal weight* (18.5 < BMI < 24.9), *overweight* (25 < BMI < 29.9) and *obese* (BMI > 30). Data from the World Health Organization (WHO) show that more than one billion adults are overweight while 300 million are obese (6). The epidemics of obesity can also affect children and adolescents. In Europe, 10-30% of children between the ages of 7 and 11 years and 25% of adolescents are overweight or obese (7), while in USA the estimate was for 16% of children and adolescents (6-19 years old) to be overweight (8).

According to the Center for Disease Control and Prevention (CDC) the percentage of obese and extremely obese people in USA increased continuously since 1960 (Table 1) and the trends predicted for 2010 indicate that the percentage of obese people is expected to increase (9). In Europe, similar percentages have been observed in some countries with a higher prevalence of obesity in central, southern and eastern Europe (10).

Table 1 Trends of overweight, obesity and extreme obesity percentage among USA adults (20-74 years old). Data from National Health and Nutrition Examination Survey (NHANES).

	NHES I 1960 - 1962	NHANES I 1971-1974	NHANES II 1976-1980	NHANES III 1988-1994	NHANES 1999-2000	NHANES 2001-2002	NHANES 2003-2004	NHANES 2005-2006
Overweight	31.5	32.3	32.1	32.7	33.6	34.4	33.4	32.2
Obese	13.4	14.5	15.0	23.2	30.9	31.3	32.9	35.1
Extremely obese	0.9	1.3	1.4	3.0	5.0	5.4	5.1	6.2

The race/ethnicity is also an important factor to predict the tendency for obesity. Black individuals have a higher tendency to develop obesity an effect specially pronounced in black women being expected that 55% of this ethnic group are expect to have a BMI greater than 30 Kg/m^2 (9).

1.2. Obesity-associated mortality

Increases in body weight are associated with increased mortality (11-13). By plotting mortality risk against BMI one can see that the minimum of mortality occurs for BMI within the normal weight range while there is a steady increase in mortality as BMI increases (Figure 1). This increased mortality associated with higher BMI is mainly due to the development of risk factors for cardiovascular disease such as hypertension, dyslipidemia and diabetes (14-16).

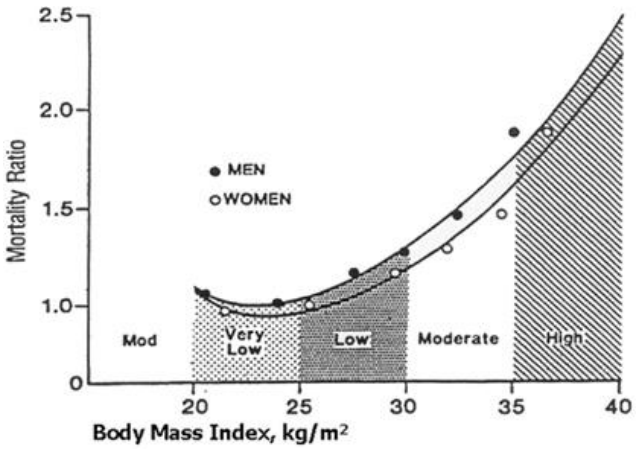

Figure 1 Association of mortality with body mass index (BMI) for men and women (Taken from (17)). Values of BMI between 20 and 25 Kg/m^2 are associated with the lowest risk of mortality. This risk increases dramatically with increasing values of BMI.

CVD is the main cause of mortality in obese people (18). The increased accumulation of fat is also associated with the development of insulin resistance (19-22). Early work from Vague suggested that fat distribution, rather than fat content, plays an important role in the pathogenesis of insulin resistance (23). In this study, it was shown that the accumulation of fat in the upper body, android obesity, was more strongly associated with diabetes than accumulation of fat in the lower body, gynoid obesity, and that there was a strong correlation between the waist and hip circumference ratio and the development of insulin resistance. More recently this concept has been extended to show a negative correlation between fat deposition in non-adipose tissue and insulin resistance (24, 25). In these studies, the authors showed, using non-invasive ^{1}H NMR, a strong inverse relationship between intramyocellular accumulation of triglycerides (TG) and peripheral insulin sensitivity.

1.3. Role of insulin on substrate selection, *in vivo*

There are two major oxidative substrates that can be used by tissues to meet their energy requirements – glucose and fatty acids – and insulin plays a crucial role in

controlling the relative contribution of each for oxidation. Studies on substrate selection started in the early 1960's when Krebs *et al* (26), and later Randle *et al* (27), observed that glucose uptake and glycolysis could be inhibited by the products of fatty acid metabolism. More recently, it has been demonstrated that insulin plays a crucial role in the concerted regulation of metabolism between adipose tissue, liver and skeletal muscle (28).

1.3.1. Fasting

1.3.1.1. Adipose tissue

During fasting, 80% of the endogenously produced glucose is metabolized by brain while the remaining 20% is metabolized mainly by red blood cells and peripheral nerves (29). Due to the high dependence of the brain on glucose, other substrates must be available for the remaining tissues. With prolonged fasting, lipolysis in the adipose tissue is increased, with consequent release of free fatty acids (FFA) into the bloodstream providing extra-adipose tissues with lipid as a source of energy (30, 31). This efflux of fatty acids from the adipose tissue seems to be driven by concentration gradients generated by two key enzymes that regulate fatty acid homeostasis in this tissue: lipoprotein lipase (LPL) and hormone-sensitive lipase (HSL). During fasting, the translocation of HSL from the cytosol to the lipid droplet, controlled by a protein kinase A (PKA)-dependent mechanism, allows a net flow of fatty acids from the adipocytes to plasma (32, 33).

1.3.1.2. Liver

During fasting, a drop of plasma glucose concentrations is prevented due to a constant output of glucose by the liver and kidneys with the liver being responsible for approximately 80% of the total output (34). The two major metabolic routes responsible for this endogenous glucose production are gluconeogenesis (*de novo* synthesis of glucose from 3 carbon unit precursors such as pyurvate) and glycogenolysis (breakdown of glycogen). Significant quantities of glycogen are stored in the liver and during the first hours of fasting these stores are readily used, becoming severely reduced after a 12h fasting (35). As the glycogen stores become depleted, gluconeogenesis assumes a greater

role in the production of glucose and by 24h of fasting it is the main process of glucose production (36). Gluconeogenesis has two main rate limiting steps at the level of the phosphoenolpyruvate carboxykinase (PEPCK) and glucose-6-phosphatase (G6Pase). PEPCK is responsible for the conversion of oxaloacetate into phosphoenolpyruvate while G6Pase catalyses the dephosphorylation of glucose-6-phosphate (G6P) into glucose to be released into the bloodstream. The expression of these enzymes increases with fasting as insulin concentration decreases and are fully repressed in the postprandial state revealing the important role of insulin in regulating these processes (37).

1.3.1.3. Skeletal muscle

Skeletal muscle is composed by several types of fibers that differ in their physical and metabolic properties. There are three major muscle fiber types – type I, type IIA and type IIB. Type I fibers, also known as slow twitch fibers, are characterized by a long twitch contraction time and high fatigue resistance. These fibers display high mitochondrial density, high myoglobin content and high capillary density. On the contrary, type II fibers have short twitch contraction time, lower fatigue resistance and a lower oxidative capacity relative to type I fibers. However, the subtype IIA displays a higher capacity for oxidation than subtype IIB (38).

Despite the differences in fiber types, the oxidative preference of resting skeletal muscle during fasting is towards fatty acids. This was shown using indirect calorimetry to study fasting substrate preferences of resting muscle from the forearm and hindlimb (5, 39). The transport of fatty acids into skeletal muscle is known to occur through passive diffusion (40) and also through a protein-mediated mechanism (41). The main transporter identified in muscle is known as fatty acid translocase (FAT/CD36). FAT/CD36 null mice injected with radio-iodinated fatty acid derivatives showed reduced uptake and esterification of fatty acids in skeletal muscle and heart (42). The deficiency of FAT/CD36 is also associated with reduced rates of fatty acid oxidation in heart (43). FAT/CD36 transporters are located in small vesicles in the cytosol that can be translocated to the plasma membrane by the stimulus of insulin (44). Contraction-induced translocation of FAT/CD36 is also known to occur through an AMP-activated protein kinase dependent mechanism (45).

1.3.2. Fed state

After a meal the circulating concentration of substrates is challenged. Typically, in healthy individuals, the amount of glucose in circulation under fasting conditions is around 100mg/dL. A meal containing roughly 50g of carbohydrates would drastically change its plasma concentration (up to 10-fold difference) if no mechanisms of disposal existed. However, in glucose tolerance tests performed in healthy individuals, a 75g glucose meal only increases plasma glucose to a maximum of 50% before returning to the basal level (46). In response to increases in plasma glucose, insulin is secreted by pancreas in a biphasic way. The first phase, cephalic, occurs before plasma glucose is impacted by the meal and is thought to be mediated by the vagus nerve stimulation (Figure 2) (47), and is followed by a more sustained release of insulin as plasma glucose concentrations rise. It is believed that this anticipatory approach elicits a faster response to the impending metabolic changes evoked by the meal (47).

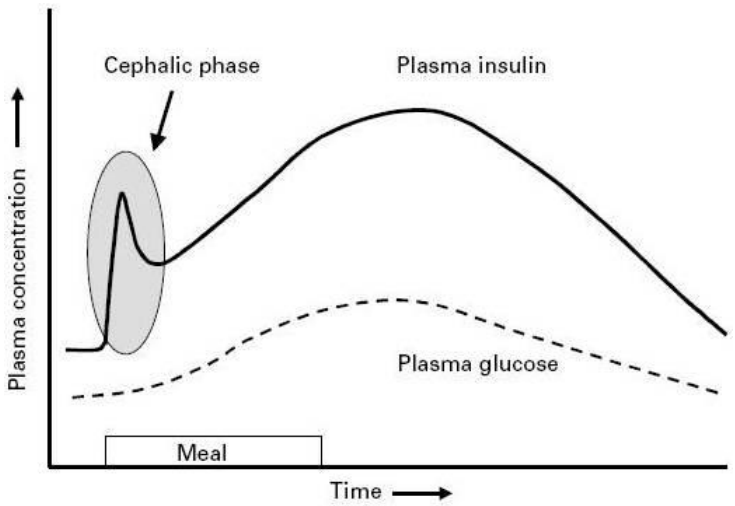

Figure 2 The pattern of insulin release in response to a meal is divided in two phases. The cephalic phase occurs before the increase is plasma glucose and is followed by a phase of continuous release of insulin until plasma concentrations of glucose decrease. Picture taken from (48).

1.3.2.1. Liver

As the plasma insulin concentration rises following a meal, hepatic glucose output is suppressed with concomitant stimulation of glucose utilization and storage, via glycolysis and synthesis of glycogen. Excess of glucose can also be converted into lipids in a process known as *de novo* lipogenesis (49-51). For this to occur, gluconeogenic flux and glycogenolysis must be suppressed while glycolysis and the synthesis of lipids and glycogen must be stimulated. All of these effects are mediated through the activation of the insulin signaling cascade (explored in section 1.4.).

The expression of PEPCK and G6Pase genes is tightly controlled by the presence of a forkhead group O protein, FoxO (reviewed in (52)). There are several isoforms of this protein with FoxO1 being the most highly expressed in liver. During fasting FoxO1 is found in the nucleus, bound to the *cis*-elements in the promoters of PEPCK and G6Pase genes, which leads to an increase in their expression. In the presence of insulin, the Akt/Protein Kinase B (PKB) complex, an intermediate of the insulin signaling pathway, phosphorylates FoxO1 and promotes its translocation to the cytosol decreasing the expression of these gluconeogenic enzymes. This mechanism was confirmed by knock-down experiments of FoxO1 in liver using an antisense oligonucleotide-mediated (ASO) approach (53). In this experiment, a single-stranded DNA molecule, composed by 13-25 nucleotides, is synthesized with a sequence complimentary to a specific portion of the gene of interest. Once these two sequences hybridize, the expression of the gene is blocked. The knock-down of FoxO1 showed reduced expression levels of PEPCK and G6Pase and consequent decrease of hepatic glucose output.

At the same time, storage, in the form of glycogen and esterified fatty acids, is stimulated. Liver cells contain high capacity glucose transporters (GLUT2, Km = 8-9mM) and also a high affinity enzyme for glucose phosphrylation (glucokinase (GK), Km = 8mM) which enable the rapid import and phosphorylation of glucose by the liver as soon as plasma concentrations increase after a meal (54). GK activity, in particular, is regulated by two major processes: an insulin-independent mechanism, accomplished by a GK regulatory protein (GKRP), and an insulin-mediated process via gene expression. During fasting, GKRP (which has a nuclear import signal) binds to GK and promotes the transport of this complex to the nucleus where it is protected from proteolytic activity. In the presence of high

concentrations of glucose or fructose, this complex dissociates and GK is transported back to cytosol (55, 56). Insulin is also known to regulate the level of expression of GK – rats deficient in insulin exhibit decreased levels of GK mRNA (57), and inhibition of insulin signaling also suppress GK gene expression (58, 59).

Once phosphorylated, glucose can be readily converted to glycogen. Glycogen metabolism is regulated by the balance of the activities of glycogen phosphorylase and glycogen synthase. During fasting both the enzymes are phosphorylated. While the phosphorylated form of glycogen phosphorylase is activated, phosphorylation of glycogen synthase results in its inhibition. This situation is reversed by the raise of insulin in the postprandial state. In these state, glycogen synthase kinase 3 (GSK3) is inhibited preventing the phosphorylation and inactivation of glycogen synthase (reviewed at (60)). Also relevant is the allosteric activation of a protein phosphatase-1 (PP-1) by increased levels of G6P and consequent dephosphorylation of glycogen synthase (61).

In liver, insulin is also responsible for the stimulation of the *de novo* synthesis and esterification of lipids (62). This is thought to be mediated by the sterol regulatory element binding protein 1c (SREBP-1c) which induces the expression of fatty acid synthase and acetyl-CoA carboxylase (ACC) via a process that involves activation of the insulin signaling cascade (63). The expression of these enzymes in liver is increased in transgenic animals which overexpress SREBP-1c (64). In contrast, low levels of lipogenic enzymes are observed in experiments in which SREBP-1c was knocked-down (65).

1.3.2.2. Skeletal muscle

In contrast to liver, in which GLUT2 is constitutively active, muscle and adipocytes contain an insulin responsive form of glucose transporters known as GLUT4. *In vivo* metabolic control analysis applied in muscle revealed that GLUT4-mediated transport of glucose is the rate-limiting step for glucose disposal (66). This regulation is achieved due to the different locations of GLUT4 in basal and insulin-stimulated states. In the basal state, GLUT4 transporters are located in small, GLUT4 storage vesicles (GSV), located in the cytosol (67). However, upon insulin stimulation, GLUT4 transporters are translocated to the plasma membrane through a process that involves activation of components of the insulin signaling pathway such as phosphoinositide 3-kinase (PI3K) and Akt/PKB. The specific

activation of Akt-PKB was shown to increase glucose uptake (68); the translocation of GLUT4 to the membrane was inhibited in cells transfected with an inactive form of Akt/PKB (69), in small interference RNA (siRNA)-mediated knockdown (70) and in PKB beta knockout mice (71). Downstream of Akt/PKB the Akt substrate of 160KDa (AS160) plays an important role in regulating the translocation of GLUT4-enriched GSV to the membrane. AS160 can be phosphorylated by Akt/PKB in six sites, four of which, when mutated, prevent GLUT4 translocation (72). Adipocytes in which AS160 was knocked down using siRNA showed a higher number of GLUT4 transporters in the membrane suggesting that AS160 is responsible for the repression of translocation in the absence of insulin (73).

1.4. Insulin signaling

1.4.1. Mechanism of insulin signal transduction

Insulin is a peptide secreted by β-cells from pancreas and it has a central role in the regulation of fuel homeostasis. It is particularly effective in keeping glucose levels within narrow limits. After a meal, circulating levels of insulin rise in response to the increased levels of plasma glucose promoting its uptake and storage. It is also responsible for the activation of anabolic pathways such as glycogen, lipid and protein synthesis while it inhibits the oxidation of these metabolites (74).

All these effects are mediated by the binding of this hormone to the insulin receptor (IR), a process characterized by high specificity and affinity, which prompts an intracellular cascade of events that signals the presence of plasma insulin (Figure 3).

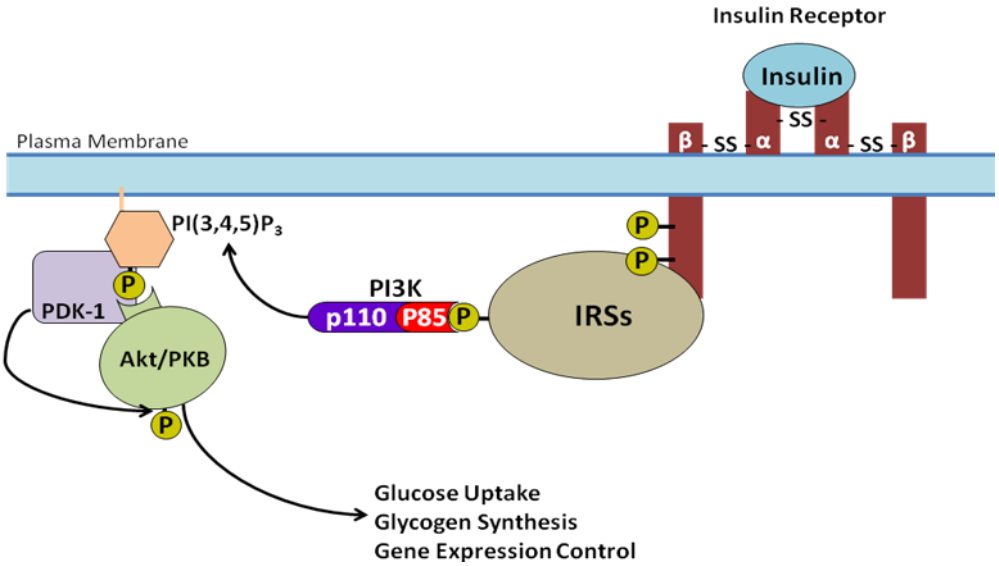

Figure 3 Insulin signaling cascade. The binding of insulin to its receptor promotes the autophosphorylation of the tyrosine residues of the β subunit of the insulin receptor (IR). This allows the docking and phosphorylation of insulin receptor substrates (IRS) which, in turn, allows the association and activation of phosphoinositide 3-kinase (PI3K). When activated, PI3K catalysis the phosphorylation of phosphatidylinositol-4,5-bisphosphate [$PI(4,5)P_2$] to phosphatidylinositol-3,4,5-bisphosphate [$PI(3,4,5)P_3$]. $PI(3,4,5)P_3$, in turn, activates phosphoinositide-dependent kinase 1 (PDK1) promoting the phosphorylation and activation of the Akt complex to regulate phenomena like glucose uptake, glycogen synthesis and gene expression.

Upon binding of insulin, the induced change in conformation of the IR activates the intrinsic tyrosine-specific kinase, located in the intracellular portion of the IR, promoting the autophosphorylation of tyrosine residues of the receptor. This promotes the recruitment, docking and phosphorylation of several proteins, termed insulin receptor substrates (IRS), thereby activating them. Once phosphorylated, IRS interact with several other signaling proteins in order to modulate metabolism. In particular, they serve as docking sites for phosphoinositide 3-kinase (PI3K) activating it. Once activated, PI3K promotes phosphorylation and activation of the serine/threonine kinase, Akt/PKB, which is directly involved in the regulation of processes like glycogen synthesis, glucose uptake in muscle and inhibition of gluconeogenesis in liver (74).

1.4.2. Structure and function of the insulin receptor (IR)

The IR is a heterotetrameric transmembrane protein containing two types of subunits – α (MW = 140KDa) and β (MW = 95KDa) – linked by disulphide bonds in a β-α-α-β configuration (Figure 4) (75-77). A single chain of 30 aminoacids is synthesized in the endoplasmic reticulum where is then cleaved, glycosylated and dimerized (78, 79). This glycosylation assumes an important role in the normal maturation of the IR as well as for its affinity towards insulin (80). Once dimerized, this IR precursor is transported to the Golgi complex where it matures to its final form and is subsequently transported to the plasma membrane. The α-subunit consists of two successive homologous globular domains, L1 and L2 which are separated by a cysteine-rich region. The β-subunits are imbedded in the plasma membrane, and are linked to the α-subunits via disulfide bridges and noncovalent interactions. The intracellular part of the β-subunit contains the tyrosine kinase catalytic domain flanked by two regulatory regions: a juxtamembrane region, involved in receptor internalization and docking of the IRS molecules, and a carboxy-terminal tail, which contains two phosphotyrosine-binding sites (81).

Upon binding to insulin, the conformational change induces the activation of the tyrosine kinase domain by phosphorylating seven tyrosine residues, distributed along the 3 domains of the β subunits, all required for full kinase activity (81-83). The juxtamembrane domain contains two phosphotyrosine residues (Tyr965 and Tyr972) responsible for the binding of substrates such as IRS and Shc essential for insulin signal transduction (84). The tyrosine kinase domain contains three phosphotyrosine residues (Tyr1158, Tyr1162, and Tyr1163) essential for full activity of the kinase (85). Phosphorylation of both juxtamembrane and kinase domains are also involved in the process of internalization of the complex insulin-IR (85, 86). The key step in this process is the recognition, by the endocytic machinery, of the tyrosine motifs in the juxtamembrane domain which are exposed once the receptor is activated. The acidic pH of the endosomes causes the release of insulin which is degraded by proteases (87, 88), and the IR is then recycled to the plasma membrane after inactivation by phosphotyrosine phosphatases (89, 90). The importance of phosphorylation of the C-Terminus is yet to be determined (77).

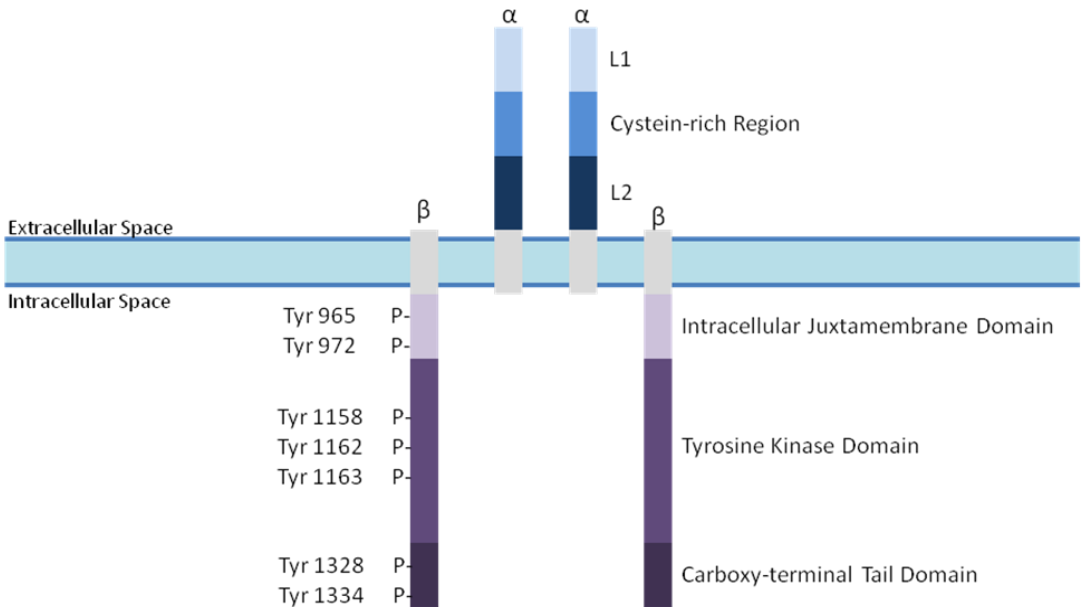

Figure 4 Configuration of α and β subunits to form the IR. The α subunits, located in the extracellular space are responsible for the binding of insulin while the β subunits, located in the intracellular milieu, are responsible for the insulin signaling transduction. β subunits comprise three distinct domains: juxtamembrane, tyrosine kinase and carboxy-terminal tail.

1.4.3. Insulin receptor substrate (IRS)

The initial mediators of the insulin signaling cascade are the IRS proteins; once phosphorylated by IR tyrosine kinase, IRS proteins serve as docking sites for other signaling molecules such as substrates possessing *src* homology 2 (SH2) domains, including PI3K regulatory subunits (p85, p55 p50, p85, and p55PIK) (91-93).

There are four isoforms of IRS (IRS-1 to 4). IRS-1 was the first substrate to be identified (94). This protein shows several sites for tyrosine phosphorylation responsible for the docking of other signaling molecules such as PI3K (95, 96). IRS-2 is another form of IRS that share many structural and functional characteristics with IRS-1 (97). The relative importance of IRS-1 and 2 was unveiled by knockout studies. Mice lacking IRS-1 (IRS-$1^{-/-}$) showed growth retardation (98, 99) and insulin resistance (100, 101). In liver from these mice, insulin signaling seemed to be intact due to compensatory expression of IRS-2 (102,

103). On the other side, mice lacking IRS-2 (IRS-$2^{-/-}$) showed marked insulin resistance in adipose tissue (102) and in liver (104, 105) but normal basal and insulin-stimulated glucose transport in muscle (105). Overall these experiments show that IRS-2 plays an important role in liver while IRS-1 is more important in muscle. In opposition to these two isoforms, IRS-3 and IRS-4 knockout showed a mild phenotype (106).

1.4.4. Phosphatidylinositol-3 kinase (PI3K)

The next step of insulin signal transduction is the recruitment of PI3K which is a heterodimer protein composed of a regulatory and a catalytic subunit (p85 and p110 respectively). There are two isoforms of PI3K that respond to different receptors: type 1A, involved in the transduction of signal triggered by the insulin receptor, and type 1B, activated by heterotrimeric G-proteins. Upon insulin stimulation, type 1A PI3K is brought to the membrane through interaction with phosphorylated IRS via the p85 subunit, and subsequently activated (107). PI3K 1A is responsible for the phosphorylation of the plasma membrane lipid phosphatidylinositol-4,5-bisphosphate ($PI(4,5)P_2$) to form phosphatidylinositol-3,4,5-trisphosphate ($PI(3,4,5)P_3$) which is involved in stimulatory effects on glucose transport, glycogen synthesis and protein synthesis and inhibitory effects on lypolisis covered in section 1.3.2. The crucial role of this enzyme in mediating the effects of insulin was demonstrated by experiments where the inhibition of PI3K by wortmannin decreased the responses of glucose uptake, glycogen synthesis and DNA synthesis to insulin stimulation (108-110).

1.4.5. Akt/Protein kinase B (PKB)

The activation of PI3K by insulin is essential to the phosphorylation and consequent activation of Akt/PKB. The presence of $PI(3,4,5)P_3$ in the membrane serve as docking site for Akt/PKB exposing the phosphorylation sites. $PI(3,4,5)P_3$ also recruits and activates phosphoinositide-dependent kinase 1 (PDK1) whose role is to phosphorylate threonine 308 of Akt/PKB. For full activation of this enzyme, serine 473 must also be phosphorylated.

Akt/PKB has several roles in cell survival and maintenance (reviewed in (74)); one of its primary functions is to stimulate glucose uptake in response to insulin. The initial observation that strongly implicated Akt/PKB as a mediator of insulin signaling was that the expression of a constitutively active form of allowed high levels of glucose transport and GLUT4 translocation in adipocytes in the absence of insulin (111). Subsequently, it was found that Akt2 directly associates with GLUT4-containing vesicles upon insulin stimulation of adipocytes (112). The importance of Akt/PKB in the regulation of glucose transport was further revealed by inhibition studies of Akt/PKB activity, either by interfering antibodies or expression of a dominant-negative form that resulted in reduced insulin-stimulated GLUT4 translocation in fat and muscle cells (69, 113). In liver, the repression of gluconeogenic genes during insulin stimulation is mediated by Akt2 (114). For example, mice deficient in Akt2 exhibit mild insulin resistance in muscle and an inability to suppress hepatic glucose production. In contrast, Akt1(-/-) produces growth retardation but has a limited effect on glucose tolerance (71, 115). Activated Akt/PKB is also known to regulate glycogen synthesis by phosphorylate serine 9 of GSK3, inhibiting it. As explained in section 1.3.2.1., inhibition of GSK3 is important for the synthesis of glycogen to occur (116).

1.5. Glucose-fatty acid cycle and normal physiology

As one can infer from the previous sections, insulin plays a key role on glucose disposal and metabolism. In 1963, Randle and co-workers, questioned whether this was the only level at which substrate selection was regulated and proposed an insulin-independent, level of control of substrate selection, termed the glucose-fatty acid, or Randle cycle (117). These experiments demonstrated a nutrient-mediated regulation of metabolism, a consequence of constant competition between glucose and fatty acids for oxidation in muscle and adipose tissue.

It was proposed that the excess glucose in plasma, that characterizes the postprandial state, is taken by adipose tissue inhibiting the release of FFA into the blood stream and thus the flux of lipid supply to muscle. The consequence is decreased muscle fatty acid oxidation releasing the inhibition upon glucose oxidation and switching, therefore, substrate preference towards glucose. In contrast, during fasting, the increased lipolysis in

adipocytes and subsequent increased availability of FFA in the blood stream inhibits glucose uptake and oxidation in muscle sparing it to be used by glucose-dependent tissues like brain (Figure 5). The glucose-fatty acid cycle suggests that the regulation of substrate preferences happens at two levels: nutrient and hormonal-mediated. According to the authors, even though the first mechanism of regulation is independent of hormone control, the presence of insulin is crucial to mediate the effects of glucose metabolism on fatty acid oxidation due to the stimulation of glucose uptake in muscle and adipose tissue.

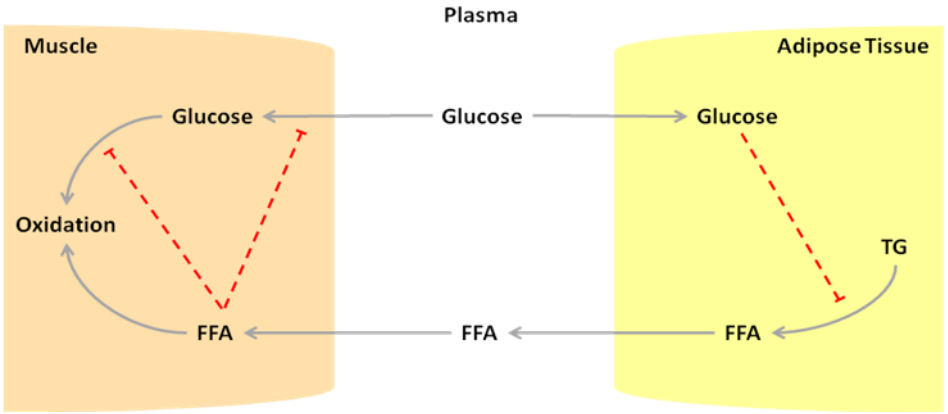

Figure 5 The glucose-fatty acid cycle proposed by Randle *et al* (117). The dashed arrows represent the inhibitory effect of glucose on lipolysis in adipose tissue and the inhibition of glucose uptake and oxidation in muscle by free fatty acids (FFA). (Adapted from (118)).

1.5.1. Inhibition of glucose metabolism by fatty acids

The initial work from Randle, showing a decrease in glucose uptake in heart and diaphragm muscle incubated with fatty acids, suggested that the inhibitory effect of fatty acids on glucose utilization was achieved by allosteric regulation of key steps in that pathway, namely, at the level of glucose transport and phosphorylation, 6-phosphofructo-1-kinase (PFK-1) and pyruvate dehydrogenase (PDH) (119). His studies revealed that the level of inhibition was not the same in all the three steps. The inhibition effect was most severe at the level of PDH having less influence at the levels of PFK-1 and glucose transport/phosphorylation. During high fluxes of β-oxidation, intramitochondrial concentrations of acetyl-CoA and NADH increase which inhibit PDH activity. At the same

time, the excess of mitochondrial citrate is transported to the cytosol where it regulates glucose metabolism by inhibiting PFK-1 and glucose phosphorylation (Figure 6).

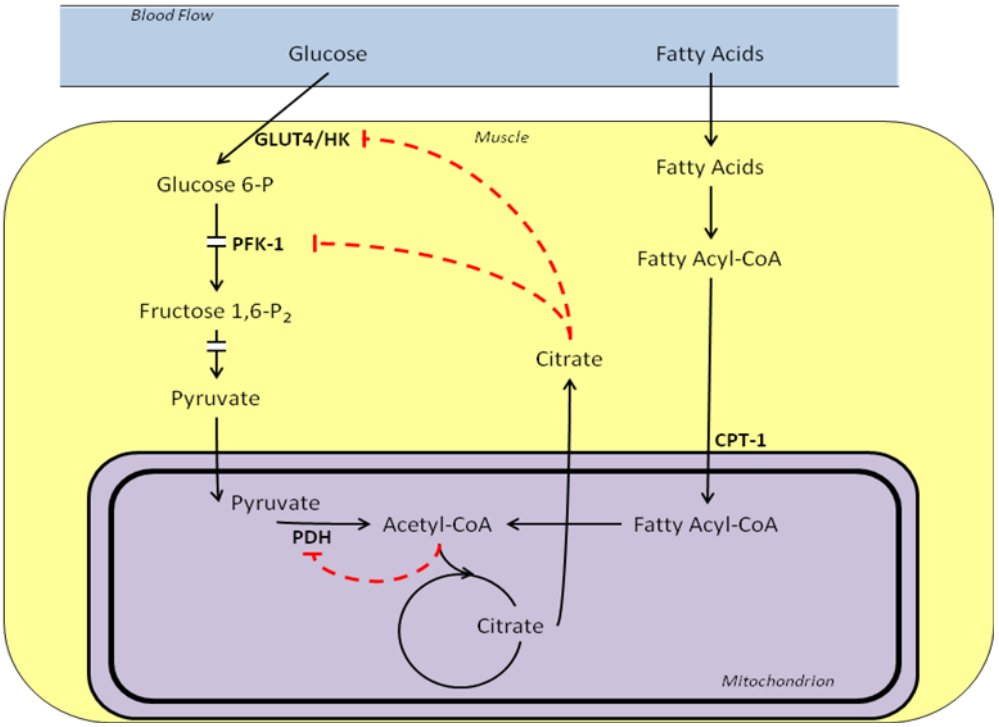

Figure 6 Mechanism of inhibition (dashed arrows) of glucose metabolism by fatty acids proposed by Randle *et al* (119, 120). In a setting of high rates of fatty acid oxidation, the accumulation of acetyl-CoA in the intramitochondrial space leads to the inhibition of the flux through PDH. Simultaneously, the excess of citrate, produced in the tricarboxylic acid (TCA) cycle, is exported to the cytosol where it can inhibit 6-phosphofructo-1-kinase (PFK-1) and glucose transport (GLUT4) and phosphorilation by hexokinase (HK). (Adapted from (118)).

1.5.1.1. Pyruvate dehydrogenase (PDH)

PDH is an intramitochondrial multienzyme complex responsible for the oxidative decarboxylation of pyruvate into acetyl-CoA with concomitant reduction of NAD^+ to NADH (Figure 7). This enzyme assumes a particularly important role in the regulation of fuel selection since it controls the entry of glucose carbons into the tricarboxylic acid (TCA) cycle. PDH is tightly regulated by several factors including allosteric inhibition by the end-

products of the reaction and a cycle of phosphorylation/dephosphorylation (reviewed in (121, 122)).

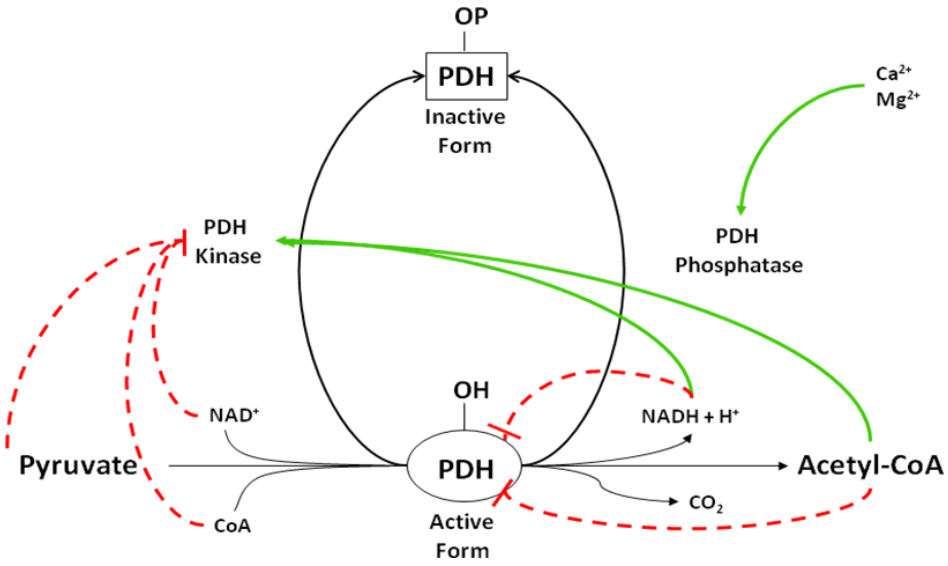

Figure 7 Reaction catalyzed by pyruvate dehydrogenase (PDH). The dashed arrows represent negative allosteric regulation while the continuous arrows represent positive allosteric regulation.

The core of this complex is composed of several subunits of dihydrolipoamide acetyltransferase, E2, that interact with thirty subunits of pyruvate dehydrogenase activity, E1. A third group of subunits of FAD-containing dihydrolipoamide dehydrogenase, E3, interacts with the complex (123). The E1 subunit is central for the regulatory mechanisms involving covalent modification by a serine phosphorylation/dephosphorylation cycle. Phosphorylation, and consequent inactivation, of PDH is achieved by the enzyme pyruvate dehydrogenase kinase (PDK); the restoration of PDH activity is the responsibility of pyruvate dehydrogenase phosphatase (PDP). These two regulatory enzymes are part of the complex through binding to the E2 subunit.

There are four isoforms of PDK (PDK1-4) expressed in a tissue specific manner. PDK1 is present mostly in the heart, PDK2 has ubiquitous expression, PDK3 is expressed mainly in testis while PDK4 expression occurs in higher amounts in heart and skeletal muscle (124). Three serine residues have been originally reported as phosphorylation sites with regulatory properties - site 1 (Ser264), site 2 (Ser271) and site 3 (Ser203) (125). Studies

conducted to distinguish between the three sites revealed that the phosphorylation of each single site can inactive the complex; however the phosphorylation rate is faster for site 1 and slower for site 3 (126). Each PDK isoform has different specificity for each phosphorylation site. For site 1 PDK2 had the maximum activity followed by PDK4, PDK1 and PDK3. For site 2 PDK3 had maximum activity PDK3 followed by PDK4, PDK2 and PDK1. PDK1 was the only isoenzyme having activity with site 3 (127). Recently three other serine phosphorylation sites were discovered – ser232, ser293 and ser300 (128). Short-term regulation of PDK is achieved by fluctuations in the concentrations of pyruvate and NADH/NAD^+ and acetyl-CoA/CoA ratios. High concentrations of pyruvate are known to inhibit the kinase activity (129). High concentrations of acetyl-CoA and NADH, products of β-oxidation, also inhibit PDK (121, 122). The extent of inhibition by these metabolites is different for each isoform. For instance, PDK2 is more sensitive to the regulation by pyruvate, acetyl-CoA and NADH than the other isoforms (129).

The opposite effect is mediated by PDH phosphatases (PDP). Mammalian tissues contain two distinct PDP isoforms (PDP1 and PDP2). This enzyme is formed by two subunits of 52 and 96Kda (130) and its activity is Mg^{2+}-dependent for both isoforms. However PDP1 and PDP2 have different sensitiveness to Ca^{2+} influencing the tissue distributions (131). PDP1, the Ca^{2+}-sensitive isoform, is more abundant in skeletal muscle while PDP2 is present in liver.

1.6. Reversed glucose-fatty acid cycle

Glucose metabolism can also compete with fatty acids as shown by the work of McGarry *et al* (132). Once glucose is oxidized to acetyl-CoA, it enters TCA cycle through condensation with oxaloacetate to form citrate. This metabolite, when in excess, can be transported to the cytosolic pool where it is converted back to acetyl-CoA and carboxylated to malonyl-CoA, in a reaction catalysed by the enzyme ACC. Malonyl-CoA is a potent inhibitor of the palmitoyltransferase-1 (CPT-1), which controls the entry and oxidation of long chain fatty acids (LCFA) in mitochondria redirecting fatty acid metabolism towards esterification (Figure 8).

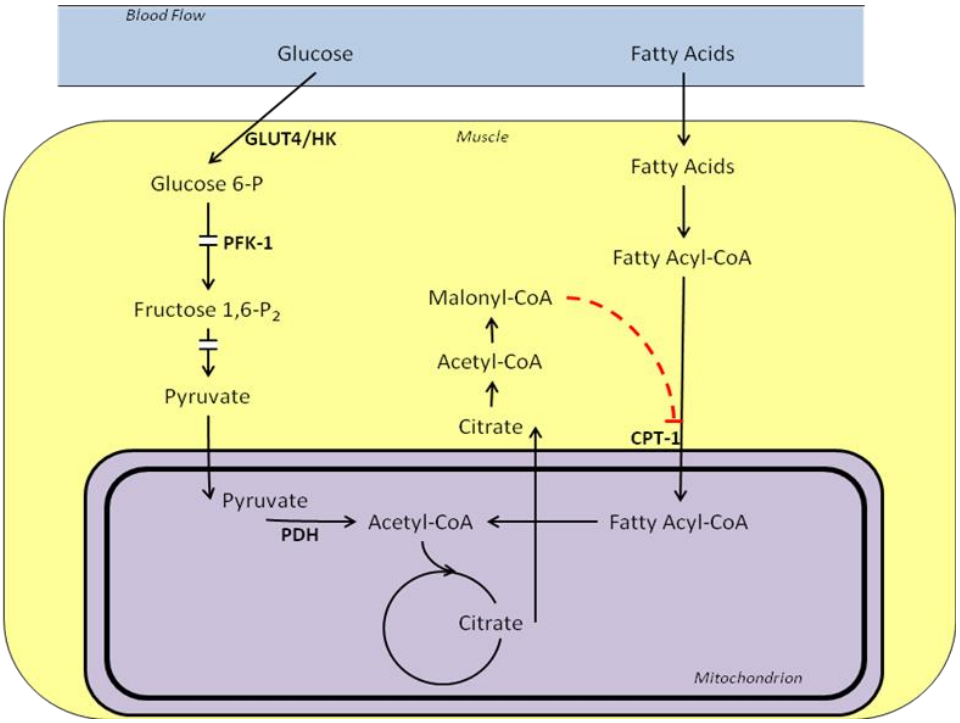

Figure 8 Inhibition of fatty oxidation by glucose metabolism. When glucose is abundant, it is metabolized to pyruvate through glycolysis. This activates pyruvate dehydrogenase (PDH) allowing pyruvate to be further oxidized to acetyl-CoA and then to form citrate. Excess of citrate is exported to the cytosol where it is cleaved, by the action of the enzyme citrate lyase, to form acetyl-CoA. The enzyme acetyl-CoA carboxylase (ACC) carboxylates acetyl-CoA to malonyl-CoA which in turn inhibits carnitine palmitoyl transferase 1 (CPT-1). This decreases fatty acid uptake and oxidation. (Adapted from (118)).

This mechanism of regulation, known as reversed glucose-fatty acid cycle, is present in both lipogenic and non-lipogenic tissues, such as liver and muscle, respectively. There are two isoforms of ACC. ACC1 is present in liver and mice lacking this isoform are not viable indicating the central role of fatty acid metabolism in survival (133). ACC2 is present in liver, heart and muscle and its major role is the regulation of fatty acid oxidation as evidenced in whole-body knockout mice models in which a 30% increase in β-oxidation was observed in soleus muscle (134). This is consistent with the subcellular location of each isoform. While ACC1 is a cytosolic enzyme, and thus involved in lipogenic activity, ACC2 is directly associated with the mitochondrial membrane supporting its role as CPT-1 regulator (135).

Sensitivity of CPT-1 to malonyl-CoA varies in different tissues (reviewed at (136)). In liver the half-maximal inhibition concentration is close to 2μM while in muscle this value is 100-fold lower, 0.02μM, showing that liver CPT-1 is less sensitive to malonyl-CoA than muscle. Also, the concentrations of malonyl-CoA in both tissues are in the micromolar range (1–5 μM) in rat suggesting that CPT-1 would be permanently inactive if no other mechanism existed to modulate its sensitivity. Recent work indicates that muscle CPT-1 sensitivity to malonyl-CoA is modulated by interaction between its NH_2 and COOH termini, depending on the physiological state (137). In mitochondria isolated from fasted rats this interaction was absent decreasing the sensitivity of CPT-1 towards malonyl-CoA.

1.7. Insulin resistance

Insulin resistance is a state of reduced sensitivity in peripheral tissues to the actions of insulin. It is characterized by impaired insulin-stimulated glucose disposal and storage by skeletal muscle and adipose tissue as well as inefficient suppression of hepatic glucose output (reviewed in (138)). It is also a good predictor of future development of T2D (139). Insulin resistance has been correlated with increased levels of fatty acids in plasma (140) and a higher TG content in non-adipose tissues (141), assessed *in vitro*. With the increasing development of non-invasive techniques such as ^{1}H-NMR, strong correlations between intramyocellular TG content and reduced glucose disposal have been established (24, 25). The direct influence of lipid on insulin sensitivity was emphasized by Perseghin *et al* (142). In this study, the intramyocellular lipid content in normal-weight, non-diabetic subjects was correlated with insulin resistance but not with BMI reinforcing the idea that the accumulation of lipids in extra-adipose tissues is essential in the development of insulin resistance. The same correlations have been obtained in animal models. In particular, in a transgenic mouse model of severe lipodystrophy, in which all the white adipose tissue was absent, lipid content in liver and muscle doubled relative to control mice. In these animals the development of severe insulin resistance was linked to the accumulation of fat (143).

Insulin resistance in skeletal muscle has also been shown to be induced by raising plasma concentrations of FFA through infusions of TG/heparin emulsions (144, 145). According to the glucose-fatty acid cycle hypothesis these results would be a direct consequence of the inhibition of glycolysis by fatty acids which would lead to accumulation

of G6P and consequent inhibition of glucose transport and phosphorilation. However, Roden *et al*, using ^{31}P NMR during a continuous lipid infusion, failed to see the predicted increase in G6P levels in skeletal muscle (146). In fact, both glucose oxidation and G6P levels decreased before the inhibitory effect of lipids on insulin-stimulated glucose uptake was observed. Instead, the effect of fatty acids on glucose uptake was attributed to impaired insulin signaling (147, 148). *T*he mechanism of lipid induced insulin resistance has been recently uncovered. The key step is the activation of novel serine-threonine protein kinase C (PKC) – PKCθ in muscle, (149), and PKCε in liver (150) – by accumulated diacylglycerol (DAG) (149). Once activated, PKC is translocated to the membrane and phosphorylates IRS-1 and IRS-2 inhibiting the autophosphorylation of tyrosine residues (149, 150). The same mechanism has been observed in other models displaying insulin resistance (151-153).

1.8. Effect of insulin resistance on substrate selection

Skeletal muscle is considered the predominant tissue responsible for the insulin-stimulated disposal of glucose (154). It also displays a high metabolic flexibility evidenced by a quick glucose uptake in response to insulin and high sensitivity of CPT-1 to malonyl-CoA concentrations. In order to study the effects of intramyocellular lipid accumulation, and consequent development of insulin resistance, on substrate selection in resting muscle, Kelly *et al* (5) measured the respiratory quotient (RQ) across the leg of lean and obese individuals during fasting and insulin-stimulating conditions (Figure 9).

In these experiments catheters are inserted in the radial artery and femoral vein and used to sample blood to measure the mass balance of CO_2 and O_2 across the leg muscle. The RQ, a measure of glucose *versus* fatty acid oxidation, is calculated as the ratio of CO_2 production over O_2 consumption. RQ values ~1 indicate a total reliance on glucose oxidation while RQ ~ 0.7 indicate a total dependence on fatty acid oxidation. The results from lean individuals revealed a shift from a fasting RQ of 0.83 to 0.9 during insulin stimulation showing that insulin promotes a change of oxidative substrate preference from fatty acid to glucose. Surprisingly, in obese subjects, while insulin stimulation had no effect on RQ values, fasting reliance on glucose oxidation was significantly higher than those

obtained for lean individuals. This unresponsive pattern observed in the presence of insulin was coined by the authors as “metabolic inflexibility” and used to explain the metabolic consequences of skeletal muscle insulin resistance on the ability to switch between oxidative substrates. The development of this metabolic inflexibility is thought to be linked to the expression of PDK4 since increased levels of this enzyme would lead to inactivation of PDH and consequent inability to oxidize pyruvate in response to insulin. In fact, higher expression of PDK4 has been associated with increased lipid content in heart (155). In line with these results, the heart-specific overexpression of PDK4 in mice led to decreased capacity to oxidize glucose and a higher reliance on fatty acid oxidation (156). On the other side, high fat fed mice lacking PDK4 showed lower fasting levels of glucose and insulin and higher insulin sensitivity during glucose tolerance tests, confirming the important role of this enzyme in the regulation of the insulin-stimulated glucose oxidation (157).

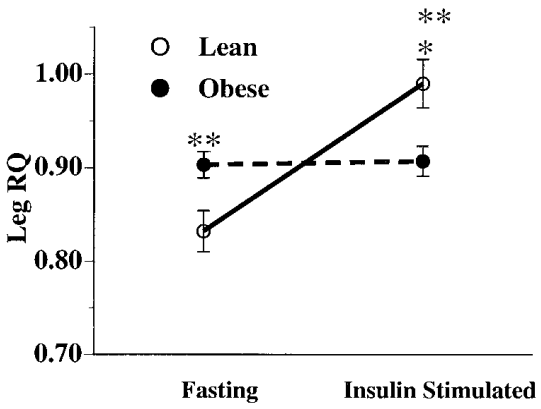

Figure 9 Respiratory quotient (RQ) measured in lean and obese individuals during fasting and insulin-stimulated conditions (Adapted from (5)). *P<0.01 relative to the fasting state; **P<0.01 relative to the lean individuals.

The use of indirect calorimetry has given important information about the *in vivo* substrate preferences. However some limitations associated with the lack of tissue specificity should be highlighted. The RQ measurement across the legs of individuals has necessarily contributions from other tissues such as adipose tissue which can lead to inaccurate estimates of substrate preferences. Therefore, the results reported here were obtained using a sensitive NMR sequence that allowed the determination of the tissue-

specific contribution of PDH to TCA cycle flux (V_{PDH}/V_{TCA}) in response to several stimuli. In particular, the influence of insulin and plasma substrate concentrations on V_{PDH}/V_{TCA} was explored in several tissues.

2. Aims

The *in vivo* study of substrate selection has been accomplished using indirect calorimetry. However several limitations are associated with this technique. It was initially developed to measure whole-body substrate oxidation and how it varied under different conditions (reviewed in (158)). However the fact that CO_2 is in equilibrium with bicarbonate in plasma leads to the existence of several interchanging compartments and, therefore, an increased delay to rich steady-state. This and the lack of tissue specificity led to the use of this technique in smaller and more localized systems such as forearm or hindlimb to avoid contributions from other organs (159). This approach involves the placement of catheters in the major artery and vein and the sampling of blood to measure the circulating concentration of O_2 and CO_2. Nevertheless, tissue specificity is still a major concern especially in the study of skeletal muscle metabolism. The existence of tissues, such as adipose tissue, bone and skin, has the potential to significantly alter the value of RQ. Adipose tissue, in particular, with an RQ≈1 (160), can be a potential source of error in the RQ determination especially in obese individuals, despite its lower oxygen consumption rate compared with skeletal muscle. Another inherent problem with indirect calorimetry is its reliance on blood flood. Factors like temperature or hormonal stimulation can affect blood flow and therefore have the potential to drastically influence the RQ obtained (161).

To overcome these limitations a method was developed to measure the relative contribution of glucose oxidation to total TCA cycle by combining NMR analysis with infused ^{13}C-labeled substrates to follow metabolism *in vivo*. In 1987, a study performed by Shulman et al (162) showed that, at the steady state, the ratio of [4-^{13}C]glutamate to labeled [3-^{13}C]alanine equals V_{PDH}/V_{TCA}. In this study, ^{13}C-NMR was used to determine the enrichments of glutamate, lactate and alanine. ^{13}C-NMR has been widely used to study intermediary metabolism (163). The low natural abundance of ^{13}C, ~1.1%, grants high specificity to this technique with which only the ^{13}C-enriched metabolites can be analyzed. Also, its wide spectral range (1 – 220ppm) avoids superposition of resonances facilitating the analysis. The downside of this approach is related to the low sensitivity of ^{13}C which limits its *in vivo* analysis of metabolites existing in high concentrations. Even the analysis of

enrichments in tissue extracts requires several hours of acquisition in order to derive spectra with high signal to noise ratios. The use of ^{1}H-NMR can overcome the low sensitivity of ^{13}C-NMR. ^{1}H is one of the NMR-visible nuclei with the highest sensitivity and natural abundance (near 100%) which makes its detection very simple. Furthermore, the coupling between ^{1}H and ^{13}C allows a straightforward determination of the enrichments. However, the small spectral width inherent to a ^{1}H spectrum (1-10ppm) makes it difficult to distinguish between overlapping frequencies. To overcome the limitations of these two approaches a new sequence, named proton-observed carbon-edited NMR (POCE-NMR), was developed (164). This is a heteronuclear spectral editing method that combines the higher sensitivity of ^{1}H-NMR with the higher specificity of ^{13}C by providing a final spectrum in which only the ^{1}H signals bonded to ^{13}C are shown (see section 3 for details) (165). POCE-NMR has been used in several experiments assuming an important role in the improvement of ^{13}C -enrichment analysis (166).

The work presented in this dissertation was conducted to achieve 3 main goals: 1) to study the tissue-specific metabolic flexibility in awake and unrestrained rats by determining V_{PDH}/V_{TCA} under basal (overnight fast) and insulin stimulated (hyperinsulinemic-euglycemic clamp) conditions in liver, heart and soleus muscle; 2) to assess the impact of insulin resistance on the development of metabolic inflexibility in animals subjected to a 3-week period of high fat feeding; 3) to explore possible mechanisms of regulation of V_{PDH}/V_{TCA} by manipulating plasma concentrations of glucose and FFA.

3. Methods

3.1. Animals

All experiments were conducted in accordance with the National Institutes of Health Guidelines for the Care and Use of Laboratory Animals and all protocols were approved by the Yale Animal Care and Use Committee. Male Sprague Dawley rats (Charles River), weighting 300-350g, were housed in an environmentally controlled room with a 12h light/dark cycle and free access to water and food. Animals were fed either with a low-fat diet - Purina 5008 chow: 60% carbohydrates, 10% fat and 30% protein calories (Ralston-Purina, St. Louis, MO) – or with a high fat diet – TD.97070: 21% carbohydrates, 60% saturated fat and 19% protein calories (Harlan Teklad, Madison, WI) for a 3 weeks period. One week before the end of the study, an internal jugular catheter and a carotid artery catheter were implanted and externalized through a skin incision at the back of the head as previously described (167). Essentially, rats were anesthetized and two catheters were placed in order to allow the infusion experiments to occur in the awake state. One catheter, for blood sampling, was inserted in the jugular vein while the second catheter, used as the infusion line, was inserted in the left carotid. These catheters were sealed and externalized through a skin incision in the back of the neck. Before the experiment the catheters were opened by flushing a saline/heparin solution.

3.2. Infusion experiments

As was presented in section 2, the primary goal of these experiments was to assess the effect of insulin on V_{PDH}/V_{TCA}. To achieve that, animals from each diet were divided, after an overnight fast, into two groups (6-8 animals *per* group). Fasting V_{PDH}/V_{TCA} was studied during an infusion of 99% [1-^{13}C]glucose for a 2h period at a rate of 1 mg/Kg/min. This represents 15% of the rate of glucose uptake by muscle and was chosen to avoid endogenous release of insulin stimulated by eventual increases of glucose concentration in plasma. The effect of insulin stimulation on V_{PDH}/V_{TCA} was assessed during a hyperinsulinemic-euglycemic clamp, the gold standard technique to study glucose

metabolism (168). In this experimental setup a continuous infusion of human insulin (Humulin; Eli Lilly, Indianapolis, IN) for 2h at a rate of 4mU/kg/min was used to raise plasma insulin concentrations to postprandial levels. At the same time a variable infusion of 25% [1-^{13}C]glucose/20% of dextrose was used to maintain glucose at 100-110 mg/dL. In these experiments, the rates of glucose infusion are dependent on the glucose uptake by the periphery and therefore an indication of the whole body insulin sensitivity.

The regulation of PDH was further studied by modulating plasma substrate concentrations. The effect of plasma glucose concentrations on V_{PDH}/V_{TCA} in animals fed with low-fat or high-fat diet was assessed during a hyperinsulinemic-hyperglycemic clamp. Plasma glucose levels were maintained at 200mg/dL using a variable infusion of 25% [1-^{13}C]glucose/20% dextrose. In a group of low-fat fed animals, fatty acid levels were manipulated instead to keep fasting levels of FFA unchanged during insulin-stimulation. For that, a simultaneous infusion of a TG emulsion (Lyposin II 20%) plus heparin at a rate of 5.56µL/min/Kg was used during the hyperinsulinemic-euglycemic clamp.

Blood samples were taken every 15 min to estimate plasma glucose concentration and adjust the rates of glucose infusion. The remaining plasma was used to determine [1-^{13}C]glucose enrichments, insulin and FFA concentrations. At the end of the experiments, animals were euthanized with sodium pentobarbital and the tissues quickly excised in the following order: soleus, liver and heart. Each tissue was frozen immediately using liquid N_2-cooled aluminium blocks and stored at -80ºC until further analysis.

3.3. Model assumptions and calculation of V_{PDH}/V_{TCA}

Once in the cells, [1-^{13}C]glucose is metabolized to [3-^{13}C]pyruvate in the glycolytic pathway. Through the action of PDH, it is then converted to [2-^{13}C]acetyl-CoA and shuttled into the TCA cycle where, through a series of reactions, forms α-[4-^{13}C]ketoglutarate. This metabolite, in equilibrium with its isotopic equivalent pool ([4-^{13}C]glutamate), can then be used to regenerate oxaloacetate (Figure 10).

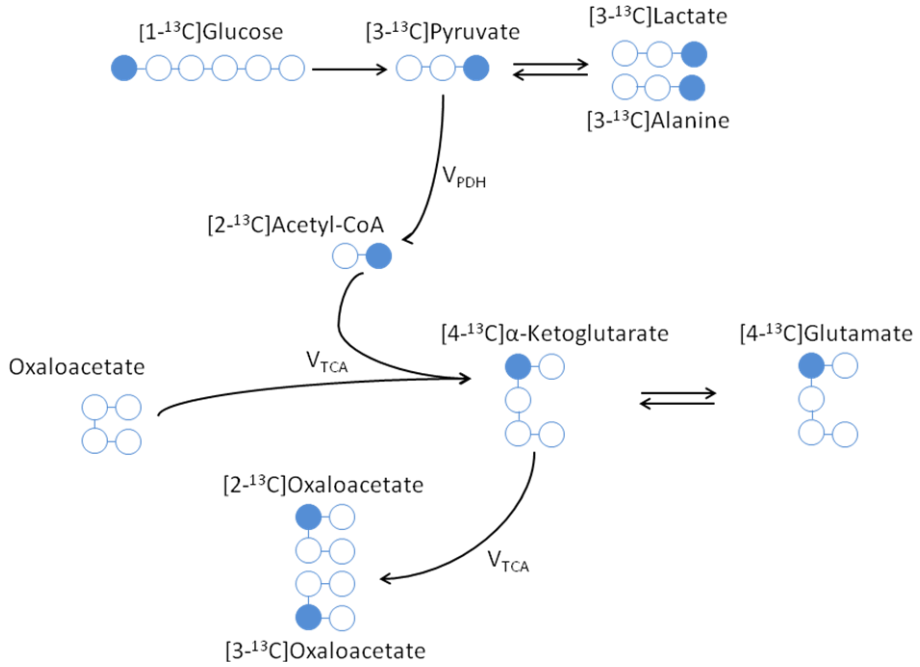

Figure 10 Schematic of metabolite labeling pattern following [1-^{13}C]glucose infusion. V_{PDH} and V_{TCA} represent the fluxes through pyruvate dehydrogenase (PDH) and tricarboxylic acid cycle (TCA), respectively.

As previously shown by Shulman *et al* (162) the ratio of [2-^{13}C]acetyl-CoA to [3-^{13}C]pyruvate equals V_{PDH}/V_{TCA} at steady state (Appendix A). However the small size of these two pools difficult their analysis by NMR. Therefore, the following assumptions must be made: 1) since glucose is the only source of labeling, the enrichment of [4-^{13}C]glutamate can be used as a surrogate of [2-^{13}C]acetyl-CoA; 2) due to the fast exchange between lactate, alanine and pyruvate, [3-^{13}C]alanine can be used as a surrogate of [3-^{13}C]pyruvate enrichment at steady state. Therefore the relative contribution of glucose oxidation to TCA cycle flux can be calculated using equation 1.

$$\frac{V_{PDH}}{V_{TCA}} = \frac{[4\text{-}^{13}\text{C}]\text{Glutamate}}{[3\text{-}^{13}\text{C}]\text{Alanine}} \qquad \textit{(Equation 1)}$$

3.4. NMR analysis

Spectra from tissue extracts were recorded using a Bruker 5-mm broadband NMR probe in an 11.7-T vertical magnet. Enrichments of alanine, lactate and glutamate were determined by POCE-NMR (169). This methodology requires the realization of two different experiments stored separately (Figure 11).

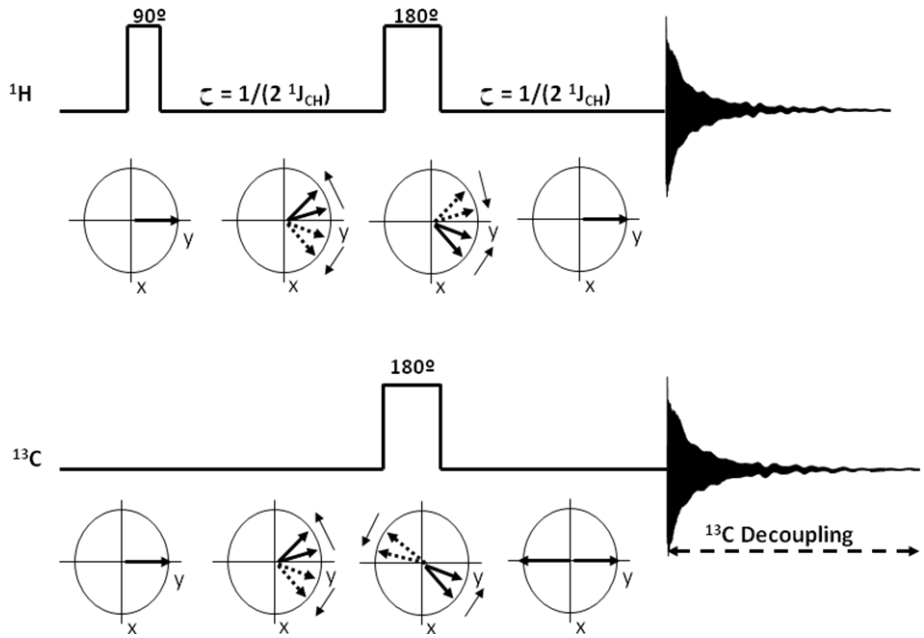

Figure 11 Pulse sequence for a proton-observe carbon-edited (POCE)-NMR experiment and its effect on the phase of spins.

On the first experiment (**S1**) a 90º pulse is used to excite all the protons present in the sample. When the excitation power is turned off the proton magnetization starts dephasing. At the end of half of the echo time (TE/2) a 180º pulse is applied reversing the direction of the magnetization evolution, along the XY plane, so that the frequencies are refocused at the end of the echo time. On a second experiment (**S2**) the sequence is modified to include a nonselective 180º pulse on the ^{13}C channel during the proton refocusing pulse. When TE is chosen as $1/J_{13C\text{-}H}$, where $J_{13C\text{-}H}$ is the heteronuclear scalar coupling constant (125-140Hz), the proton resonances from the ^{13}C-labeled metabolites appear inverted relative to the proton resonances attached to ^{12}C-nuclei. The difference of

the two spectra obtained from these two experiments represents the protons directly bound to ^{13}C. The atom percent excess (APE) for each of the metabolites of interest was calculated according to equation 2.

$$APE = \frac{\mathbf{S2}/2}{\mathbf{S1}} \times 100 - 1.1\% \qquad \textit{(Equation 2)}$$

Water signal was suppressed by a series of six 20 ms adiabatic full passage pulses and 1ms magnetic field crusher gradients were applied. Also, a composite decoupling pulse was used during the acquisition to collapse satellite resonances into single lines. The free induction decay (FID) obtained (under fully relaxed conditions, with a repetition time of 10s) were subjected to an exponential multiplication of 1.0 Hz before the fourier transformation and phase corrected manually. The areas of interest were quantified using NUTS software.

3.5. Analytical methods

Plasma glucose was quantified during the infusion experiments by a glucose oxidase method on a Beckman glucose analyzer II (Beckman). Plasma [1-^{13}C]glucose enrichment was determined, after derivatisation, by GC/MS as previously described (170). Insulin circulating levels were measured using double-antibody RIA kits (Linco, St. Louis, MO). Plasma concentrations of FFA were measured using an enzymatic kit (Roche Diagnostics, Mannheim, Germany). Tissue extractions were performed using perchloric acid 7% followed by neutralization of the supernatant with KOH. The salt formed ($KClO_4$) was spin-down and the supernatant lyophilized and ressuspended in 50 mM KH_2PO_4 buffer containing 50% of D_2O.

3.6. Insulin signalling

3.6.1. Akt/PKB activity

Insulin signaling was determined by measuring Akt/PKB activity in protein extracts using the Akt/PKB Kinase Activity Assay Kit (Assay Designs, MI, USA) and the protocol

provided by the supplier. Shortly, the assay was performed in 96-well plates coated with a specific synthetic peptide as substrate for Akt/PKB. In each well, the substrate was incubated with ~100mg of protein from homogenized tissue and the reaction was initiated with the addition of ATP. A primary polyclonal antibody was used to recognize the phosphorylated form of the substrate. The phosphorylated substrate was quantified using a secondary antibody conjugated with a horseradish peroxidase. Absorbance was read at 450nm.

3.6.2. Akt/PKB phosphorylation

Phosphorilation of serine 473 residue of Akt/PKB is essential for its activity. The phosphorilation levels of this enzyme were detected by western blot analysis after separating 50µg of total protein lysate on a 4–12% tris-glycine gel (Invitrogen) and transferring to a polyvinylidene difluoride membrane (Immobilon-P 0.45 µm, Millipore). Primary antibodies anti-phospho-Akt(Ser473) and anti-Akt (Cell Signaling), as well as the secondary antibodies anti-rabbit (Sigma) were used in a BSA 5% solution (dilution 1/1000). The intensity of the bands obtained was quantified using ImageJ software.

3.7. Glycogen concentration

Tissues were treated with perchloric acid 0.6N followed by neutralization with KOH. A sample of this extract was taken to measure free glucose and the remaining was incubated with acetate buffer, 0.40M, pH4.8, containing 2mg/mL of amyloglucosidase (Sigma, Aldrich) for 3h at 37ºC. Glycogen concentration was given by the difference between the amount of glucose hydrolysed by the incubation with amyloglucosidase and the amount of free glucose before the digestion.

3.8. Extraction of DAG and TG

The extraction procedure for DAG species was performed as described previously (153). Between 50 to 100 mg of liver tissue were homogenized in ice-cold

chloroform/methanol (2:1 v/v) containing 0.01% butylated hydroxytoluene and the internal standards 1,3-dipentadecanoin and 1,2,3-triheptadecanoate. Organic and aqueous phases were separated by adding chloroform and H_2O. After centrifugation, the organic layer was collected, dried under nitrogen flow, and reconstituted with hexane/methylene chloride/ether (89/10/1 v/v/v). DAG were separated from TG with preconditioned columns (waters Sep Pak Cartridge WAT020845) and eluted with hexane/ethyl acetate (85/15 v/v) under a low negative pressure. Lipid metabolite extracts were subjected to LC/MS/MS analysis. A heated nebulizer source in positive mode was interfaced with an API 3000 tandem mass spectrometer (Applied Biosystems) in conjunction with a Shimadzu Prominence HPLC System (Shimadzu). Total DAG content was expressed as the sum of individual species. For muscle samples, the distinction between cytosolic and membrane fractions is necessary. Therefore, 50-100 mg of heart/soleus were homogenized in a buffer containing 20 mM Tris-HCl, pH 7.4; 1 mM EDTA; 0.25 mM EGTA; 250 mM sucrose; 2 mM phenylmethanesulfonyl fluoride; and protease inhibitor cocktail (Roche). Samples were then centrifuged at 172000**g** at 4°C for 1 hour. The resultant supernatants were considered the cytosolic fractions while the pellets were considered the membrane fractions. The membrane fractions were resuspended in the same buffer and sonicated for 30s. The extraction and quantification of DAG from each fraction was performed as described above.

TG were extracted from frozen tissue with chloroform/methanol (2:1, v/v). Tissues were homogenized in this mixture for 30s and shaken at room temperature for 4h. At the end samples were centrifuged and the bottom layer was collected and dried under N_2 flow. The samples were reconstituted in chloroform and quantified using an enzymatic kit (Roche). This assay relies on the hydrolysis of TG, by lipoprotein lipase, and quantification of the glycerol formed. Glycerol is first phosphorylated by glycerol kinase and then oxidised by glycerol phosphate oxidase producing dihydroxyacetone phosphate and hydrogen peroxide. Lastly, hydrogen peroxide is used to reduce 4-aminoantipyrine in a reaction catalysed by peroxidase. The product formed, N-Ethyl-N-(3-sulfopropyl)-*m*-anisidine, can be quantified by measuring the absorbance at 540nm.

3.9. Statistical analysis

All data are reported as means ± SE. Unpaired two-tailed Student's *t* tests were used for comparisons between groups. All differences were considered statistically significant at $P<0.05$.

4. Results & Discussion

4.1. Hepatic substrate selection

4.1.1. V_{PDH}/V_{TCA} in insulin-sensitive conditions

In order to assess the influence of insulin on tissue-specific V_{PDH}/V_{TCA}, two groups of low-fat fed animals with similar initial plasma concentrations of glucose (Figure 12A) and insulin (Figure 12B) were used. In the first group, the basal infusion of [1-^{13}C]glucose did not affect plasma concentrations of glucose during the time course of infusion while it was successfully clamped between 90-110 mg/dL in the group subjected to a hyperinsulinemic-euglycemic clamp (Figure 12C). In this group, plasma concentration of insulin was significantly raised from low fasting levels to concentrations observed in a postprandial state (Figure 12D).

At the end of these infusions the POCE-NMR technique was used to determine the ^{13}C-enrichment of alanine, lactate and glutamate present in liver extracts (Figure 13) to assess the influence of fasting and insulin stimulation on V_{PDH}/V_{TCA}.

An important assumption of our model is the use of [3-^{13}C]alanine as a surrogate of [3-^{13}C]pyruvate enrichment. For such assumption to be valid, isotopic steady-state must be achieved. As can be seen in table 2, the enrichments of [3-^{13}C]lactate and [3-^{13}C]alanine were similar in both fasting and insulin stimulating experiments which indicates that the time length of the infusions was adequate to achieve a complete isotopic equilibrium. Under fasting conditions the fraction of glycolytic flux supported by plasma glucose was ~10% while it was increased by 2-fold in the presence of high circulating levels of insulin (Table 2).

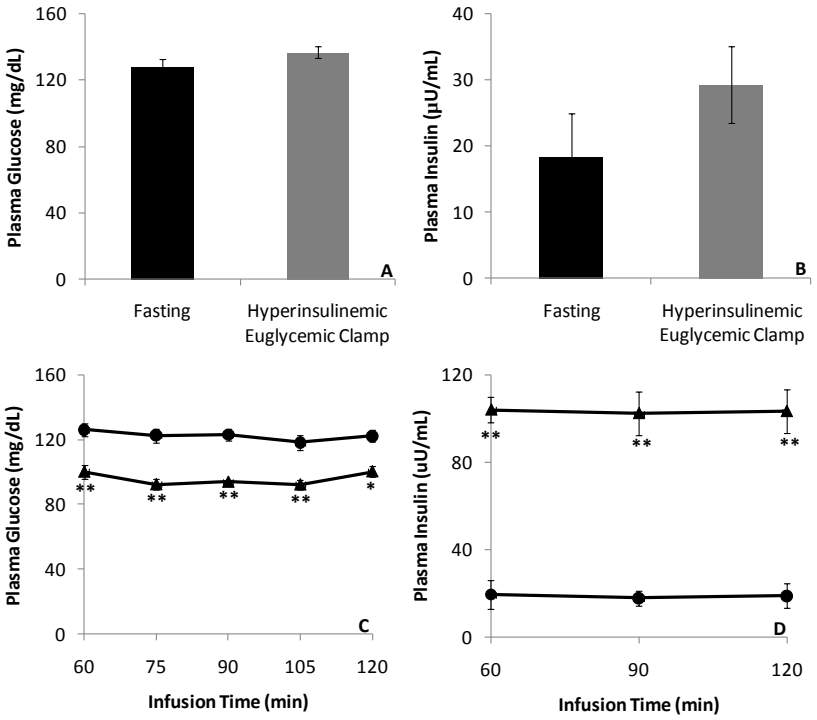

Figure 12 Fasting plasma concentrations of glucose (A) and insulin (B). Plasma concentration of glucose (C) and insulin (D) during the last hour of basal infusion of [1-^{13}C]glucose (●) and hyperglycemic-euglycemic clamp (▲), performed in low fat-fed animals. *P<0.005, **P<0.0005 *versus* fasting.

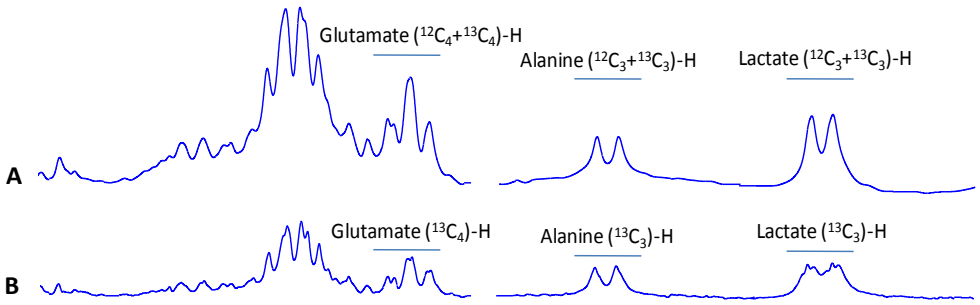

Figure 13 Representative spectra from POCE-NMR analysis of liver extracts. The spectrum in (A) is the result of the proton signals attached to both ^{12}C and ^{13}C whereas (B) contains only the proton signals attached to ^{13}C (result of the difference between (a) and (^{13}C-H)-inverted spectrum (not shown).

Table 2 Fraction of glycolytic flux supported by plasma glucose measured as the ratio of [3-^{13}C]lactate and [3-^{13}C]alanine to [1-^{13}C]glucose in livers from low-fat fed animals during fasting and hyperinsulinemic-euglycemic clamp.

		[3-^{13}C]lactate / [1-^{13}C]glucose	**[3-^{13}C]alanine / [1-^{13}C]glucose**
Low-fat diet	*Fasting*	12.8 ± 1.1%	10.2 ± 1.3%
	Hyperinsulinemic-euglycemic clamp	20.0 ± 1.1%**	17.6 ± 1.2%*

*P<0.001, **P<0.0005 *versus* Fasting

The observed increase of lactate and alanine enrichments during the hyperinsulinemic euglycemic clamp is likely linked to an increase in glycolysis stimulated by the insulin. When these and the [4-^{13}C]glutamate enrichments were applied in equation 1, it was possible to determine that, in the fasting state, PDH flux contributed with 17.1±1.5% to the total TCA cycle flux revealing a high dependence on fatty acid oxidation. Unexpectedly, during the hyperinsulinemic-euglycemic clamp no increase was observed in the V_{PDH}/V_{TCA} - 19.0±3.2% (Figure 14).

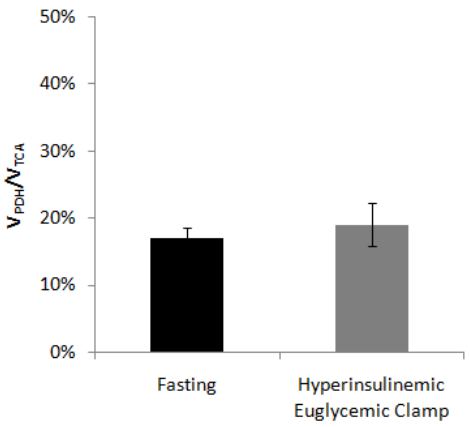

Figure 14 Hepatic contribution of PDH flux (V_{PDH}) to total TCA cycle flux (V_{TCA}) in low-fat fed rats during fasting and hyperinsulinemic-euglycemic clamp.

PDH plays a crucial role determining the fate of pyruvate in liver. Inhibition of PDH during fasting allows pyruvate to be directed towards gluconeogenesis in order to maintain constant concentrations of glucose in plasma. High intramitochondrial acetyl-CoA/CoA and

$NADH/NAD^+$ ratios are known to inhibit PDH complex through allosteric action on the enzymatic complex and through the activation of the PDK enzyme (122, 171). For this reason oxidation of fatty acids is a major factor that determines the extent of inhibition of the PDH complex. In fact, palmitate has been shown to inhibit glucose oxidation and glycolysis in hepatocytes (172, 173). This is particularly relevant to avoid futile oxidation of pyruvate supporting, at the same time, the necessary gluconeogenic flux. This dependence of gluconeogenesis on β-oxidation has been shown in many studies. By injecting very-low-density lipoproteins (VLDL) containing labeled fatty acids Moir *et al* showed that, in awake and unrestrained rats, the β-oxidation flux after a 24h fast is twice as high as in the fed state (62). Reduction of plasma FFA, by administration of nicotinic acid (174) and inhibition of CPT-1 (175), promoted reduced gluconeogenic fluxes and concomitantly decreases in plasma glucose concentration. Therefore, a small contribution of glucose oxidation to TCA cycle was expected after an overnight fasting due to the higher reliance on fatty acid oxidation that characterizes this state. This result, a fasting V_{PDH}/V_{TCA} of 17.1±1.5%, is also further supported from a study performed by Kaempfer *et al* in which the sampling of cytosolic acetyl-CoA with a xenobiotic probe (acetylated sulfamethoxazole) revealed that in fasting only 20% of acetyl-CoA is originated from glucose oxidation (176).

In vivo studies have shown that insulin is able to shift fatty acid metabolism from oxidation to esterification (62, 177). In parallel, insulin is known to increase the percentage of active PDH (178). However, the results reported here, showed for the first time that the *in vivo* contribution of PDH flux to TCA cycle during the hyperinsulinemic-euglycemic clamp was not changed compared to an overnight fast. These reveal an unexpected ineffectiveness of insulin to switch, *per se,* the relative contributions of the major oxidative substrates. Insulin concentrations similar to those reported here have also been reported to fail to reduce hepatic gluconeogenic flux in humans (179, 180). This inability to inhibit gluconeogenic activity can be responsible for the consumption of pyruvate that becomes unavailable for oxidation even under insulin stimulating conditions.

4.1.2. V_{PDH}/V_{TCA} in insulin-resistant conditions

The effects of a chronic exposure to fatty acids on hepatic substrate selection were assessed after a 3 week feeding period with a high-fat content diet. At the end of this

period, animals were subjected to either a basal infusion of [1-^{13}C]glucose or a hyperinsulinemic-euglycemic clamp and the results were compared with the respective low-fat fed groups. High-fat feeding promoted fasting hyperglycemia (Figure 15A), typically seen in insulin resistant animals (131.8±3.5 mg/dL *versus* 145.1±4.6 mg/dL, $P<0.05$). Paralleled to this, fasting levels of insulin were also increased in the high-fat diet fed animals (Figure 15B). In the animals subjected to the hyperinsulinemic-euglycemic clamp, for the same plasma concentrations of glucose (Figure 15C), the rate of glucose infusion in the high-fat fed group was smaller when compared with the control group – from 28.3±3.5mg/dL to 7.5±1.4mg/dL, $P<0.005$, indicating severe whole-body insulin resistance (Figure 15D).

The same whole body insulin resistance was also observed in liver. High fat diet is known to induce hepatic insulin resistance in just 3 days (150) due to the intracellular accumulation of DAG (149, 181). After a 3-week period of high-fat feeding a trend for higher intracellular concentrations of TG was observed (Figure 16A) while the total level of DAG was significantly increased (Figure 16B). As a consequence, the insulin stimulated activity of Akt/PKB was decreased by 25% after the 3-week feeding period (Figure 16C).

Due to the development of hepatic insulin resistance, changes in the liver metabolism were expected. In fact, NMR analysis of liver extracts revealed decreased fasting enrichments of [3-^{13}C]lactate compared to those obtained for the low-fat fed animals (Table 3). During insulin stimulation, contrary to what happened in the low-fat fed animals, there was no increase in the glycolytic flux supported by glucose extracted from plasma stimulated by insulin, supporting the idea of an insulin resistance state shown in figure 16C.

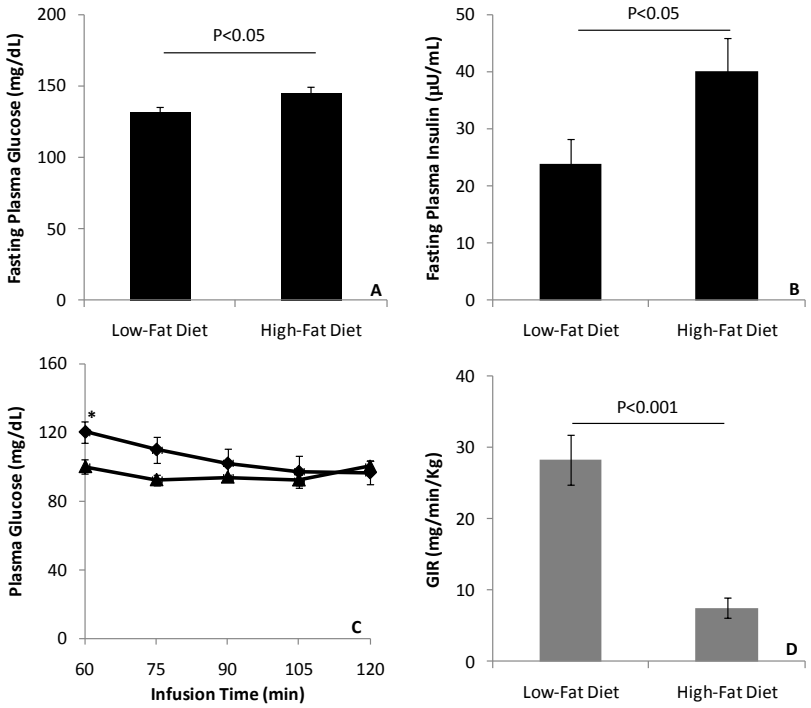

Figure 15 Effect of high-fat diet on fasting plasma concentrations of glucose (A) and insulin (B). Plasma glucose concentrations during the last hour of the hyperinsulinemic-euglycemic clamp performed on low-fat fed (▲) and high-fat fed (◆) animals (C) and respective glucose infusion rates (GIR) necessary to maintain euglycemia (D). *P<0.05 *versus* low-fat diet group.

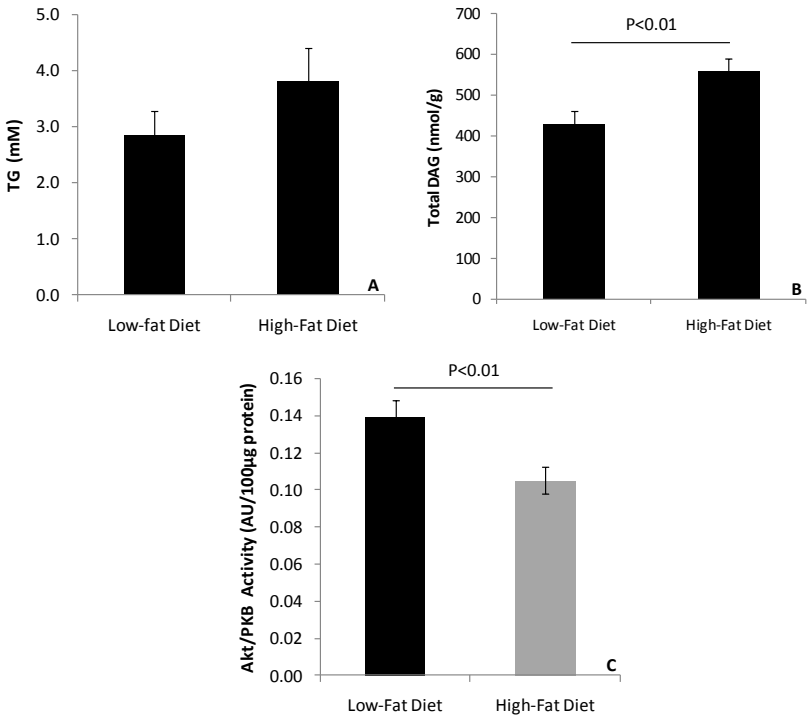

Figure 16 Effect of high-fat diet on hepatic fasting concentrations of triglycerides (TG) (A), total diacylglycerol (DAG) (B) and consequent impact on total insulin stimulated Akt/PKB activity (C).

Table 3 Fraction of glycolytic flux supported by plasma glucose measured as the ratio of [3-^{13}C]lactate and [3-^{13}C]alanine to [1-^{13}C]glucose in livers from low-fat and high-fat fed animals during fasting and hyperinsulinemic-euglycemic clamp.

		[3-^{13}C]lactate / [1-^{13}C]glucose	**[3-^{13}C]alanine / [1-^{13}C]glucose**
Low-fat diet	*Fasting*	12.8 ± 1.1%	10.2 ± 1.3%
	Hyperinsulinemic-euglycemic clamp	20.0 ± 1.1%**	17.6 ± 1.2%*
High-fat diet	*Fasting*	7.5 ± 0.5%‡	10.6 ± 2.2%
	Hyperinsulinemic-euglycemic clamp	6.1 ± 1.4%‡‡	5.4 ± 2.0%‡

*P<0.001, **P<0.0005 *versus* Fasting
‡P<0.005, ‡‡P<0.00005 *versus* Low-fat diet

By plugging the enrichments from table 3, and those calculated for [4-^{13}C]glutamate, into equation 1 it was possible to determine the influence on insulin resistance on V_{PDH}/V_{TCA}. Livers from high-fat fed animals showed a fasting V_{PDH}/V_{TCA} of 1.3±0.7% which

represents a ~90% reduction from what was calculated for the low-fat fed animals (P<0.00001). The presence of high levels of circulating insulin after chronic exposure to fatty acids was again unable to increase V_{PDH}/V_{TCA} from the fasting values – 4.0±3.5% (Figure 17).

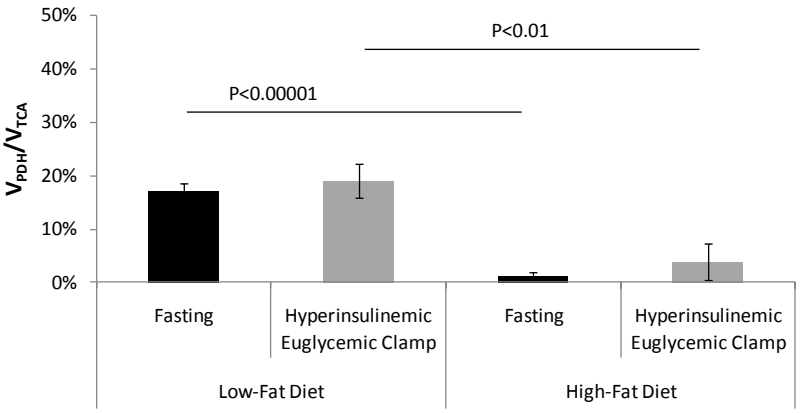

Figure 17 Hepatic contribution of PDH flux (V_{PDH}) to total TCA cycle flux (V_{TCA}) in low-fat and high-fat fed rats during fasting and hyperinsulinemic-euglycemic clamp.

The results of hepatic V_{PDH}/V_{TCA} under insulin-sensitive and insulin-resistant states clearly showed which oxidative substrate is mainly used by liver. A ~80% dependence on fatty acid oxidation, aggravated by high fat feeding, demonstrated that fatty acids are the most important source of energy in this organ. It also showed, for the first time, that the concept of metabolic flexibility cannot be applied to liver since insulin was infective to change the relative contributions of glucose and fatty acids to TCA cycle flux in both low-fat and high-fat fed animals. Acute action of insulin is very important in the regulation of hepatic metabolism particularly in the suppression of hepatic glucose output (182). However, the acute regulation of oxidative metabolism seems to be largely dependent on substrate concentrations. It has been shown that in hepatocytes, insulin, *per se*, was unable to suppress the conversion of fatty acids into acid-soluble products and ketone bodies. Only in the presence of high concentrations of glucose this conversion was suppressed (183). This suggests that the main mechanism that regulates substrate oxidation in liver is through a substrate-driven mechanism similar to the reversed glucose-fatty acid cycle in which the activation of PDH by pyruvate is essential to the production of malonyl-CoA and inhibition of fatty acid oxidation. This hypothesis was tested with hyperinsulinemic-

hyperglycemic clamps in which plasma glucose was clamped at a value twice as high as in the euglycemic clamp. The results of this experiment will be explored in the section 4.1.4.

The ~90% decrease of V_{PDH}/V_{TCA} observed after chronic exposure to fat was associated with a reduced activity of the insulin signaling pathway. It is known that hepatic insulin resistance is associated with high gluconeogenic fluxes (184) which can have important consequences on liver metabolism. On one side, high gluconeogenic fluxes can remove pyruvate away from PDH re-directing it towards carboxylation (first step of gluconeogenesis). This would lead to a reduction of pyruvate oxidation and of V_{PDH}/V_{TCA}. On the other side, the high rates of fatty acid oxidation lead to increased intramitochondrial concentrations of acetyl-CoA and consequent reduced flux through PDH (122). However other mechanisms, related to the ability of insulin to regulate the expression of genes associated with glucose metabolism, might take place. PDH activity has been reported to decrease by 75% after high-fat diet exposure despite high plasma concentrations of insulin (185). This decrease in PDH activity has been attributed to increases of PDK activity and expression. From the identified isoforms of PDK only PDK2 and PDK4 are highly expressed in liver. The expression of PDK4, in particular, is known to be increased with fasting and in insulin resistant conditions (186-188) while insulin stimulation represses it (189). The mechanism of PDK4 repression by insulin involves the PI3K/PKB pathway and FoxO (190) and in a setting of insulin resistance the stimulation of PDH activity is blunted due to the inability to suppress PDK activity (191). Therefore, the hepatic insulin resistance observed in the livers studied could lead to increased expression of PDK enzymes increasing phosphorilation levels of PDH and inhibiting it.

4.1.3. *In vivo* regulation of V_{PDH}/V_{TCA} by fatty acids

During the hyperinsulinemic-euglycemic clamp experiments, the high circulating concentration of insulin promoted a reduction in the plasma levels of FFA from 0.8±0.1mM in the fasting state to 0.2±0.0mM at the end of the infusion ($P<0.001$). However, in the high-fat fed animals the infusion of insulin was ineffective to reduce plasma FFA concentrations from fasting levels (Figure 18A). Due to the inhibitory effect of fatty acid metabolism on PDH, the high levels of FFA during the hyperinsulinemic-euglycemic clamp in the high-fat fed animals could explain the ~90% decrease of V_{PDH}/V_{TCA}. For that reason,

and to assess if high plasma levels of FFA produce effects similar to what was observed in the chronic exposure to fat, low-fat fed animals received a continuous infusion of TG and heparin to keep FFA levels constant during the hyperinsulinemic-euglycemic clamp (Figure 18A).

The infusion of TG/heparin was able to counteract the drop of plasma FFA concentrations during insulin stimulation (Figure 18A). However these high levels of FFA had no effect on the whole body glucose disposal (Figure 18B). The NMR analysis of the extracts revealed a 50% reduction of glycolysis supported by plasma glucose to values similar to those obtained during fasting (Table 4).

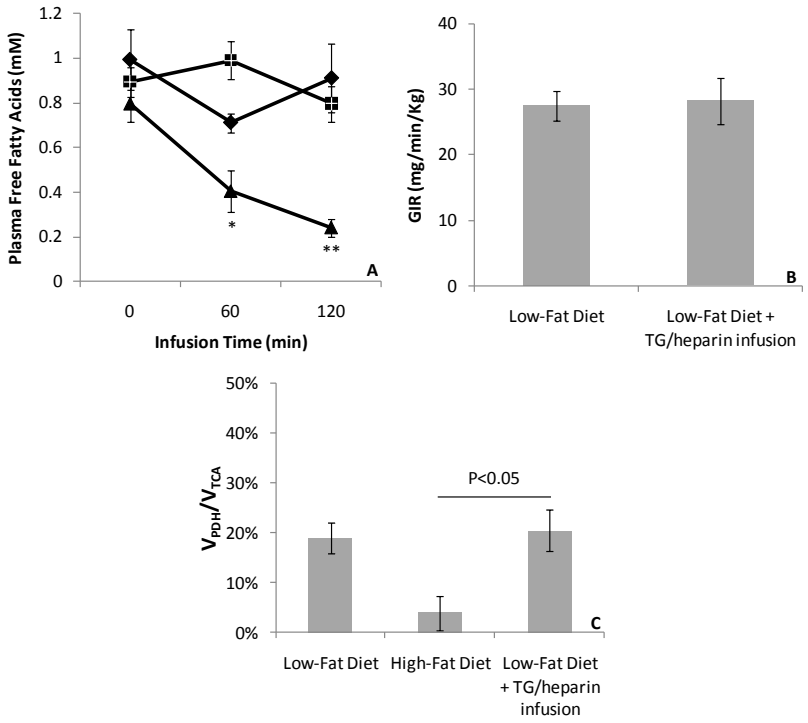

Figure 18 Plasma concentration of free fatty acids (FFA) during the hyperinsulinemic-euglycemic clamp experiments performed in low-fat fed (▲), high-fat fed animals (◆) and during the triglycerides (TG)/heparin infusion (⊞) (A). Effect of sustained plasma levels of FFA on the glucose infusion rate (GIR) (B) and insulin stimulated V_{PDH}/V_{TCA} (C). *P<0.01, **P<0.005 *versus* fasting concentrations.

Table 4 Fraction of glycolytic flux supported by plasma glucose measured as the ratio of [3-^{13}C]lactate and [3-^{13}C]alanine to [1-^{13}C]glucose in livers from low-fat and high-fat fed animals during fasting and hyperinsulinemic-euglycemic clamp.

		[3-^{13}C]lactate / [1-^{13}C]glucose	**[3-^{13}C]alanine / [1-^{13}C]glucose**
Low-fat diet	*Fasting*	12.8 ± 1.1%	10.2 ± 1.3%
	Hyperinsulinemic-euglycemic clamp	20.0 ± 1.1%	17.6 ± 1.2%
	Hyperinsulinemic-euglycemic clamp + TG/heparin	14.2±2.2%*	12.8±1.7%*

*P<0.01 *versus* Hyperinsulinemic-euglycemic clamp

The decrease of alanine and lactate enrichments, observed during the infusion of TG/ heparin, to levels observed in fasting demonstrates the inhibitory effect of fatty acids on glycolysis as shown before (172, 173). It has also been shown that increased plasma concentration of fatty acids reduces insulin clearance by the liver, which can also explain the absence of the insulin effect on these enrichments (192). Regardless of this, V_{PDH}/V_{TCA} was the same as the one obtained without lipid infusion (Figure 18C). The inhibitory effect of fatty acids on glucose metabolism, proposed by Randle *et al* for muscle tissue, has also been shown in isolated hepatocytes (172, 173). Elevated concentrations of FFA, achieved by TG/heparin infusions, have been implicated to affect hepatic glucose metabolism. In humans, using D_2O as tracer for gluconeogenesis, Roden *et al* observed a higher contribution of gluconeogenesis to total endogenous glucose production during a continuous lipid infusion (193)**.** The same conclusions were obtained after manipulation of FFA levels using nicotinic acid (194). However, the effect on glucose oxidation has not been assessed *in vivo*. In the experiments reported here it was shown that the continuous presence of fasting levels of FFA during insulin stimulation had no effect on the V_{PDH}/V_{TCA}. It is possible, however, that the excess of fatty acids in liver were directed to esterification rather than oxidation. The use of a higher rate of TG/heparin infusion could increase plasma concentrations of FFA and eventually increase fatty acid oxidation. Under these conditions an effect on V_{PDH}/V_{TCA} could possibly be observed. However the conclusion to retain from figure 18C is that the high plasma concentrations of FFA were not the responsible factor for the decrease of V_{PDH}/V_{TCA} after high fat feeding. Another mechanism such as increased activity of PDK must take place as proposed before.

4.1.4. *In vivo* regulation of V_{PDH}/V_{TCA} by glucose

Pyruvate is a positive regulator of PDH flux both through activation of PDH and inhibition of PDK activities (122). Therefore, in a different set of experiments, the effect of higher plasma concentration of glucose on V_{PDH}/V_{TCA} was assessed. Higher availability of glucose has the potential to increase glycolysis and, through pyruvate, stimulate the flux through PDH. For these experiments, animals fed with both diets were subjected to a hyperinsulinemic-hyperglycemic clamp. In these experiments, plasma glucose was clamped at 200 mg/dL (Figure 19A). During the last hour of infusion, circulating levels of insulin were significantly higher in the high-fat fed animals relative to the low-fat fed ones suggesting, like before, the development of diet-induced insulin resistance (Figure 19B). This was confirmed by the rates of glucose infusion (Figure 19C) which were significantly reduced in the high-fat fed animals (45.4±3.8 mg/min/Kg *versus* 62.7±2.0 mg/min/Kg in the low-fat fed group, $P<0.005$).

The NMR analysis of liver extracts from low-fat fed animals revealed that the amount of lactate and alanine metabolized from plasma glucose increased ~40% when compared with the values obtained during the euglycemic clamp (Table 5, $P<0.05$). The analysis of livers from the high-fat fed animals showed similar enrichments to the low-fat diet group.

The increase of [3-^{13}C]lactate/[1-^{13}C]glucose and [3-^{13}C]alanine/[1-^{13}C]glucose is associated with increased uptake and metabolization of plasma glucose. The high Km of GLUT2 allows the uptake of glucose when its concentration in plasma is higher than the euglycemic levels. In these clamps, glucose was kept constant at 11mM, therefore, a higher uptake of glucose and mobilization to glycogen synthesis and to glycolysis was expected. It is important to highlight the similar enrichments obtained in the high-fat fed group suggesting that the higher concentration of glucose was able to overcome the reduced glycolytic activity observed before and consequence of the insulin resistance induced by the diet.

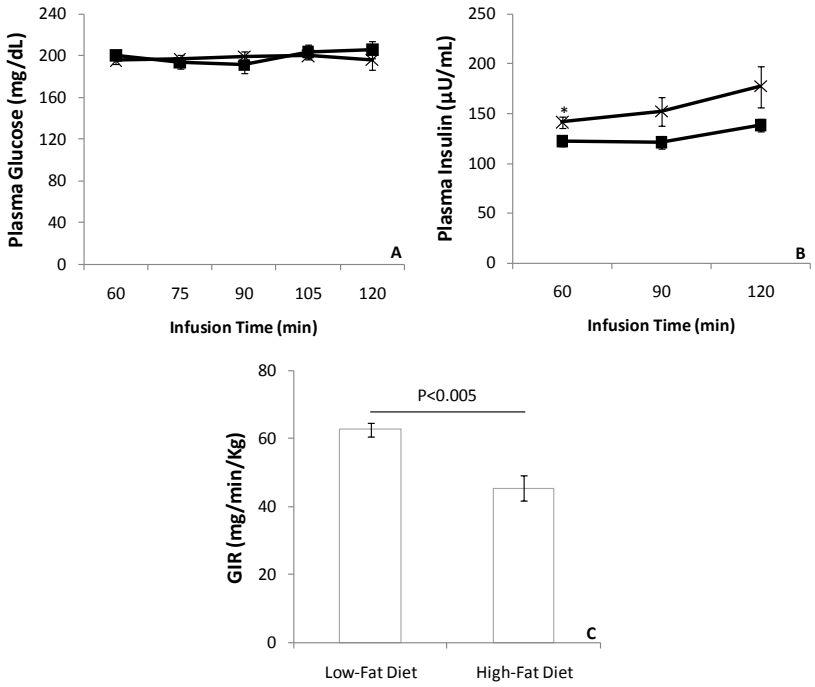

Figure 19 Plasma concentration of glucose (A), insulin (B) and glucose infusion rate (GIR) (C) obtained during the hyperinsulinemic-hyperglycemic clamp experiments performed in low-fat (■) and high-fat (✕) fed animals. *P<0.05 *versus* low-fat diet group.

Table 5 Fraction of hepatic glycolytic flux supported by plasma glucose measured as the ratio of [3-^{13}C]lactate and [3-^{13}C]alanine to [1-^{13}C]glucose in livers from low-fat and high-fat fed animals during hyperinsulinemic-euglycemic clamp and hyperinsulinemic-hyperglycemic clamp.

		[3-^{13}C]Lactate / [1-^{13}C]Glucose	**[3-^{13}C]Alanine / [1-^{13}C]Glucose**
Low-fat diet	*Hyperinsulinemic-euglycemic clamp*	20.0 ± 1.1%	17.6 ± 1.2%
	Hyperinsulinemic-hyperglycemic clamp	31.8 ± 3.6%†	31.4 ± 3.0%††
High-fat diet	*Hyperinsulinemic-euglycemic clamp*	6.1 ± 1.4%	5.4 ± 2.0%
	Hyperinsulinemic-hyperglycemic clamp	27.6 ± 1.3%††	26.8 ± 1.9%††

†P<0.05, ††P<0.005 *versus* Hyperinsulinemic-euglycemic clamp

These enrichments were translated into a V_{PDH}/V_{TCA} of 44.6±3.2%, in the low-fat fed group, representing a 2-fold increase relative to what was obtained in the

hyperinsulinemic-euglycemic clamps (P<0.0001, figure 20). In the high-fat fed group, the higher enrichment of lactate and alanine was also paralleled by a significant increase in V_{PDH}/V_{TCA} relative to the hyperinsulinemic-euglycemic group (12.9±2.6%, P<0.05). However, it was significantly lower than the low-fat fed animals suggesting that the mechanism responsible for the inhibition of PDH flux cannot be overridden by increased levels of substrate (Figure 20). A possible mechanism to explain this strong inhibition is through increased activities and/or expression of PDK2 and PDK4. Even though these activities were not measured an extensive phosphorilation of PDH could severely inhibit the flux through this enzyme.

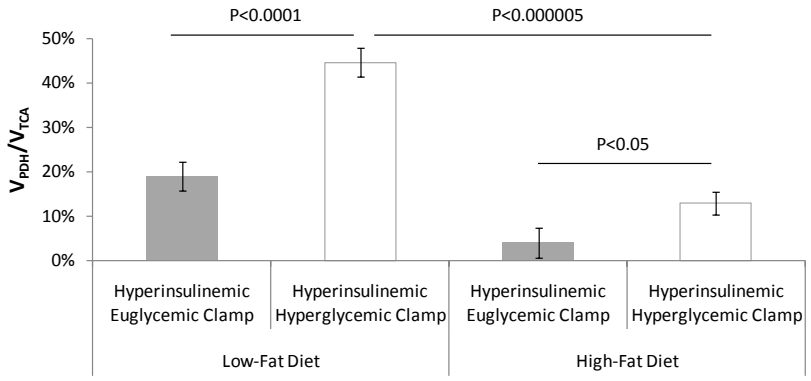

Figure 20 Hepatic contribution of PDH flux (V_{PDH}) to total TCA cycle flux (V_{TCA}) in low-fat and high-fat fed rats during hyperinsulinemic-euglycemic and hyperinsulinemic-hyperglycemic clamps.

From these results important conclusions can be drawn about the regulation mechanisms of PDH flux. Insulin, a traditional positive modulator of PDH activity, was unable to increase V_{PDH}/V_{TCA} even in insulin sensitive animals. Only high concentrations of glucose and insulin were able to increase V_{PDH}/V_{TCA} suggesting that the main mechanism of V_{PDH}/V_{TCA} regulation is substrate-driven. This is a particularly important conclusion since it perfectly fits with the physiological function of liver as an energy storage organ. In the liver, the excess of energy provided by a meal is stored in the form of glycogen and *de novo* synthesized fatty acids. It has been shown, using ^{13}C-NMR, that glycogen synthesis is stimulated by a high glucose load (195). Also, a strong correlation has been established

between glycogen concentrations and PDH activity in liver (196). This suggests that during a glucose load, the increase in plasma glucose stimulates the synthesis of glycogen and as these stores begin to be replenished a fraction of glucose is then consumed through glycolysis leading to the activation of PDH. In fact, in our experiments there was also a strong association between glycogen concentration and V_{PDH}/V_{TCA} (Figure 21). An increase in V_{PDH}/V_{TCA} was only observed when glycogen concentrations were also increased further supporting this idea proposed.

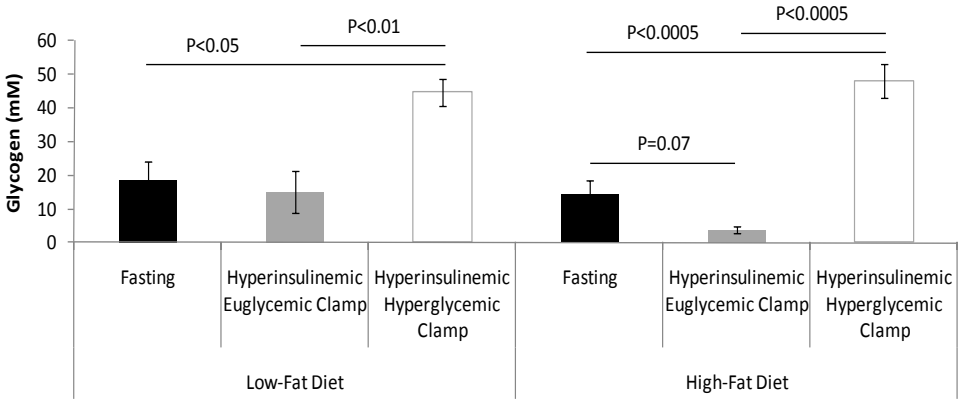

Figure 21 Hepatic concentration of glycogen for low-fat and high-fat diet during fasting and during hyperinsulinemic-euglycemic and hyperinsulinemic-hyperglycemic clamps.

Activation of PDH is relevant since it allows the conversion of glucose into acetyl-CoA that can be used in the *de novo* lipogenesis – a phenomenon observed after a glucose load (49-51). This further supports the hypothesis that PDH flux is regulated by a "substrate-push" mechanism in which higher amounts of glucose in combination with insulin can increase V_{PDH}/V_{TCA} in order to promote *de novo* lipogenesis.

4.2. Heart and skeletal muscle substrate selection

4.2.1. V_{PDH}/V_{TCA} in insulin-sensitive conditions

At the end of the basal and hyperinsulinemic-euglycemic clamp infusions, discussed in figure 12, heart and soleus tissues were extracted and analyzed by POCE-NMR to determine ^{13}C-enrichment of alanine, lactate and glutamate (Figure 22).

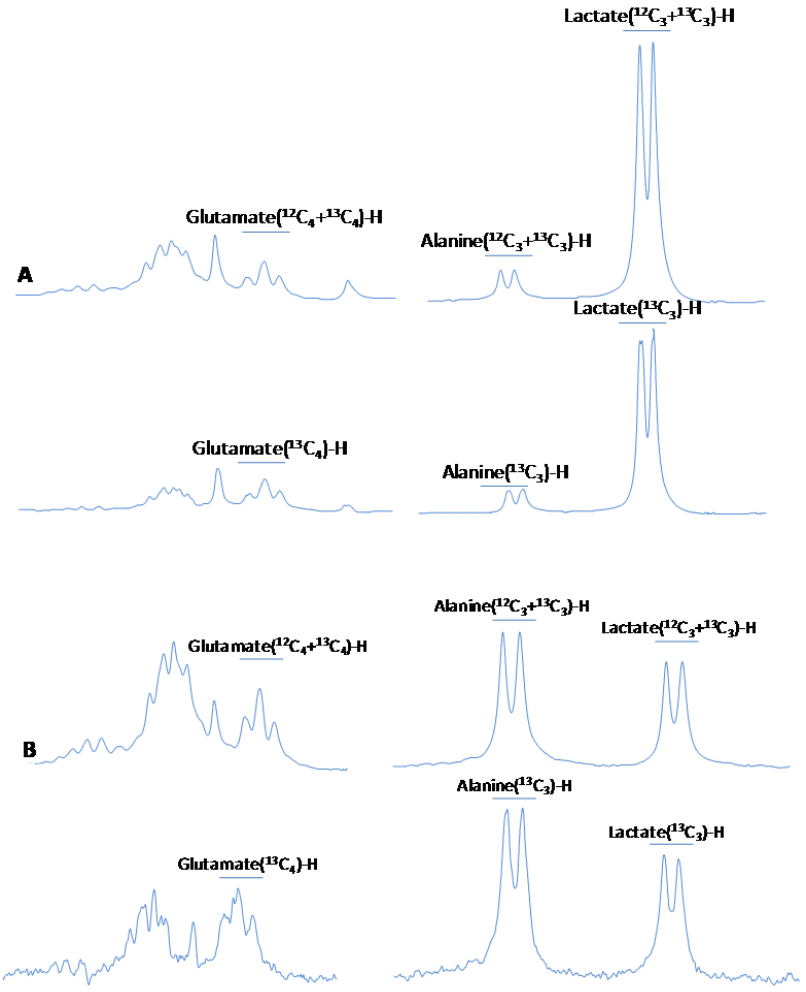

Figure 22 Representative spectra from POCE-NMR analysis of heart (A) and soleus (B) extracts. The first spectrum in A and B is the result of the proton signals attached to both ^{12}C and ^{13}C whereas in the second spectrum only the proton signals attached to ^{13}C are observed.

After extraction, the analysis of [3-^{13}C]lactate and [3-^{13}C]alanine enrichment using POCE-NMR revealed that, in heart, the enrichment of this metabolites in fasting was around 20% and that no change was observed after the hyperinsulinemic-euglycemic clamp (Table 6). On the contrary, in soleus, the fasting lactate and alanine enrichments of ~20% increased to around 35% during the hyperinsulinemic-euglycemic clamp (Table 6).

Table 6 Fraction of glycolytic flux supported by plasma glucose measured as the ratio of [3-^{13}C]lactate and [3-^{13}C]alanine to [1-^{13}C]glucose in heart and soleus from low-fat fed animals during fasting and hyperinsulinemic-euglycemic clamp.

		[3-^{13}C]lactate / [1-^{13}C]glucose	**[3-^{13}C]alanine / [1-^{13}C]glucose**
Heart	*Fasting*	21.8±5.0%	19.7±3.5%
	Hyperinsulinemic-euglycemic clamp	21.4±2.6%	23.3±1.4%
Soleus	*Fasting*	20.4±2.0%	18.2±1.7%
	Hyperinsulinemic-euglycemic clamp	26.0±1.8%*	27.8±2.3%**

*P=0.05, **P<0.01 *versus* Fasting

Interestingly, the relative enrichments of [3-^{13}C]lactate and [3-^{13}C]alanine in heart were not different between fasting and hyperinsulinemic conditions. Insulin is known to stimulate glucose transport as well as glycolysis (197) and an increase in these enrichments was expected. However it has been shown that the activation of PDH is followed by an increase in lactate oxidation (198, 199). Therefore it is possible that the enriched 3-carbon pools were diluted due to a higher uptake of lactate. Nonetheless, when both the alanine and glutamate enrichments were plugged into equation 1, it was possible to determine that, in heart, insulin promoted a ~3-fold increase of V_{PDH}/V_{TCA} from 30.9±2.1% in fasting to 86.1±7.3% during the hyperinsulinemic-euglycemic clamp (P<0.00005, Figure 23). A similar effect was observed in soleus in which insulin promoted a ~2-fold increase of V_{PDH}/V_{TCA} from 29.7±6.6% in fasting to 65.2±5.2% during the hyperinsulinemic-euglycemic clamp (P<0.005, Figure 23).

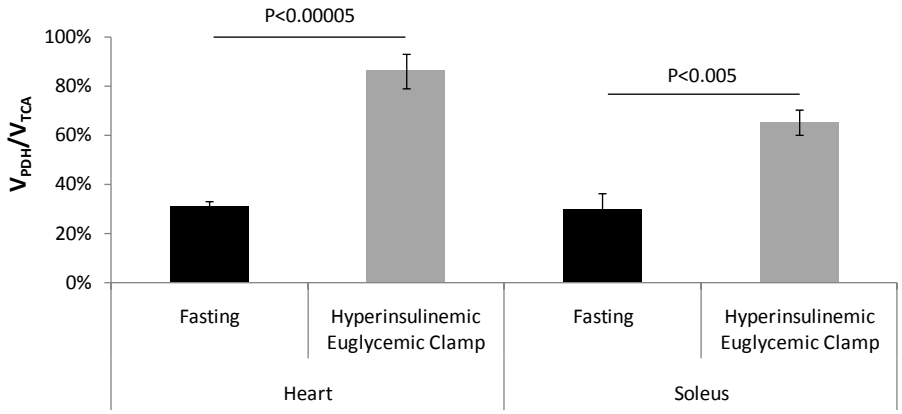

Figure 23 Relative contribution of PDH flux (V_{PDH}) to total TCA cycle flux (V_{TCA}) in heart and soleus muscle of in low-fat fed rats during fasting and hyperinsulinemic-euglycemic clamp.

The idea of skeletal muscle as a tissue able to switch between carbohydrates and fatty acids as its main oxidative substrate is not recent. The first studies that pointed towards this were done in the beginning of last century (reviewed in (200)). In 1927 one of the first studies measuring the arteriovenous balance of O_2 consumed and CO_2 produced across the leg muscle of dogs determined a significant increase of the RQ values between fast and fed states from 0.8 to 0.9, respectively (201)**.** More than 70 years later the same studies applied in the skeletal muscle of humans revealed a similar shift towards glucose oxidation in the presence of insulin (5). This metabolic flexibility proposed by Kelley *et al* to characterize the dynamics of skeletal muscle substrate selection was reproduced in the studies reported here. In two types of muscle, heart and soleus, the fasting preference towards fatty acid oxidation was altered in the presence of insulin during which glucose was the preferred substrate.

Soleus and heart are two examples of high oxidative capacity tissues. Soleus is mainly constituted by type 1 fibers, also known as slow-twitch fibers, which are characterized by high capillary density, high myoglobin content and high mitochondrial density endowing this muscle with a high oxidative capacity (38). The oxidative preference of skeletal muscle during fasting is towards fatty acids. The RQ values during this state vary between 0.80 and 0.85 which is the equivalent to 50% contribution of fatty acids to total oxidative metabolism (38). In the studies reported here the fasting reliance on fatty acids in soleus is

even higher (~70%) a probable consequence of tissue specific analysis instead of a RQ value that results from several muscle groups with different fiber type composition.

In heart, due to its continuous activity, the demand for energy is high: 35Kg of ATP are produced *per* day which represents 10,000 times the total amount of ATP it is able to store (202). To meet these extremely high energy requirements heart is able to oxidize a variety of substrates ranging from glucose and fatty acids – the major substrates – to lactate, ketone bodies and amino acids. It is also characterized by a high flexibility since it can switch between these substrates in order to oxidize the most efficiently one for a given stimulus. Some of these stimuli include substrate availability, oxygen supply, circulating hormones and cardiac work load (203). Cardiac substrate selection is strongly linked to the circulating concentrations of each metabolite. During fetal life the main substrate is lactate (204). However, after birth, plasma concentrations of lactate drop while fatty acids availability increase switching its preference towards fatty acid oxidation (205). In fact, this tendency remains constant throughout the adult life with the contribution of glucose to TCA cycle varying between 0% and 40% (206-208). Thus, the V_{PDH}/V_{TCA} of 30% reported here fits with what has been described in literature confirming the higher reliance on fatty acid oxidation in a resting and fasted state. The main source of fatty acids to be metabolized by muscle comes from plasma through the hydrolysis of TGs by LPL (209). Once inside the cell, fatty acids serve as ligands for the peroxisome proliferator-activated receptor α (PPARα) promoting, in both heart and skeletal muscle, the upregulation of genes involved in the mitochondrial β-oxidation (acyl-CoA dehydrogenase, 3-ketoacyl-CoA thiolases, acyl-CoA oxidase), in the transport of fatty acids and other enzymes such as CPT-1 and malonyl-CoA decarboxylase (MCD) (210, 211).

In the presence of insulin important changes occur at the level of glucose metabolism. Glucose uptake is stimulated by insulin through the activation of PI3K pathway and consequent translocation of glucose transporter GLUT4 to the plasma membrane (197). Paralleled to this, heart perfusion studies have shown that insulin also stimulates glycolysis (212), glucose oxidation (213) and the translocation of FAT/CD36, to the plasma membrane promoting their uptake and esterification (44). However this was the first time, to the best of our knowledge, that a study performed *in vivo* showed an almost total reliance on glucose oxidation during insulin stimulation. This confirms the high capacity of heart to choose the best substrate in each situation. Fatty acids are a more energy-efficient

substrate than glucose, i.e., for each mole of CO_2 produced by oxidation of these two fuels, more energy is produced oxidizing fatty acids than glucose. For this reason, during fasting, when glucose is scarce and must be spared for brain metabolism, fatty acids are naturally the chosen substrate for oxidation. However, glucose is more energy-efficient than fatty acids, i.e., for each mole of oxygen consumed glucose produces more energy than fatty acids. Therefore, in times of glucose abundance, it becomes the major substrate sparing fatty acids.

4.2.2. V_{PDH}/V_{TCA} in insulin-resistant conditions

An extensive body of literature have shown that a mismatch between fatty acid uptake and oxidation leads to the accumulation of lipid species, in particular TG and DAG, and consequent development of insulin resistance in heart (214) and skeletal muscle (138). As demonstrated before, insulin resistance has been linked with the loss of metabolic flexibility in skeletal muscle (28). Therefore, eventual changes in the metabolically flexible pattern shown in figure 23 were assessed in heart and soleus muscle after a chronic exposure to fatty acids. In heart, the result of this high-fat feeding period was a ~2-fold increase in fasting TG content from 0.5±0.2mM to 1.1±0.1mM in the high-fat fed animals ($P<0.05$, Figure 24A). Parallel to this, an increase in DAG concentration in the membrane fraction was observed (Figure 24B). Consequently, serine-phosphorylation of Akt was significantly reduced in the high-fat fed animals after 20min of insulin stimulation showing the existence of cardiac insulin resistance (Figure 24C).

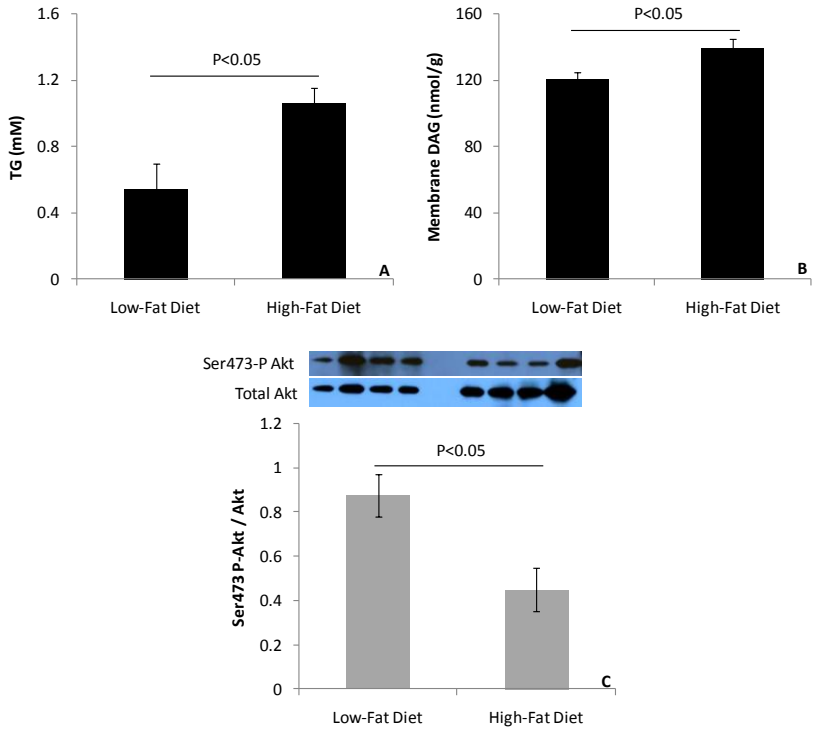

Figure 24 Effect of high-fat diet on cardiac intracellular concentration of triglycerides (TG) (A), diacylglycerol (DAG) levels present in the membrane fraction (B) and on total Ser473-phosphorylated Akt levels after 20min of insulin stimulation (C).

In soleus, the high-fat feeding failed to induce intracellular accumulation of TG content (Figure 25A) but a significant increase in the level of DAG present in the membrane fraction was observed (Figure 25B). As a consequence, Akt serine-phosphorylation levels were significantly reduced in the high-fat fed animals after 20min of insulin stimulation showing also in the soleus the development of insulin resistance induced by high-fat diet (Figure 25C).

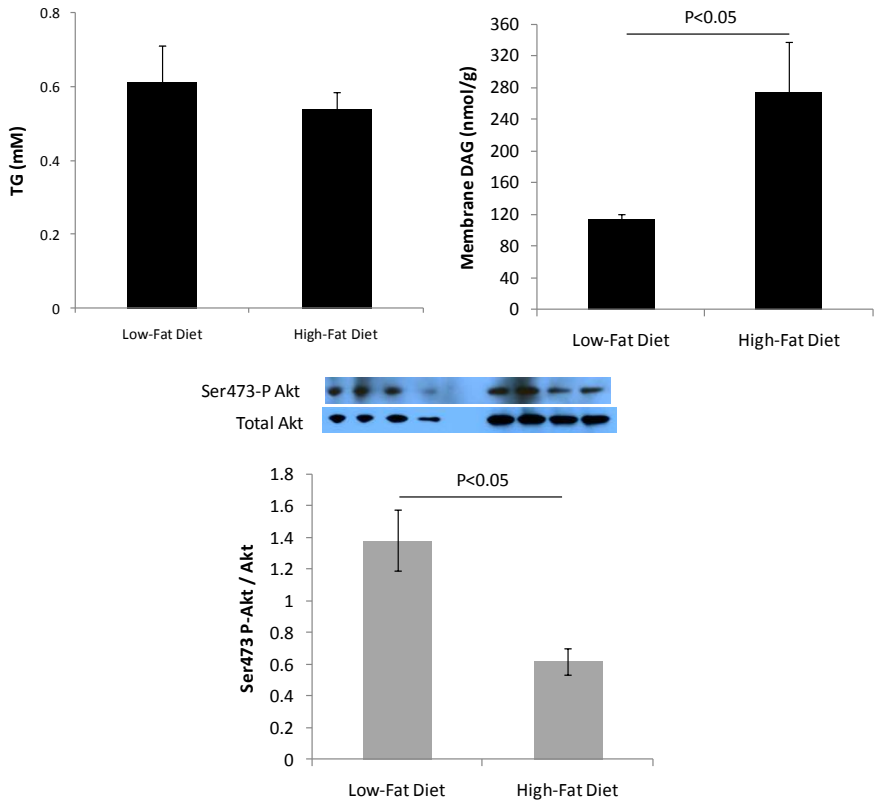

Figure 25 Effect of high-fat diet on soleus intracellular concentration of triglycerides (TG) (A), diacylglycerol (DAG) levels present in the membrane fraction (B) and on total Ser473-phosphorylated Akt levels after 20min of insulin stimulation (C).

The uptake of fatty acids by heart and skeletal muscle is dependent on their plasma concentrations and on the regulation of its transporter. FAT/CD36 is the main transporter of fatty acids in both heart and skeletal muscle being responsible for 68% of the total uptake occurring in heart (43). Like GLUT4, FAT/CD36 exists in small vesicles in the cytosol that can be translocated to the plasma membrane by insulin through a mechanism that involves the PI3K pathway (44). The localization of this transporter is affected in insulin resistant conditions. Higher amounts of FAT/CD36 were found in the plasma membrane of hearts from obese Zucker rats (215) and db/db mice (216). The same observation was made for skeletal muscle (151, 217). This leads to higher rates of fatty acid uptake and accumulation of TG. In the results reported here, TG concentration increased in hearts from high-fat fed animals but not in soleus. Regardless, the levels of DAG associated with

plasma membrane were elevated in both tissues. As discussed previously (151), when evaluating the effect of DAG on insulin signaling, the compartmentation of these metabolites is very important. Only increases of DAG associated with the membrane are correlated with PKCθ translocation and activity (151). In these studies, PKCθ translocation was not assessed. However, the direct consequence of its activity is the phosphorilation of serine residues of IRS-1 which leads to its inactivation. Under these conditions, the phosphorylation of IRS downstream targets is expected to be decreased which was observed by western blot.

Due to the insulin resistance developed, alterations in the enrichments of [3-^{13}C]lactate and [3-^{13}C]alanine, as well as in the V_{PDH}/V_{TCA}, were expected during the fasting and hyperinsulinemic euglycemic clamp infusions (figure 15). In heart, high-fat diet had no significant effect on the enrichments of lactate and alanine. However a strong tendency for decreased lactate enrichment was observed (Table 7). In the presence of insulin no significant change was observed which is coherent with the status of insulin resistance determined. In soleus was observed once again the tendency for decreased enrichment of lactate relative to alanine which was in fact significantly different from what was obtained in the low-fat fed animals (Table 7). However, in the presence of insulin the enrichment of both lactate and alanine were significantly higher than those in the fasting and similar to those obtained in the low-fat fed animals (Table 7).

When the enrichments from table 7 and [4-^{13}C]glutamate were plugged into equation 1 important tissue specific effects of high-fat diet were uncovered. In heart, a fasting V_{PDH}/V_{TCA} of 24.7±4.9% after high-fat diet showed that chronic exposure to lipids had no effect on fasting V_{PDH}/V_{TCA}. However, during the hyperinsulinemic-euglycemic clamp, the insulin-stimulated increase in V_{PDH}/V_{TCA} observed in the low-fat diet was reduced by ~50% (86.1±7.3% *versus* 45.1±7.2%, $P<0.005$, Figure 26A). Despite this reduced response to insulin, V_{PDH}/V_{TCA} was still significantly higher than the fasting state (Figure 26A). In soleus, similarly to what happened in heart, high-fat diet had no effect on fasting V_{PDH}/V_{TCA} (Figure 26B). However, during the hyperinsulinemic-euglycemic clamp, the insulin-stimulated response was completely abolished by high-fat diet (Figure 26B).

Table 7 Fraction of glycolytic flux supported by plasma glucose measured as the ratio of [3-^{13}C]lactate and [3-^{13}C]alanine to [1-^{13}C]glucose in heart and soleus from low-fat and high-fat fed animals during fasting and hyperinsulinemic-euglycemic clamp.

			[3-^{13}C]lactate/ [1-^{13}C]glucose	**[3-^{13}C]alanine/ [1-^{13}C]glucose**
Heart	**Low-fat diet**	*Fasting*	21.8±5.0%	19.7±3.5%
		Hyperinsulinemic-euglycemic clamp	21.4±2.6%	23.3±1.4%
	High-fat diet	*Fasting*	10.0±3.4%	15.7±3.0%
		Hyperinsulinemic-euglycemic clamp	15.0±2.2%	20.2±2.6%
Soleus	**Low-fat diet**	*Fasting*	20.4±2.0%	18.2±1.7%
		Hyperinsulinemic-euglycemic clamp	26.0±1.8%*	27.8±2.3%**
	High-fat diet	*Fasting*	11.7±2.2%†	16.8±1.8%
		Hyperinsulinemic-euglycemic clamp	26.1±2.5%**	27.0±2.7%*

*P≤0.05, **P<0.01 *versus* Fasting
†P<0.05 *versus* Low-fat diet

The work developed by Kelley *et al* was of significant importance in the study of in vivo substrate selection (5). By determining the RQ values across the tissue bed in the leg of lean and obese subjects, two major conclusions were drawn. First and foremost, the authors showed that skeletal muscle from lean and fit individuals is able to switch between oxidizing fatty acids and glucose in response to the stimulus of insulin or fasting. This means that during fasting higher rates of fatty acid oxidation are stimulated while insulin suppresses this preference and stimulates a higher reliance on glucose oxidation. In opposition, obese and unfit individuals are characterized by a metabolic inflexibility, a situation where both fasting and insulin fail to increase the reliance on fatty acid and glucose oxidation, respectively. From this, another conclusion was derived related to the difference in fasting RQ values between lean and obese individuals. It was shown that higher fasting RQ values were associated with higher indexes of obesity and insulin resistance. Fasting RQ could therefore serve, according to the authors, as a predictor of the severity of insulin resistance. Previously, a similar conclusion was obtained where 24h RQ were positively correlated with increases in body weight (218). The results reported here however, challenge this idea of higher glucose oxidation in skeletal muscle of insulin

resistant individuals. No changes were observed in the fasting V_{PDH}/V_{TCA} determined in both heart and soleus muscle of animals subjected to low-fat and high-fat diet. Because only relative fluxes were measured, the results from figure 26 have no direct implication on the absolute fluxes of glucose and fatty acid oxidation. However it shows that insulin resistance has no effect on fasting contribution of glucose oxidation to total TCA cycle; only the response towards insulin was affected.

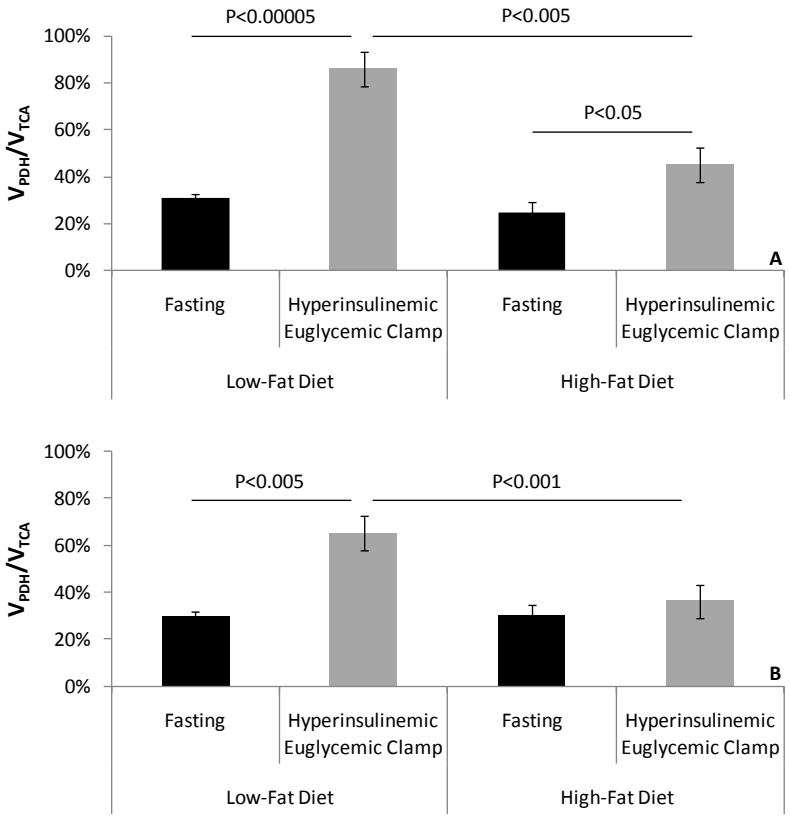

Figure 26 Relative contribution of PDH flux (V_{PDH}) to total TCA cycle flux (V_{TCA}) in heart (A) and soleus muscle (B) of low-fat and high-fat fed rats during fasting and hyperinsulinemic-euglycemic clamp.

Upon insulin stimulation, the obtained values of V_{PDH}/V_{TCA} revealed different responses to insulin after fat accumulation in heart and soleus. In heart the chronic exposure to fat decreased the insulin-stimulating effect on V_{PDH}/V_{TCA}. In contrary, in soleus, high-fat diet

totally abolished the effect of insulin on V_{PDH}/V_{TCA}. These results are very important since they show that *in vivo*, two highly oxidative tissues respond differently to insulin resistance: while insulin resistant soleus muscle is severely metabolically inflexible, the insulin resistant heart conserves some of its metabolic flexibility.

Decreases of insulin-stimulated glucose oxidation have been described due to high-fat diet. These have been associated to decreased PDH activity (219). The PDH complex is known to alternate between an active and an inactive form in a process that involves a cycle of phosphorilation and dephosphorilation. PDK is responsible for the phosphorilation and inactivation of PDH while PDP dephosphorilates PDH returning this complex to an active form (122). From all the isoforms of PDK, PDK4 has been given the main focus in heart and skeletal muscle. Due to its high abundance in skeletal muscle and PPARα-dependent regulation, PDK4 is a good candidate to explain the reduced oxidation of glucose in insulin-resistant tissues. For instance, the cardiac-specific over-expression of PPARα mimicked the metabolic derangement observed in a diabetic heart: increased expression of CPT-1, increased fatty acid oxidation, reduced expression of glucose transporters and reduced glucose oxidation (220). Similar results were obtained in skeletal muscle (221). Increases in total PDK activity and PDK4 protein have been shown to occur after only a 3- to 6-day period of high-fat diet (222, 223), making the activation of the PDH complex more difficult during an oral glucose challenge. Diet induced increases in PDK4 could therefore explain the differences in the insulin-stimulated values of V_{PDH}/V_{TCA} obtained for heart and soleus after the chronic exposure to lipids. These results would also match the higher expression of PDK4 in skeletal muscle relative to the heart (124, 224). Nevertheless, it should be emphasized how a chronic exposure to lipids can affect differently each tissue. The ability of heart to maintain intact some of its metabolic flexibility is most likely associated with its physiological function. Cardiac glucose oxidation has been closely associated with the level of workload (225). Therefore it is possible that the fatty acid induced differences in the insulin-stimulated V_{PDH}/V_{TCA} in heart and soleus reside in the different energy demands between constant contraction and a resting state. The high energy requirements of the heart might suffice to overcome the inhibition of glucose metabolism imposed by fatty acids making it possible to retain its necessary metabolic flexibility.

4.2.3. *In vivo* regulation of V_{PDH}/V_{TCA} by fatty acids

The studies conducted by Randle *et al*, on the inhibitory effect of fatty acid oxidation of glucose metabolism, were originally performed on skeletal muscle and cardiac tissue (117). Therefore, it was important to assess if the loss of metabolic flexibility by high-fat diet (Figure 26) was due to the high plasma levels of FFA (Figure 18A). As explained before, plasma concentrations of FFA were kept constant during the hyperinsulinemic-euglycemic clamp through an infusion of a TG/heparin emulsion. The NMR analysis of the tissue extracts revealed that 2h of constant levels of plasma FFA had no effect on the relative enrichments of [3-^{13}C]lactate and [3-^{13}C]alanine in both heart and soleus (Table 8).

Table 8 Fraction of glycolytic flux supported by plasma glucose measured as the ratio of [3-^{13}C]lactate and [3-^{13}C]alanine to [1-^{13}C]glucose in hearts and soleus from low-fat fed animals during fasting and hyperinsulinemic-euglycemic clamp with and without a lipid infusion.

		[3-^{13}C]lactate / [1-^{13}C]glucose	**[3-^{13}C]alanine / [1-^{13}C]glucose**
Heart	*Hyperinsulinemic-euglycemic clamp*	21.4±2.6%	23.3±1.4%
	Hyperinsulinemic-euglycemic clamp + TG/heparin Infusion	21.7±3.9%	25.4±3.8%
Soleus	*Hyperinsulinemic-euglycemic clamp*	24.8±2.0%	27.8±2.5%
	Hyperinsulinemic-euglycemic clamp + TG/heparin Infusion	22.9±2.1%	32.7±4.3%

However after plugging the enrichments from table 8 and the values of [4-^{13}C]glutamate, different responses were observed towards the higher availability of fatty acids. While no effect on insulin-stimulated V_{PDH}/V_{TCA} was observed in the heart, when compared to the low-fat fed group with no lipid infusion (Figure 27A), the higher level of FFA abolished it in soleus (Figure 27B).

Due to its central role in metabolism, by controlling the entry of glucose carbons in TCA cycle, PDH complex is subjected to a high level of regulation. The importance of this enzymatic complex was demonstrated in PDH deficient mice. The knockout of PDH in heart and skeletal muscle in mice led to death of the male pups after weaning. Only the weaning on high-fat diet was effective in their survival (226).

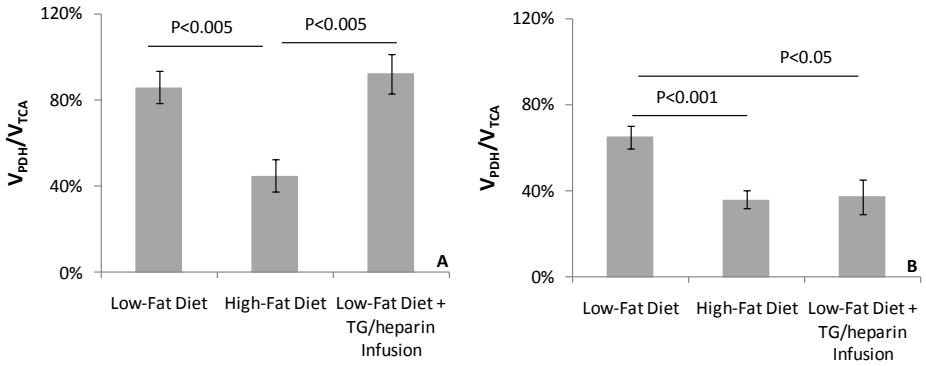

Figure 27 Relative contribution of PDH flux (V_{PDH}) to total TCA cycle flux (V_{TCA}) in heart (A) and soleus muscle (B) of low-fat and high-fat fed rats during fasting and hyperinsulinemic-euglycemic clamp with and without triglyceride (TG)/heparin infusion.

The long term regulation of PDH, discussed in the previous section, involves a stable increase of the expression of PDK isoforms responsible for the phosphorylation and inhibition of PDH. However short-term regulation, mediated by allosteric interactions with the substrates and the products of the reaction catalyzed by PDH, is no less important in the regulation of PDH activity. Increases of [acetyl-CoA]/[CoA] and [NADH]/[NAD^+] are known to inhibit PDH both directly and indirectly (through stimulation of PDK activity). This mechanism was central in the theory of a glucose-fatty acid cycle in which high fatty acid oxidation rates increased the mentioned ratios leading to inhibition of glucose oxidation. According to this theory this is also paralleled by inhibition of glycolysis by citrate, leading to the accumulation of G6P which would in turn inhibit HK and glucose transport. However, some conflicting results surround the validation of this theory as an *in vivo* occurring mechanism of substrate competition. It has been shown that increases in plasma fatty acids resulted in an increase (227), decrease (228, 229) or in no change (230, 231) in muscle glucose uptake. In healthy humans lipid/heparin infusions inhibited glucose uptake by skeletal muscle in the forearm (232, 233) supporting Randle's theory. However, the same was not observed in other studies (234). The effects of fatty acids on PDH activity have also been contradictory. Fatty acids were shown to inhibit PDH in some (145, 235) but not all (236) biopsies. Also, a different mechanism to mediate the effects of fatty acid on glucose metabolism seems to take place in humans and rats. In vivo studies on human subjects

showed that the decline of glucose oxidation induced by elevated plasma concentrations of fatty acids was accompanied by a decrease of G6P (146). Contrary to the glucose-fatty acid cycle theory, these results indicated that excessive fatty acids, in humans, induce insulin resistance through inhibition of glucose uptake, i.e., the reduced uptake of glucose leads to a decreased oxidation of glucose and not the opposite as proposed by Randle. On the contrary, in a similar experiment performed in rats, FFA induced increases in intracellular concentrations of G6P, decreased glycolysis and decreased flux through PDH, fully supporting the glucose-fatty acid cycle (237).

The results reported here, however, show that in *in vivo* conditions the inhibitory effect of fatty acids on glucose oxidation is not present in all tissues to the same extent. The acute increase in plasma fatty acids completely abolished the insulin-stimulated increase of V_{PDH}/V_{TCA} in soleus. In contrast, no effect was observed in heart. These results resemble what was obtained after the 3-week of high-fat diet. The chronic exposure to fatty acids was more effective to reduce the metabolic flexibility of soleus than heart. From these results two important conclusions can be drawn. First, they give further support to the idea that the high energy requirements for heart to maintain its physiological function are a key factor to overcome the inhibitory effect of fatty acids on glucose metabolism. Second, they further support the idea that defects in skeletal muscle metabolism are the first event that results from increased and continuous exposure to fatty acids which culminates in the development of T2D (138).

4.2.4. *In vivo* regulation of V_{PDH}/V_{TCA} by glucose

As was discussed before, increased availability of glucose reduces the reliance on fatty acid oxidation through malonyl-CoA (132). The next experiments were performed to assess how the V_{PDH}/V_{TCA} is regulated, in heart and soleus muscle, by high plasma concentrations of glucose during insulin stimulation.

In this setting, when glucose was clamped at 200mg/dL, the enrichments of [3-^{13}C]lactate and [3-^{13}C]alanine increased significantly in hearts from low-fat fed animals when compared to the hyperinsulinemic-euglycemic clamp (Table 9). In soleus muscle from low-fat fed animals, even though not statistically different, a strong tendency was observed for increased enrichments between euglycemic and hyperglycemic clamps (P<0.08 for [3-

^{13}C]lactate and P<0.07 for [3-^{13}C]alanine). After the 3-week feeding period, the simultaneous stimulation of insulin and glucose in heart promoted a significant increase of [3-^{13}C]lactate and [3-^{13}C]alanine enrichments while no effect was observed in soleus muscle (Table 9).

Table 9 Fraction of glycolytic flux supported by plasma glucose measured as the ratio of [3-^{13}C]lactate and [3-^{13}C]alanine to [1-^{13}C]glucose in heart and soleus from low-fat and high-fat fed animals during hyperinsulinemic-euglycemic clamp and hyperinsulinemic-hyperglycemic clamp.

			[3-^{13}C]lactate/ [1-^{13}C]glucose	**[3-^{13}C]alanine/ [1-^{13}C]glucose**
Heart	**Low-fat diet**	*Hyperinsulinemic-euglycemic clamp*	21.4±2.5%	23.2±1.4%
		Hyperinsulinemic-hyperglycemic clamp	37.7±2.5%**	39.3±2.5%**
	High-fat diet	*Hyperinsulinemic-euglycemic clamp*	15±2.2%	20.2±2.6%
		Hyperinsulinemic-hyperglycemic clamp	26.5±2.5%*	29.4±2.7%*
Soleus	**Low-fat diet**	*Hyperinsulinemic-euglycemic clamp*	24.8±2.0%	27.8±2.5%
		Hyperinsulinemic-hyperglycemic clamp	32.3±3.4%	36.9±3.8%
	High-fat diet	*Hyperinsulinemic-euglycemic clamp*	26.1±2.5%	27.0±2.7%
		Hyperinsulinemic-hyperglycemic clamp	22.7±3.5%	33.1±2.5%

*P<0.05, **P<0.001 *versus* Hyperinsulinemic-euglycemic clamp
†P<0.05 *versus* Hyperinsulinemic-hyperglycemic clamp
‡P<0.05 *versus* [3-^{13}C]alanine

With the enrichments from table 9 plugged into equation 1 it was observed that the hyperglycemia had no significant effect on the V_{PDH}/V_{TCA} in hearts of low-fat fed animals (86.1±7.3% in the hyperinsulinemic-euglycemic clamp *versus* 100.8±8.8% in hyperinsulinemic-hyperglycemic clamp, Figure 28A). However, in the high-fat fed animals, the hyperinsulinemic-hyperglycemic clamp was able to increase of V_{PDH}/V_{TCA} to the levels observed in the low-fat fed animals (45.1±7.2% in the hyperinsulinemic-euglycemic clamp *versus* 104.7±6.9% in the hyperinsulinemic-hyperglycemic clamp, P<0.0001, Figure 28A).

In soleus, the simultaneous stimulation of glucose and insulin, in low-fat fed animals, increased V_{PDH}/V_{TCA} from 65.2±5.2%, in the hyperinsulinemic-euglycemic clamp, to 95.6±8.2% (Figure 28B, $P<0.05$). In the high-fat fed animals, in which the presence of insulin alone (euglycemic clamp) was ineffective to raise V_{PDH}/V_{TCA}, the hyperinsulinemic-hyperglycemic clamp significantly increased V_{PDH}/V_{TCA} from 36.1±4.1% to 78.4±11.3% ($P<0.05$, figure 28B).

In the original work developed by Randle *et al* the intracellular effect of glucose on fatty acid metabolism was not completely known (120). It was not until several years later (132) that this was uncovered. The discovery of malonyl-CoA and its effects on the inhibition of fatty acid oxidation was key to understand one of the mechanisms of substrate competition. The mechanism of glucose signaling through malonyl-CoA, initially discovered in liver, also occurs in non-lipogenic tissues as heart and skeletal muscle. When the PDH complex is in its active form, the acetyl-CoA produced is used in the first reaction of the TCA cycle to produce citrate. When high concentrations of pyruvate are oxidized, the excess of citrate is transported to the cytosol where it used to replenish the pool of acetyl-CoA. This metabolite is then carboxylated by the enzyme ACC to produced malonyl-CoA. This sequence of reactions happens in liver and skeletal muscle. However, in muscle, the existing isoform of ACC, named ACC2, is located in the outer membrane of the mitochondria (135) restricting the use of malonyl-CoA, exclusively, for the inhibition of CPT1. The importance of malonyl-CoA in the regulation of the relative fluxes of glucose and fatty acid oxidation in muscle was shown in mice lacking MCD (238, 239). In these mice, with an inexistent pathway for malonyl-CoA degradation, the decrease in fatty acid oxidation is paralleled by increased glucose oxidation.

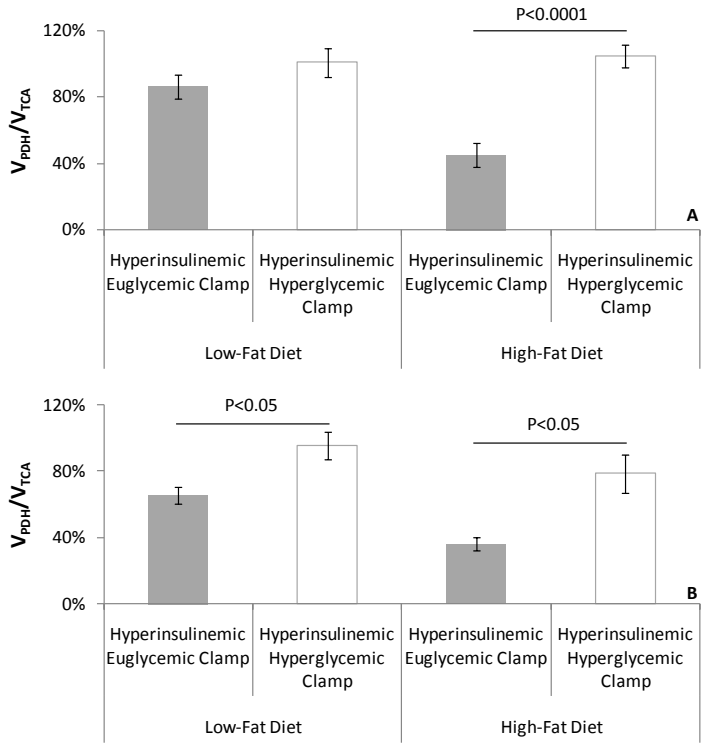

Figure 28 Relative contribution of PDH flux (V_{PDH}) to total TCA cycle flux (V_{TCA}) in heart (A) and soleus muscle (B) of low-fat and high-fat fed rats during hyperinsulinemic-euglycemic clamp and hyperinsulinemic-hyperglycemic clamp.

Our results showed that, like in the liver, glucose availability plays an important role in the regulation of PDH flux in both heart and soleus muscle. In insulin sensitive animals, glucose further increased the insulin-stimulated value of V_{PDH}/V_{TCA} by ~45%. In heart, because the reliance on glucose was almost total during the hyperinsulinemic-euglycemic clamp, the higher availability of glucose had no further effect on V_{PDH}/V_{TCA}. This reinforces the idea of higher metabolic flexibility of heart: similar levels of insulin promoted a greater shift towards glucose oxidation in heart than in soleus. In the former, only the combination of insulin with higher concentrations of glucose was able to increase V_{PDH}/V_{TCA} to values closer to 100%. The importance of glucose was also evidenced in the insulin resistant animals in which the higher availability of glucose rescued the values of V_{PDH}/V_{TCA} observed in the low-fat fed animals. Unlike liver, where insulin alone was not able to change V_{PDH}/V_{TCA}, the regulation of substrate selection in heart and soleus seems to be more

complex. While glucose availability is also here important in the stimulation of higher V_{PDH}/V_{TCA}, insulin has a more preponderant role in regulating this. The reason for this is likely associated with its ability to stimulate the transport of glucose increasing the possibility to metabolize glucose to pyruvate and therefore stimulate PDH.

5. Conclusions

The results reported here showed important tissue specific differences in terms of substrate selection in fasting and insulin-stimulating conditions that were not previously detected by indirect calorimetry in the studies performed by Kelley *et al* (120). Important conclusions could also be drawn that further elucidated the mechanisms of insulin resistance development as well as the regulation of glucose oxidation.

The combined use of stable isotope infusions and POCE-NMR analysis was a key methodological approach to uncover the tissue specific substrate preferences reported here. There are several advantages associated with the use of this approach over indirect calorimetry. The infusion of [1-^{13}C]glucose as a tracer during fasting had no effect on plasma glucose concentrations nor on the circulating levels of insulin which was essential to characterize this state accurately. The other advantage is related to the non-dependence on blood flow. Changes in blood flow can drastically influence the results obtained by indirect calorimetry (161). However, the fact that plasma [1-^{13}C]glucose enrichments depend solely on the balance between the rates of [1-^{13}C]glucose infusion and glucose uptake by the tissues, makes this method robust to the blood flow influence. Also, the most significant advantage of this methodology is the ability to study V_{PDH}/V_{TCA} without the contributions from other tissues. In the studies performed by Kelley *et al* (120), the indirect calorimetry was performed in the muscle across the legs of insulin-sensitive and resistant individuals. Even though this approach limits the tissues analyzed it is not completely efficient. The different muscle groups present in the legs are composed by different fiber types. For instance, while the gastrocnemius and quadriceps muscles are composed by ~50% of type 1 and type 2, soleus muscle is mainly composed by type 1 fibers. Due to the different oxidative capacities of both fiber types, the values of RQ obtained by indirect calorimetry are an average of the total fiber types present in all muscle groups. In contrast, the NMR-based approach used in this work allowed the study of individual muscle groups.

With this work an attempt was made to extend the concept of metabolic flexibility to other tissues, like liver and heart, and bring new insights into the *in vivo* regulation of substrate selection. The results obtained from liver showed that insulin, surprisingly, had

no effect on V_{PDH}/V_{TCA}. The evidence for this came from the hyperinsulinemic-euglycemic clamp experiments. The fasting V_{PDH}/V_{TCA} obtained, ~20%, was unchanged in the presence of postprandial levels of insulin. The small value of V_{PDH}/V_{TCA} during fasting is supported by several studies that showed that a higher reliance on fatty acid oxidation is necessary to support gluconeogenesis in liver. However the inability of insulin to increase it, during the 2h infusions, shows that the concept of metabolic flexibility cannot be applied to liver. The hyperinsulinemic-hyperglycemic clamps gave important information about the regulation of V_{PDH}/V_{TCA}. Only in these experimental conditions an increase in V_{PDH}/V_{TCA} was observed. Also, the association of these results with increased glycogen concentrations suggested a substrate dependent mechanism of PDH activation. When the plasma glucose is abundant, a fraction of it is used to refill glycogen stores while the rest is metabolized to pyruvate stimulating the flux through PDH. This hypothesis would be coincident with the role of liver as an energy reservoir. In the presence of high concentrations of glucose, and in association with insulin, the excess of glucose is directed to the *de novo* synthesis of lipids, which requires the activation of PDH. Similar results were obtained in insulin resistant livers. After the period of high fat feeding, the contribution of glucose oxidation to the TCA cycle was totally abolished and the presence of postprandial levels of insulin had, again, no effect on $V_{PDH}/V_{TCA.}$ The high concentrations of glucose significantly increased V_{PDH}/V_{TCA} but not to the same extent observed in the low-fat fed animals suggesting that a mechanism other than allosteric regulation takes place in these conditions. The chronic exposure to lipids is known to increase the expression PDK enzymes that phosphorylate and inhibit PDH. This is a possible mechanism to explain these results and so PDK activity must be determined in the future.

The analysis of heart and soleus extracts revealed a fasting V_{PDH}/V_{TCA} of 30% confirming the expected high reliance of muscle on fatty acid oxidation during fasting. In contrast to liver, the V_{PDH}/V_{TCA} calculated for heart and soleus showed that these tissues possess high metabolic flexibility: insulin stimulated a 3-fold and 2-fold increase of V_{PDH}/V_{TCA} in heart and soleus, respectively. However it was after the high-fat diet induced insulin resistance that important tissue responses to the insulin stimulus were observed. In contrary to the proposed by Kelley *et al* (120), insulin resistance had no effect on the fasting values of V_{PDH}/V_{TCA} in both these tissues. These authors determined that the fasting state of insulin resistant individuals was characterized by a higher reliance on glucose

oxidation than in the insulin sensitive subjects and proposed that fasting RQ values could be a good indicator of the severity of insulin resistance. However, the results reported here challenge that view by showing that insulin resistant does not influence fasting V_{PDH}/V_{TCA}. Also, the metabolic inflexibility induced by insulin resistance was more severe in soleus than in heart, showing that even though these are highly oxidative tissues, substrate selection is differently affected by chronic exposure to fat. Also relevant was the modulation of V_{PDH}/V_{TCA} in response to changes in plasma concentrations of glucose and FFA. When fasting concentrations of FFA were kept constant during the hyperinsulinemic-euglycemic clamps, only in soleus the effect of insulin on V_{PDH}/V_{TCA} was abolished. This shows that PDH from soleus is more sensitive to inhibition by fatty acids than heart which might be related to the energy requirements of both tissues. Because heart is in constant contraction-relaxation cycles, the necessity for a constant supply of energy is high. Therefore the ability to rely on glucose oxidation, even in the presence of high levels of FFA, is important. This hypothesis is further supported by the results obtained after the high fat diet. The importance of glucose in the regulation of V_{PDH}/V_{TCA} was evidenced in the hyperinsulinemic-hyperglycemic clamps in which further increased insulin-stimulated V_{PDH}/V_{TCA} in both insulin sensitive and resistant animals.

In conclusion, the results reported here, in terms of tissue-specific substrate selection and V_{PDH}/V_{TCA} regulation, showed that POCE-NMR can also be a useful technique in a clinical setting. The combined use of tissue biopsies with POCE-NMR analysis can determine the degree of insulin resistance of an individual, by calculating the magnitude of the insulin-stimulated shift from fatty acids to glucose oxidation, and assess the effectiveness of any clinical intervention used to reverse it. With this approach the development of insulin resistance can be closely followed and individually analyzed in order to find the best treatment.

6. Appendix A

In this appendix, equation 1 will be derived. Assuming that [1-^{13}C]glucose is the only source of label (Figure 10), the temporal variation of label in the pool of acetyl-CoA is dependent on its production through pyruvate dehydrogenase (V_{PDH}) and on its consumption through the tricarboxylic acid cycle (V_{TCA}). This balance can be written as in equation A1 where [2-^{13}C]acetyl-CoA and [3-^{13}C]pyruvate represent the concentration of ^{13}C-label in each pool.

$$d[2\text{-}^{13}C]\text{Acetyl-CoA}/dt = [3\text{-}^{13}C]\text{Pyruvate} \times V_{PDH} - [2\text{-}^{13}C]\text{Acetyl-CoA} \times V_{TCA} \quad \textit{(Equation A1)}$$

At isotopic steady state:

$$0 = [3\text{-}^{13}C]\text{Pyruvate} \times V_{PDH} - [2\text{-}^{13}C]\text{Acetyl-CoA} \times V_{TCA} \quad \textit{(Equation A2)}$$

Equation A3 follows directly from A2:

$$\frac{V_{PDH}}{V_{TCA}} = \frac{[2\text{-}^{13}C]\text{Acetyl-CoA}}{[3\text{-}^{13}C]\text{Pyruvate}} \quad \textit{(Equation A3)}$$

Due to the limitations associated with the sensitivity of NMR [4-^{13}C]glucose can be used as a surrogate of [2-^{13}C]acetyl-CoA enrichments (assuming the inexistence of other sources of label). Also, because of the fast exchange between the pools of lactate, pyruvate and alanine, one can assume that the enrichments of these three pools are similar at steady-state. Therefore one can use equation 1 as an approximation to equation A3.

$$\frac{V_{PDH}}{V_{TCA}} = \frac{[4\text{-}^{13}C]\text{Glutamate}}{[3\text{-}^{13}C]\text{Alanine}} \quad \textit{(Equation 1)}$$

7. References

1. Roth, J., Qiang, X., Marban, S.L., Redelt, H., and Lowell, B.C. 2004. The obesity pandemic: where have we been and where are we going? *Obes Res* 12 Suppl 2:88S-101S.

2. Mensah, G.A., Mokdad, A.H., Ford, E., Narayan, K.M., Giles, W.H., Vinicor, F., and Deedwania, P.C. 2004. Obesity, metabolic syndrome, and type 2 diabetes: emerging epidemics and their cardiovascular implications. *Cardiol Clin* 22:485-504.

3. Chan, J.M., Rimm, E.B., Colditz, G.A., Stampfer, M.J., and Willett, W.C. 1994. Obesity, fat distribution, and weight gain as risk factors for clinical diabetes in men. *Diabetes Care* 17:961-969.

4. Rexrode, K.M., Carey, V.J., Hennekens, C.H., Walters, E.E., Colditz, G.A., Stampfer, M.J., Willett, W.C., and Manson, J.E. 1998. Abdominal adiposity and coronary heart disease in women. *JAMA* 280:1843-1848.

5. Kelley, D.E., Goodpaster, B., Wing, R.R., and Simoneau, J.A. 1999. Skeletal muscle fatty acid metabolism in association with insulin resistance, obesity, and weight loss. *Am J Physiol* 277:E1130-1141.

6. Organization, W.H. 2003. Controlling the global obesity epidemic.

7. Lobstein, T., and Frelut, M.L. 2003. Prevalence of overweight among children in Europe. *Obes Rev* 4:195-200.

8. Ben-Sefer, E., Ben-Natan, M., and Ehrenfeld, M. 2009. Childhood obesity: current literature, policy and implications for practice. *Int Nurs Rev* 56:166-173.

9. Wang, Y.C., Colditz, G.A., and Kuntz, K.M. 2007. Forecasting the obesity epidemic in the aging U.S. population. *Obesity (Silver Spring)* 15:2855-2865.

10. Berghofer, A., Pischon, T., Reinhold, T., Apovian, C.M., Sharma, A.M., and Willich, S.N. 2008. Obesity prevalence from a European perspective: a systematic review. *BMC Public Health* 8:200.

11. Troiano, R.P., Frongillo, E.A., Jr., Sobal, J., and Levitsky, D.A. 1996. The relationship between body weight and mortality: a quantitative analysis of combined information from existing studies. *Int J Obes Relat Metab Disord* 20:63-75.

12. Engeland, A., Bjorge, T., Selmer, R.M., and Tverdal, A. 2003. Height and body mass index in relation to total mortality. *Epidemiology* 14:293-299.

13. Durazo-arvizu, R., McGee, D., Li, Z., and Cooper, R. 1997. Establishing the nadir of the body mass index-mortality relationship: a case study. *J Am Stat Assoc* 92:1,312-319.

14. Eckel, R.H. 1997. Obesity and heart disease: a statement for healthcare professionals from the Nutrition Committee, American Heart Association. *Circulation* 96:3248-3250.

15. Bray, G.A., Clearfield, M.B., Fintel, D.J., and Nelinson, D.S. 2009. Overweight and obesity: the pathogenesis of cardiometabolic risk. *Clin Cornerstone* 9:30-40; discussion 41-32.

16. Flint, A.J., Hu, F.B., Glynn, R.J., Caspard, H., Manson, J.E., Willett, W.C., and Rimm, E.B. 2009. Excess Weight and the Risk of Incident Coronary Heart Disease Among Men and Women. *Obesity (Silver Spring)*.

17. Bray, G.A., and Gray, D.S. 1988. Obesity. Part I--Pathogenesis. *West J Med* 149:429-441.

18. McGee, D.L. 2005. Body mass index and mortality: a meta-analysis based on person-level data from twenty-six observational studies. *Ann Epidemiol* 15:87-97.

19. Bloomgarden, Z.T. 1998. Insulin resistance: current concepts. *Clin Ther* 20:216-231; discussion 215.

20. O'Dea, K. 1992. Obesity and diabetes in "the land of milk and honey". *Diabetes Metab Rev* 8:373-388.

21. Knowler, W.C., Saad, M.F., Pettitt, D.J., Nelson, R.G., and Bennett, P.H. 1993. Determinants of diabetes mellitus in the Pima Indians. *Diabetes Care* 16:216-227.

22. Haffner, S.M. 1998. Epidemiology of type 2 diabetes: risk factors. *Diabetes Care* 21 Suppl 3:C3-6.

23. Vague, J. 1956. The degree of masculine differentiation of obesities: a factor determining predisposition to diabetes, atherosclerosis, gout, and uric calculous disease. *Am J Clin Nutr* 4:20-34.

24. Szczepaniak, L.S., Babcock, E.E., Schick, F., Dobbins, R.L., Garg, A., Burns, D.K., McGarry, J.D., and Stein, D.T. 1999. Measurement of intracellular triglyceride stores by H spectroscopy: validation in vivo. *Am J Physiol* 276:E977-989.

25. Sinha, R., Dufour, S., Petersen, K.F., LeBon, V., Enoksson, S., Ma, Y.Z., Savoye, M., Rothman, D.L., Shulman, G.I., and Caprio, S. 2002. Assessment of skeletal muscle triglyceride content by (1)H nuclear magnetic resonance spectroscopy in lean and obese adolescents: relationships to insulin sensitivity, total body fat, and central adiposity. *Diabetes* 51:1022-1027.

26. Williamson, J.R., and Krebs, H.A. 1961. Acetoacetate as fuel of respiration in the perfused rat heart. *Biochem J* 80:540-547.

27. Newsholme, E.A., Randle, P.J., and Manchester, K.L. 1962. Inhibition of the phosphofructokinase reaction in perfused rat heart by respiration of ketone bodies, fatty acids and pyruvate. *Nature* 193:270-271.

28. Kelley, D.E. 2005. Skeletal muscle fat oxidation: timing and flexibility are everything. *J Clin Invest* 115:1699-1702.

29. Baron, A.D., Brechtel, G., Wallace, P., and Edelman, S.V. 1988. Rates and tissue sites of non-insulin- and insulin-mediated glucose uptake in humans. *Am J Physiol* 255:E769-774.

30. Bickerton, A.S., Roberts, R., Fielding, B.A., Hodson, L., Blaak, E.E., Wagenmakers, A.J., Gilbert, M., Karpe, F., and Frayn, K.N. 2007. Preferential uptake of dietary Fatty acids in adipose tissue and muscle in the postprandial period. *Diabetes* 56:168-176.

31. Ruge, T., Hodson, L., Cheeseman, J., Dennis, A.L., Fielding, B.A., Humphreys, S.M., Frayn, K.N., and Karpe, F. 2009. Fasted to fed trafficking of Fatty acids in human adipose tissue reveals a novel regulatory step for enhanced fat storage. *J Clin Endocrinol Metab* 94:1781-1788.

32. Frayn, K.N., Coppack, S.W., Fielding, B.A., and Humphreys, S.M. 1995. Coordinated regulation of hormone-sensitive lipase and lipoprotein lipase in human adipose tissue in vivo: implications for the control of fat storage and fat mobilization. *Adv Enzyme Regul* 35:163-178.

33. Zimmermann, R., Lass, A., Haemmerle, G., and Zechner, R. 2009. Fate of fat: the role of adipose triglyceride lipase in lipolysis. *Biochim Biophys Acta* 1791:494-500.

34. Stumvoll, M., Meyer, C., Mitrakou, A., Nadkarni, V., and Gerich, J.E. 1997. Renal glucose production and utilization: new aspects in humans. *Diabetologia* 40:749-757.

35. Kokubun, E., Hirabara, S.M., Fiamoncini, J., Curi, R., and Haebisch, H. 2009. Changes of glycogen content in liver, skeletal muscle, and heart from fasted rats. *Cell Biochem Funct* 27:488-495.

36. Alves, T.C., Nunes, P.M., Palmeira, C.M., Jones, J.G., and Carvalho, R.A. 2008. Estimating gluconeogenesis by NMR isotopomer distribution analysis of [^{13}C]bicarbonate and [1-^{13}C]lactate. *NMR Biomed* 21:337-344.

37. O'Brien, R.M., Streeper, R.S., Ayala, J.E., Stadelmaier, B.T., and Hornbuckle, L.A. 2001. Insulin-regulated gene expression. *Biochem Soc Trans* 29:552-558.

38. Hultman, E. 1995. Fuel selection, muscle fibre. *Proc Nutr Soc* 54:107-121.

39. Andres, R., Cader, G., and Zierler, K.L. 1956. The quantitatively minor role of carbohydrate in oxidative metabolism by skeletal muscle in intact man in the basal state; measurements of oxygen and glucose uptake and carbon dioxide and lactate production in the forearm. *J Clin Invest* 35:671-682.

40. Hamilton, J.A. 1999. Transport of fatty acids across membranes by the diffusion mechanism. *Prostaglandins Leukot Essent Fatty Acids* 60:291-297.

41. Su, X., and Abumrad, N.A. 2009. Cellular fatty acid uptake: a pathway under construction. *Trends Endocrinol Metab* 20:72-77.

42. Coburn, C.T., Knapp, F.F., Jr., Febbraio, M., Beets, A.L., Silverstein, R.L., and Abumrad, N.A. 2000. Defective uptake and utilization of long chain fatty acids in muscle and adipose tissues of CD36 knockout mice. *J Biol Chem* 275:32523-32529.

43. Kuang, M., Febbraio, M., Wagg, C., Lopaschuk, G.D., and Dyck, J.R. 2004. Fatty acid translocase/CD36 deficiency does not energetically or functionally compromise hearts before or after ischemia. *Circulation* 109:1550-1557.

44. Luiken, J.J., Koonen, D.P., Willems, J., Zorzano, A., Becker, C., Fischer, Y., Tandon, N.N., Van Der Vusse, G.J., Bonen, A., and Glatz, J.F. 2002. Insulin stimulates long-chain fatty acid utilization by rat cardiac myocytes through cellular redistribution of FAT/CD36. *Diabetes* 51:3113-3119.

45. Luiken, J.J., Coort, S.L., Willems, J., Coumans, W.A., Bonen, A., van der Vusse, G.J., and Glatz, J.F. 2003. Contraction-induced fatty acid translocase/CD36 translocation in rat cardiac myocytes is mediated through AMP-activated protein kinase signaling. *Diabetes* 52:1627-1634.

46. Petersen, K.F., Dufour, S., Befroy, D., Garcia, R., and Shulman, G.I. 2004. Impaired mitochondrial activity in the insulin-resistant offspring of patients with type 2 diabetes. *N Engl J Med* 350:664-671.

47. Power, M.L., and Schulkin, J. 2008. Anticipatory physiological regulation in feeding biology: cephalic phase responses. *Appetite* 50:194-206.

48. Storlien, L., Oakes, N.D., and Kelley, D.E. 2004. Metabolic flexibility. *Proc Nutr Soc* 63:363-368.

49. Hudgins, L.C., Hellerstein, M., Seidman, C., Neese, R., Diakun, J., and Hirsch, J. 1996. Human fatty acid synthesis is stimulated by a eucaloric low fat, high carbohydrate diet. *J Clin Invest* 97:2081-2091.

50. Acheson, K.J., Schutz, Y., Bessard, T., Anantharaman, K., Flatt, J.P., and Jequier, E. 1988. Glycogen storage capacity and de novo lipogenesis during massive carbohydrate overfeeding in man. *Am J Clin Nutr* 48:240-247.

51. Holness, M.J., MacLennan, P.A., Palmer, T.N., and Sugden, M.C. 1988. The disposition of carbohydrate between glycogenesis, lipogenesis and oxidation in liver during the starved-to-fed transition. *Biochem J* 252:325-330.

52. Gross, D.N., van den Heuvel, A.P., and Birnbaum, M.J. 2008. The role of FoxO in the regulation of metabolism. *Oncogene* 27:2320-2336.

53. Samuel, V.T., Choi, C.S., Phillips, T.G., Romanelli, A.J., Geisler, J.G., Bhanot, S., McKay, R., Monia, B., Shutter, J.R., Lindberg, R.A., et al. 2006. Targeting foxo1 in mice using antisense oligonucleotide improves hepatic and peripheral insulin action. *Diabetes* 55:2042-2050.

54. Colville, C.A., Seatter, M.J., Jess, T.J., Gould, G.W., and Thomas, H.M. 1993. Kinetic analysis of the liver-type (GLUT2) and brain-type (GLUT3) glucose transporters in Xenopus oocytes: substrate specificities and effects of transport inhibitors. *Biochem J* 290 (Pt 3):701-706.

55. van Schaftingen, E., Veiga-da-Cunha, M., and Niculescu, L. 1997. The regulatory protein of glucokinase. *Biochem Soc Trans* 25:136-140.

56. de la Iglesia, N., Veiga-da-Cunha, M., Van Schaftingen, E., Guinovart, J.J., and Ferrer, J.C. 1999. Glucokinase regulatory protein is essential for the proper subcellular localisation of liver glucokinase. *FEBS Lett* 456:332-338.

57. Iynedjian, P.B., Gjinovci, A., and Renold, A.E. 1988. Stimulation by insulin of glucokinase gene transcription in liver of diabetic rats. *J Biol Chem* 263:740-744.

58. Ribaux, P.G., and Iynedjian, P.B. 2003. Analysis of the role of protein kinase B (cAKT) in insulin-dependent induction of glucokinase and sterol regulatory element-binding protein 1 (SREBP1) mRNAs in hepatocytes. *Biochem J* 376:697-705.

59. Iynedjian, P.B. 2005. Lack of evidence for a role of TRB3/NIPK as an inhibitor of PKB-mediated insulin signalling in primary hepatocytes. *Biochem J* 386:113-118.

60. Lee, J., and Kim, M.S. 2007. The role of GSK3 in glucose homeostasis and the development of insulin resistance. *Diabetes Res Clin Pract* 77 Suppl 1:S49-57.

61. Ferrer, J.C., Favre, C., Gomis, R.R., Fernandez-Novell, J.M., Garcia-Rocha, M., de la Iglesia, N., Cid, E., and Guinovart, J.J. 2003. Control of glycogen deposition. *FEBS Lett* 546:127-132.

62. Moir, A.M., and Zammit, V.A. 1993. Monitoring of changes in hepatic fatty acid and glycerolipid metabolism during the starved-to-fed transition in vivo. Studies on awake, unrestrained rats. *Biochem J* 289 (Pt 1):49-55.

63. Matsumoto, M., Ogawa, W., Teshigawara, K., Inoue, H., Miyake, K., Sakaue, H., and Kasuga, M. 2002. Role of the insulin receptor substrate 1 and phosphatidylinositol 3-kinase signaling pathway in insulin-induced expression of sterol regulatory element binding protein 1c and glucokinase genes in rat hepatocytes. *Diabetes* 51:1672-1680.

64. Foufelle, F., and Ferre, P. 2002. New perspectives in the regulation of hepatic glycolytic and lipogenic genes by insulin and glucose: a role for the transcription factor sterol regulatory element binding protein-1c. *Biochem J* 366:377-391.

65. Shimano, H., Yahagi, N., Amemiya-Kudo, M., Hasty, A.H., Osuga, J., Tamura, Y., Shionoiri, F., Iizuka, Y., Ohashi, K., Harada, K., et al. 1999. Sterol regulatory element-binding protein-1 as a key transcription factor for nutritional induction of lipogenic enzyme genes. *J Biol Chem* 274:35832-35839.

66. Jucker, B.M., Barucci, N., and Shulman, G.I. 1999. Metabolic control analysis of insulin-stimulated glucose disposal in rat skeletal muscle. *Am J Physiol* 277:E505-512.

67. Slot, J.W., Geuze, H.J., Gigengack, S., Lienhard, G.E., and James, D.E. 1991. Immuno-localization of the insulin regulatable glucose transporter in brown adipose tissue of the rat. *J Cell Biol* 113:123-135.

68. Ng, Y., Ramm, G., Lopez, J.A., and James, D.E. 2008. Rapid activation of Akt2 is sufficient to stimulate GLUT4 translocation in 3T3-L1 adipocytes. *Cell Metab* 7:348-356.

69. Wang, Q., Somwar, R., Bilan, P.J., Liu, Z., Jin, J., Woodgett, J.R., and Klip, A. 1999. Protein kinase B/Akt participates in GLUT4 translocation by insulin in L6 myoblasts. *Mol Cell Biol* 19:4008-4018.

70. Katome, T., Obata, T., Matsushima, R., Masuyama, N., Cantley, L.C., Gotoh, Y., Kishi, K., Shiota, H., and Ebina, Y. 2003. Use of RNA interference-mediated gene silencing and adenoviral overexpression to elucidate the roles of AKT/protein kinase B isoforms in insulin actions. *J Biol Chem* 278:28312-28323.

71. Cho, H., Mu, J., Kim, J.K., Thorvaldsen, J.L., Chu, Q., Crenshaw, E.B., 3rd, Kaestner, K.H., Bartolomei, M.S., Shulman, G.I., and Birnbaum, M.J. 2001. Insulin resistance and a diabetes mellitus-like syndrome in mice lacking the protein kinase Akt2 (PKB beta). *Science* 292:1728-1731.

72. Sano, H., Kane, S., Sano, E., Miinea, C.P., Asara, J.M., Lane, W.S., Garner, C.W., and Lienhard, G.E. 2003. Insulin-stimulated phosphorylation of a Rab GTPase-activating protein regulates GLUT4 translocation. *J Biol Chem* 278:14599-14602.

73. Eguez, L., Lee, A., Chavez, J.A., Miinea, C.P., Kane, S., Lienhard, G.E., and McGraw, T.E. 2005. Full intracellular retention of GLUT4 requires AS160 Rab GTPase activating protein. *Cell Metab* 2:263-272.

74. Saltiel, A.R., and Kahn, C.R. 2001. Insulin signalling and the regulation of glucose and lipid metabolism. *Nature* 414:799-806.

75. Gammeltoft, S. 1984. Insulin receptors: binding kinetics and structure-function relationship of insulin. *Physiol Rev* 64:1321-1378.

76. Adams, T.E., Epa, V.C., Garrett, T.P., and Ward, C.W. 2000. Structure and function of the type 1 insulin-like growth factor receptor. *Cell Mol Life Sci* 57:1050-1093.

77. Jensen, M., and De Meyts, P. 2009. Molecular mechanisms of differential intracellular signaling from the insulin receptor. *Vitam Horm* 80:51-75.

78. Ullrich, A., Bell, J.R., Chen, E.Y., Herrera, R., Petruzzelli, L.M., Dull, T.J., Gray, A., Coussens, L., Liao, Y.C., Tsubokawa, M., et al. 1985. Human insulin receptor and its relationship to the tyrosine kinase family of oncogenes. *Nature* 313:756-761.

79. Bass, J., Chiu, G., Argon, Y., and Steiner, D.F. 1998. Folding of insulin receptor monomers is facilitated by the molecular chaperones calnexin and calreticulin and impaired by rapid dimerization. *J Cell Biol* 141:637-646.

80. Elleman, T.C., Frenkel, M.J., Hoyne, P.A., McKern, N.M., Cosgrove, L., Hewish, D.R., Jachno, K.M., Bentley, J.D., Sankovich, S.E., and Ward, C.W. 2000. Mutational analysis of the N-linked glycosylation sites of the human insulin receptor. *Biochem J* 347 Pt 3:771-779.

81. Youngren, J.F. 2007. Regulation of insulin receptor function. *Cell Mol Life Sci* 64:873-891.

82. Lee, J., O'Hare, T., Pilch, P.F., and Shoelson, S.E. 1993. Insulin receptor autophosphorylation occurs asymmetrically. *J Biol Chem* 268:4092-4098.

83. Frattali, A.L., and Pessin, J.E. 1993. Relationship between alpha subunit ligand occupancy and beta subunit autophosphorylation in insulin/insulin-like growth factor-1 hybrid receptors. *J Biol Chem* 268:7393-7400.

84. Hubbard, S.R., and Miller, W.T. 2007. Receptor tyrosine kinases: mechanisms of activation and signaling. *Curr Opin Cell Biol* 19:117-123.

85. Wilden, P.A., Siddle, K., Haring, E., Backer, J.M., White, M.F., and Kahn, C.R. 1992. The role of insulin receptor kinase domain autophosphorylation in receptor-mediated activities. Analysis with insulin and anti-receptor antibodies. *J Biol Chem* 267:13719-13727.

86. Carpentier, J.L. 1994. Insulin receptor internalization: molecular mechanisms and physiopathological implications. *Diabetologia* 37 Suppl 2:S117-124.

87. Bondy, C.A., Zhou, J., Chin, E., Reinhardt, R.R., Ding, L., and Roth, R.A. 1994. Cellular distribution of insulin-degrading enzyme gene expression. Comparison with insulin and insulin-like growth factor receptors. *J Clin Invest* 93:966-973.

88. Di Guglielmo, G.M., Drake, P.G., Baass, P.C., Authier, F., Posner, B.I., and Bergeron, J.J. 1998. Insulin receptor internalization and signalling. *Mol Cell Biochem* 182:59-63.

89. Elchebly, M., Payette, P., Michaliszyn, E., Cromlish, W., Collins, S., Loy, A.L., Normandin, D., Cheng, A., Himms-Hagen, J., Chan, C.C., et al. 1999. Increased insulin sensitivity and obesity resistance in mice lacking the protein tyrosine phosphatase-1B gene. *Science* 283:1544-1548.

90. Klaman, L.D., Boss, O., Peroni, O.D., Kim, J.K., Martino, J.L., Zabolotny, J.M., Moghal, N., Lubkin, M., Kim, Y.B., Sharpe, A.H., et al. 2000. Increased energy expenditure, decreased adiposity, and tissue-specific insulin sensitivity in protein-tyrosine phosphatase 1B-deficient mice. *Mol Cell Biol* 20:5479-5489.

91. Virkamaki, A., Ueki, K., and Kahn, C.R. 1999. Protein-protein interaction in insulin signaling and the molecular mechanisms of insulin resistance. *J Clin Invest* 103:931-943.

92. Taniguchi, C.M., Emanuelli, B., and Kahn, C.R. 2006. Critical nodes in signalling pathways: insights into insulin action. *Nat Rev Mol Cell Biol* 7:85-96.

93. White, M.F. 2002. IRS proteins and the common path to diabetes. *Am J Physiol Endocrinol Metab* 283:E413-422.

94. Sun, X.J., Rothenberg, P., Kahn, C.R., Backer, J.M., Araki, E., Wilden, P.A., Cahill, D.A., Goldstein, B.J., and White, M.F. 1991. Structure of the insulin receptor substrate IRS-1 defines a unique signal transduction protein. *Nature* 352:73-77.

95. White, M.F. 1998. The IRS-signaling system: a network of docking proteins that mediate insulin and cytokine action. *Recent Prog Horm Res* 53:119-138.

96. White, M.F. 1997. The insulin signalling system and the IRS proteins. *Diabetologia* 40 Suppl 2:S2-17.

97. Sun, X.J., Wang, L.M., Zhang, Y., Yenush, L., Myers, M.G., Jr., Glasheen, E., Lane, W.S., Pierce, J.H., and White, M.F. 1995. Role of IRS-2 in insulin and cytokine signalling. *Nature* 377:173-177.

98. Araki, E., Lipes, M.A., Patti, M.E., Bruning, J.C., Haag, B., 3rd, Johnson, R.S., and Kahn, C.R. 1994. Alternative pathway of insulin signalling in mice with targeted disruption of the IRS-1 gene. *Nature* 372:186-190.

99. Tamemoto, H., Kadowaki, T., Tobe, K., Yagi, T., Sakura, H., Hayakawa, T., Terauchi, Y., Ueki, K., Kaburagi, Y., Satoh, S., et al. 1994. Insulin resistance and growth retardation in mice lacking insulin receptor substrate-1. *Nature* 372:182-186.

100. Kulkarni, R.N., Winnay, J.N., Daniels, M., Bruning, J.C., Flier, S.N., Hanahan, D., and Kahn, C.R. 1999. Altered function of insulin receptor substrate-1-deficient mouse islets and cultured beta-cell lines. *J Clin Invest* 104:R69-75.

101. Kubota, N., Tobe, K., Terauchi, Y., Eto, K., Yamauchi, T., Suzuki, R., Tsubamoto, Y., Komeda, K., Nakano, R., Miki, H., et al. 2000. Disruption of insulin receptor substrate 2 causes type 2

diabetes because of liver insulin resistance and lack of compensatory beta-cell hyperplasia. *Diabetes* 49:1880-1889.

102. Previs, S.F., Withers, D.J., Ren, J.M., White, M.F., and Shulman, G.I. 2000. Contrasting effects of IRS-1 versus IRS-2 gene disruption on carbohydrate and lipid metabolism in vivo. *J Biol Chem* 275:38990-38994.

103. Yamauchi, T., Tobe, K., Tamemoto, H., Ueki, K., Kaburagi, Y., Yamamoto-Honda, R., Takahashi, Y., Yoshizawa, F., Aizawa, S., Akanuma, Y., et al. 1996. Insulin signalling and insulin actions in the muscles and livers of insulin-resistant, insulin receptor substrate 1-deficient mice. *Mol Cell Biol* 16:3074-3084.

104. Withers, D.J., Gutierrez, J.S., Towery, H., Burks, D.J., Ren, J.M., Previs, S., Zhang, Y., Bernal, D., Pons, S., Shulman, G.I., et al. 1998. Disruption of IRS-2 causes type 2 diabetes in mice. *Nature* 391:900-904.

105. Higaki, Y., Wojtaszewski, J.F., Hirshman, M.F., Withers, D.J., Towery, H., White, M.F., and Goodyear, L.J. 1999. Insulin receptor substrate-2 is not necessary for insulin- and exercise-stimulated glucose transport in skeletal muscle. *J Biol Chem* 274:20791-20795.

106. Fantin, V.R., Wang, Q., Lienhard, G.E., and Keller, S.R. 2000. Mice lacking insulin receptor substrate 4 exhibit mild defects in growth, reproduction, and glucose homeostasis. *Am J Physiol Endocrinol Metab* 278:E127-133.

107. Cantley, L.C. 2002. The phosphoinositide 3-kinase pathway. *Science* 296:1655-1657.

108. Standaert, M.L., Bandyopadhyay, G., and Farese, R.V. 1995. Studies with wortmannin suggest a role for phosphatidylinositol 3-kinase in the activation of glycogen synthase and mitogen-activated protein kinase by insulin in rat adipocytes: comparison of insulin and protein kinase C modulators. *Biochem Biophys Res Commun* 209:1082-1088.

109. Haruta, T., Morris, A.J., Rose, D.W., Nelson, J.G., Mueckler, M., and Olefsky, J.M. 1995. Insulin-stimulated GLUT4 translocation is mediated by a divergent intracellular signaling pathway. *J Biol Chem* 270:27991-27994.

110. Cheatham, B., Vlahos, C.J., Cheatham, L., Wang, L., Blenis, J., and Kahn, C.R. 1994. Phosphatidylinositol 3-kinase activation is required for insulin stimulation of pp70 S6 kinase, DNA synthesis, and glucose transporter translocation. *Mol Cell Biol* 14:4902-4911.

111. Kohn, A.D., Summers, S.A., Birnbaum, M.J., and Roth, R.A. 1996. Expression of a constitutively active Akt Ser/Thr kinase in 3T3-L1 adipocytes stimulates glucose uptake and glucose transporter 4 translocation. *J Biol Chem* 271:31372-31378.

112. Calera, M.R., Martinez, C., Liu, H., Jack, A.K., Birnbaum, M.J., and Pilch, P.F. 1998. Insulin increases the association of Akt-2 with Glut4-containing vesicles. *J Biol Chem* 273:7201-7204.

113. Hill, M.M., Clark, S.F., Tucker, D.F., Birnbaum, M.J., James, D.E., and Macaulay, S.L. 1999. A role for protein kinase Bbeta/Akt2 in insulin-stimulated GLUT4 translocation in adipocytes. *Mol Cell Biol* 19:7771-7781.

114. Yoon, J.C., Puigserver, P., Chen, G., Donovan, J., Wu, Z., Rhee, J., Adelmant, G., Stafford, J., Kahn, C.R., Granner, D.K., et al. 2001. Control of hepatic gluconeogenesis through the transcriptional coactivator PGC-1. *Nature* 413:131-138.

115. Whiteman, E.L., Cho, H., and Birnbaum, M.J. 2002. Role of Akt/protein kinase B in metabolism. *Trends Endocrinol Metab* 13:444-451.

116. Cross, D.A., Alessi, D.R., Cohen, P., Andjelkovich, M., and Hemmings, B.A. 1995. Inhibition of glycogen synthase kinase-3 by insulin mediated by protein kinase B. *Nature* 378:785-789.

117. Randle, P.J., Garland, P.B., Hales, C.N., and Newsholme, E.A. 1963. The glucose fatty-acid cycle. Its role in insulin sensitivity and the metabolic disturbances of diabetes mellitus. *Lancet* 1:785-789.

118. Hue, L., and Taegtmeyer, H. 2009. The Randle cycle revisited: a new head for an old hat. *Am J Physiol Endocrinol Metab* 297:E578-591.

119. Garland, P.B., Randle, P.J., and Newsholme, E.A. 1963. Citrate as an Intermediary in the Inhibition of Phosphofructokinase in Rat Heart Muscle by Fatty Acids, Ketone Bodies, Pyruvate, Diabetes, and Starvation. *Nature* 200:169-170.

120. Randle, P.J., Garland, P.B., Hales, C.N., and Newsholme, E.A. 1963. The glucose fatty-acid cycle: Its role in insulin sensitivity and the metabolic disturbances of diabetes mellitus. *Lancet* 7285:785-789.

121. Holness, M.J., and Sugden, M.C. 2003. Regulation of pyruvate dehydrogenase complex activity by reversible phosphorylation. *Biochem Soc Trans* 31:1143-1151.

122. Strumilo, S. 2005. Short-term regulation of the mammalian pyruvate dehydrogenase complex. *Acta Biochim Pol* 52:759-764.

123. Patel, M.S., and Korotchkina, L.G. 2002. Pyruvate dehydrogenase complex as a marker of mitochondrial metabolism. Inhibition by 4-hydroxy-2-nonenal. *Methods Mol Biol* 186:255-263.

124. Bowker-Kinley, M.M., Davis, W.I., Wu, P., Harris, R.A., and Popov, K.M. 1998. Evidence for existence of tissue-specific regulation of the mammalian pyruvate dehydrogenase complex. *Biochem J* 329 (Pt 1):191-196.

125. Yeaman, S.J., Hutcheson, E.T., Roche, T.E., Pettit, F.H., Brown, J.R., Reed, L.J., Watson, D.C., and Dixon, G.H. 1978. Sites of phosphorylation on pyruvate dehydrogenase from bovine kidney and heart. *Biochemistry* 17:2364-2370.

126. Korotchkina, L.G., and Patel, M.S. 1995. Mutagenesis studies of the phosphorylation sites of recombinant human pyruvate dehydrogenase. Site-specific regulation. *J Biol Chem* 270:14297-14304.

127. Korotchkina, L.G., and Patel, M.S. 2001. Site specificity of four pyruvate dehydrogenase kinase isoenzymes toward the three phosphorylation sites of human pyruvate dehydrogenase. *J Biol Chem* 276:37223-37229.

128. Rardin, M.J., Wiley, S.E., Naviaux, R.K., Murphy, A.N., and Dixon, J.E. 2009. Monitoring phosphorylation of the pyruvate dehydrogenase complex. *Anal Biochem* 389:157-164.

129. Bao, H., Kasten, S.A., Yan, X., Hiromasa, Y., and Roche, T.E. 2004. Pyruvate dehydrogenase kinase isoform 2 activity stimulated by speeding up the rate of dissociation of ADP. *Biochemistry* 43:13442-13451.

130. Chen, G., Wang, L., Liu, S., Chuang, C., and Roche, T.E. 1996. Activated function of the pyruvate dehydrogenase phosphatase through Ca2+-facilitated binding to the inner lipoyl domain of the dihydrolipoyl acetyltransferase. *J Biol Chem* 271:28064-28070.

131. Huang, B., Gudi, R., Wu, P., Harris, R.A., Hamilton, J., and Popov, K.M. 1998. Isoenzymes of pyruvate dehydrogenase phosphatase. DNA-derived amino acid sequences, expression, and regulation. *J Biol Chem* 273:17680-17688.

132. McGarry, J.D., Mannaerts, G.P., and Foster, D.W. 1977. A possible role for malonyl-CoA in the regulation of hepatic fatty acid oxidation and ketogenesis. *J Clin Invest* 60:265-270.

133. Abu-Elheiga, L., Matzuk, M.M., Kordari, P., Oh, W., Shaikenov, T., Gu, Z., and Wakil, S.J. 2005. Mutant mice lacking acetyl-CoA carboxylase 1 are embryonically lethal. *Proc Natl Acad Sci U S A* 102:12011-12016.

134. Abu-Elheiga, L., Matzuk, M.M., Abo-Hashema, K.A., and Wakil, S.J. 2001. Continuous fatty acid oxidation and reduced fat storage in mice lacking acetyl-CoA carboxylase 2. *Science* 291:2613-2616.

135. Abu-Elheiga, L., Brinkley, W.R., Zhong, L., Chirala, S.S., Woldegiorgis, G., and Wakil, S.J. 2000. The subcellular localization of acetyl-CoA carboxylase 2. *Proc Natl Acad Sci U S A* 97:1444-1449.

136. Zammit, V.A. 2008. Carnitine palmitoyltransferase 1: central to cell function. *IUBMB Life* 60:347-354.

137. Faye, A., Borthwick, K., Esnous, C., Price, N.T., Gobin, S., Jackson, V.N., Zammit, V.A., Girard, J., and Prip-Buus, C. 2005. Demonstration of N- and C-terminal domain intramolecular interactions in rat liver carnitine palmitoyltransferase 1 that determine its degree of malonyl-CoA sensitivity. *Biochem J* 387:67-76.

138. Petersen, K.F., and Shulman, G.I. 2006. Etiology of insulin resistance. *Am J Med* 119:S10-16.

139. Ferrannini, E. 1998. Insulin resistance versus insulin deficiency in non-insulin-dependent diabetes mellitus: problems and prospects. *Endocr Rev* 19:477-490.

140. Han, P., Zhang, Y.Y., Lu, Y., He, B., Zhang, W., and Xia, F. 2008. Effects of different free fatty acids on insulin resistance in rats. *Hepatobiliary Pancreat Dis Int* 7:91-96.

141. Pan, D.A., Lillioja, S., Kriketos, A.D., Milner, M.R., Baur, L.A., Bogardus, C., Jenkins, A.B., and Storlien, L.H. 1997. Skeletal muscle triglyceride levels are inversely related to insulin action. *Diabetes* 46:983-988.

142. Krssak, M., Falk Petersen, K., Dresner, A., DiPietro, L., Vogel, S.M., Rothman, D.L., Roden, M., and Shulman, G.I. 1999. Intramyocellular lipid concentrations are correlated with insulin sensitivity in humans: a ^{1}H NMR spectroscopy study. *Diabetologia* 42:113-116.

143. Moitra, J., Mason, M.M., Olive, M., Krylov, D., Gavrilova, O., Marcus-Samuels, B., Feigenbaum, L., Lee, E., Aoyama, T., Eckhaus, M., et al. 1998. Life without white fat: a transgenic mouse. *Genes Dev* 12:3168-3181.

144. Kelley, D.E., Mokan, M., Simoneau, J.A., and Mandarino, L.J. 1993. Interaction between glucose and free fatty acid metabolism in human skeletal muscle. *J Clin Invest* 92:91-98.

145. Boden, G., Chen, X., Ruiz, J., White, J.V., and Rossetti, L. 1994. Mechanisms of fatty acid-induced inhibition of glucose uptake. *J Clin Invest* 93:2438-2446.

146. Roden, M., Price, T.B., Perseghin, G., Petersen, K.F., Rothman, D.L., Cline, G.W., and Shulman, G.I. 1996. Mechanism of free fatty acid-induced insulin resistance in humans. *J Clin Invest* 97:2859-2865.

147. Dresner, A., Laurent, D., Marcucci, M., Griffin, M.E., Dufour, S., Cline, G.W., Slezak, L.A., Andersen, D.K., Hundal, R.S., Rothman, D.L., et al. 1999. Effects of free fatty acids on glucose transport and IRS-1-associated phosphatidylinositol 3-kinase activity. *J Clin Invest* 103:253-259.

148. Griffin, M.E., Marcucci, M.J., Cline, G.W., Bell, K., Barucci, N., Lee, D., Goodyear, L.J., Kraegen, E.W., White, M.F., and Shulman, G.I. 1999. Free fatty acid-induced insulin resistance is associated with activation of protein kinase C theta and alterations in the insulin signaling cascade. *Diabetes* 48:1270-1274.

149. Yu, C., Chen, Y., Cline, G.W., Zhang, D., Zong, H., Wang, Y., Bergeron, R., Kim, J.K., Cushman, S.W., Cooney, G.J., et al. 2002. Mechanism by which fatty acids inhibit insulin activation of

insulin receptor substrate-1 (IRS-1)-associated phosphatidylinositol 3-kinase activity in muscle. *J Biol Chem* 277:50230-50236.

150. Samuel, V.T., Liu, Z.X., Qu, X., Elder, B.D., Bilz, S., Befroy, D., Romanelli, A.J., and Shulman, G.I. 2004. Mechanism of hepatic insulin resistance in non-alcoholic fatty liver disease. *J Biol Chem* 279:32345-32353.

151. Choi, C.S., Fillmore, J.J., Kim, J.K., Liu, Z.X., Kim, S., Collier, E.F., Kulkarni, A., Distefano, A., Hwang, Y.J., Kahn, M., et al. 2007. Overexpression of uncoupling protein 3 in skeletal muscle protects against fat-induced insulin resistance. *J Clin Invest* 117:1995-2003.

152. Savage, D.B., Choi, C.S., Samuel, V.T., Liu, Z.X., Zhang, D., Wang, A., Zhang, X.M., Cline, G.W., Yu, X.X., Geisler, J.G., et al. 2006. Reversal of diet-induced hepatic steatosis and hepatic insulin resistance by antisense oligonucleotide inhibitors of acetyl-CoA carboxylases 1 and 2. *J Clin Invest* 116:817-824.

153. Neschen, S., Morino, K., Hammond, L.E., Zhang, D., Liu, Z.X., Romanelli, A.J., Cline, G.W., Pongratz, R.L., Zhang, X.M., Choi, C.S., et al. 2005. Prevention of hepatic steatosis and hepatic insulin resistance in mitochondrial acyl-CoA:glycerol-sn-3-phosphate acyltransferase 1 knockout mice. *Cell Metab* 2:55-65.

154. DeFronzo, R.A., Gunnarsson, R., Bjorkman, O., Olsson, M., and Wahren, J. 1985. Effects of insulin on peripheral and splanchnic glucose metabolism in noninsulin-dependent (type II) diabetes mellitus. *J Clin Invest* 76:149-155.

155. Holness, M.J., Smith, N.D., Bulmer, K., Hopkins, T., Gibbons, G.F., and Sugden, M.C. 2002. Evaluation of the role of peroxisome-proliferator-activated receptor alpha in the regulation of cardiac pyruvate dehydrogenase kinase 4 protein expression in response to starvation, high-fat feeding and hyperthyroidism. *Biochem J* 364:687-694.

156. Zhao, G., Jeoung, N.H., Burgess, S.C., Rosaaen-Stowe, K.A., Inagaki, T., Latif, S., Shelton, J.M., McAnally, J., Bassel-Duby, R., Harris, R.A., et al. 2008. Overexpression of pyruvate dehydrogenase kinase 4 in heart perturbs metabolism and exacerbates calcineurin-induced cardiomyopathy. *Am J Physiol Heart Circ Physiol* 294:H936-943.

157. Hwang, B., Jeoung, N.H., and Harris, R.A. 2009. Pyruvate dehydrogenase kinase isoenzyme 4 (PDHK4) deficiency attenuates the long-term negative effects of a high-saturated fat diet. *Biochem J* 423:243-252.

158. Ferrannini, E. 1988. The theoretical bases of indirect calorimetry: a review. *Metabolism* 37:287-301.

159. Rosdahl, H., Lind, L., Millgard, J., Lithell, H., Ungerstedt, U., and Henriksson, J. 1998. Effect of physiological hyperinsulinemia on blood flow and interstitial glucose concentration in human skeletal muscle and adipose tissue studied by microdialysis. *Diabetes* 47:1296-1301.

160. Frayn, K.N., Humphreys, S.M., and Coppack, S.W. 1995. Fuel selection in white adipose tissue. *Proc Nutr Soc* 54:177-189.

161. Macdonald, I.A. 1999. Arterio-venous differences to study macronutrient metabolism: introduction and overview. *Proc Nutr Soc* 58:871-875.

162. Shulman, G.I., Rossetti, L., Rothman, D.L., Blair, J.B., and Smith, D. 1987. Quantitative analysis of glycogen repletion by nuclear magnetic resonance spectroscopy in the conscious rat. *J Clin Invest* 80:387-393.

163. Shulman, R.G., and Rothman, D.L. 2001. ^{13}C NMR of intermediary metabolism: implications for systemic physiology. *Annu Rev Physiol* 63:15-48.

164. Fitzpatrick, S.M., Hetherington, H.P., Behar, K.L., and Shulman, R.G. 1990. The flux from glucose to glutamate in the rat brain in vivo as determined by ^{1}H-observed, ^{13}C-edited NMR spectroscopy. *J Cereb Blood Flow Metab* 10:170-179.

165. De Graaf, R.A. 2008. In Vivo NMR Spectroscopy: Principles and Techniques Wiley-Interscience. 407.

166. de Graaf, R.A., Mason, G.F., Patel, A.B., Behar, K.L., and Rothman, D.L. 2003. In vivo ^{1}H-[^{13}C]-NMR spectroscopy of cerebral metabolism. *NMR Biomed* 16:339-357.

167. Rossetti, L., Smith, D., Shulman, G.I., Papachristou, D., and DeFronzo, R.A. 1987. Correction of hyperglycemia with phlorizin normalizes tissue sensitivity to insulin in diabetic rats. *J Clin Invest* 79:1510-1515.

168. DeFronzo, R.A., Tobin, J.D., and Andres, R. 1979. Glucose clamp technique: a method for quantifying insulin secretion and resistance. *Am J Physiol* 237:E214-223.

169. de Graaf, R.A., Mason, G.F., Patel, A.B., Behar, K.L., and Rothman, D.L. 2003. In vivo H-1-[C-13]-NMR spectroscopy of cerebral metabolism. *NMR Biomed* 16:339-357.

170. Cline, G.W., and Shulman, G.I. 1995. Mass and positional isotopomer analysis of glucose-metabolism in periportal and pericentral hepatocytes. *J Biol Chem* 270:28062-28067.

171. Sugden, M.C., and Holness, M.J. 1994. Interactive regulation of the pyruvate dehydrogenase complex and the carnitine palmitoyltransferase system. *FASEB J* 8:54-61.

172. Berry, M.N., Phillips, J.W., Henly, D.C., and Clark, D.G. 1993. Effects of fatty acid oxidation on glucose utilization by isolated hepatocytes. *FEBS Lett* 319:26-30.

173. Hue, L., Maisin, L., and Rider, M.H. 1988. Palmitate inhibits liver glycolysis. Involvement of fructose 2,6-bisphosphate in the glucose/fatty acid cycle. *Biochem J* 251:541-545.

174. Chen, X., Iqbal, N., and Boden, G. 1999. The effects of free fatty acids on gluconeogenesis and glycogenolysis in normal subjects. *J Clin Invest* 103:365-372.

175. Gonzalez-Manchon, C., Martin-Requero, A., Ayuso, M.S., and Parrilla, R. 1992. Role of endogenous fatty acids in the control of hepatic gluconeogenesis. *Arch Biochem Biophys* 292:95-101.

176. Kaempfer, S., Blackham, M., Christiansen, M., Wu, K., Cesar, D., Vary, T., and Hellerstein, M.K. 1991. Fraction of hepatic cytosolic acetyl-CoA derived from glucose in vivo: relation to PDH phosphorylation state. *Am J Physiol* 260:E865-875.

177. Moir, A.M., and Zammit, V.A. 1993. Rapid switch of hepatic fatty acid metabolism from oxidation to esterification during diurnal feeding of meal-fed rats correlates with changes in the properties of acetyl-CoA carboxylase, but not of carnitine palmitoyltransferase I. *Biochem J* 291 (Pt 1):241-246.

178. Holness, M.J., and Sugden, M.C. 1990. Pyruvate dehydrogenase activities and rates of lipogenesis during the fed-to-starved transition in liver and brown adipose tissue of the rat. *Biochem J* 268:77-81.

179. Gastaldelli, A., Toschi, E., Pettiti, M., Frascerra, S., Quinones-Galvan, A., Sironi, A.M., Natali, A., and Ferrannini, E. 2001. Effect of physiological hyperinsulinemia on gluconeogenesis in nondiabetic subjects and in type 2 diabetic patients. *Diabetes* 50:1807-1812.

180. Adkins, A., Basu, R., Persson, M., Dicke, B., Shah, P., Vella, A., Schwenk, W.F., and Rizza, R. 2003. Higher insulin concentrations are required to suppress gluconeogenesis than glycogenolysis in nondiabetic humans. *Diabetes* 52:2213-2220.

181. Kim, J.K., Fillmore, J.J., Chen, Y., Yu, C., Moore, I.K., Pypaert, M., Lutz, E.P., Kako, Y., Velez-Carrasco, W., Goldberg, I.J., et al. 2001. Tissue-specific overexpression of lipoprotein lipase causes tissue-specific insulin resistance. *Proc Natl Acad Sci U S A* 98:7522-7527.

182. Moore, M.C., Cherrington, A.D., Cline, G., Pagliassotti, M.J., Jones, E.M., Neal, D.W., Badet, C., and Shulman, G.I. 1991. Sources of carbon for hepatic glycogen synthesis in the conscious dog. *J Clin Invest* 88:578-587.

183. Boyd, M.E., Albright, E.B., Foster, D.W., and McGarry, J.D. 1981. In vitro reversal of the fasting state of liver metabolism in the rat. Reevaluation of the roles of insulin and glucose. *J Clin Invest* 68:142-152.

184. Magnusson, I., Rothman, D.L., Katz, L.D., Shulman, R.G., and Shulman, G.I. 1992. Increased rate of gluconeogenesis in type II diabetes mellitus. A ^{13}C nuclear magnetic resonance study. *J Clin Invest* 90:1323-1327.

185. Sugden, M.C., Orfali, K.A., and Holness, M.J. 1995. The pyruvate dehydrogenase complex: nutrient control and the pathogenesis of insulin resistance. *J Nutr* 125:1746S-1752S.

186. Wu, P., Blair, P.V., Sato, J., Jaskiewicz, J., Popov, K.M., and Harris, R.A. 2000. Starvation increases the amount of pyruvate dehydrogenase kinase in several mammalian tissues. *Arch Biochem Biophys* 381:1-7.

187. Harris, R.A., Huang, B., and Wu, P. 2001. Control of pyruvate dehydrogenase kinase gene expression. *Adv Enzyme Regul* 41:269-288.

188. Holness, M.J., Bulmer, K., Smith, N.D., and Sugden, M.C. 2003. Investigation of potential mechanisms regulating protein expression of hepatic pyruvate dehydrogenase kinase isoforms 2 and 4 by fatty acids and thyroid hormone. *Biochem J* 369:687-695.

189. Connaughton, S., Chowdhury, F., Attia, R.R., Song, S., Zhang, Y., Elam, M.B., Cook, G.A., and Park, E.A. 2009. Regulation of pyruvate dehydrogenase kinase isoform 4 (PDK4) gene expression by glucocorticoids and insulin. *Mol Cell Endocrinol*.

190. Kwon, H.S., and Harris, R.A. 2004. Mechanisms responsible for regulation of pyruvate dehydrogenase kinase 4 gene expression. *Adv Enzyme Regul* 44:109-121.

191. Turvey, E.A., Heigenhauser, G.J., Parolin, M., and Peters, S.J. 2005. Elevated n-3 fatty acids in a high-fat diet attenuate the increase in PDH kinase activity but not PDH activity in human skeletal muscle. *J Appl Physiol* 98:350-355.

192. Svedberg, J., Stromblad, G., Wirth, A., Smith, U., and Bjorntorp, P. 1991. Fatty acids in the portal vein of the rat regulate hepatic insulin clearance. *J Clin Invest* 88:2054-2058.

193. Roden, M., Stingl, H., Chandramouli, V., Schumann, W.C., Hofer, A., Landau, B.R., Nowotny, P., Waldhausl, W., and Shulman, G.I. 2000. Effects of free fatty acid elevation on postabsorptive endogenous glucose production and gluconeogenesis in humans. *Diabetes* 49:701-707.

194. Boden, G., Chen, X., Capulong, E., and Mozzoli, M. 2001. Effects of free fatty acids on gluconeogenesis and autoregulation of glucose production in type 2 diabetes. *Diabetes* 50:810-816.

195. Petersen, K.F., Cline, G.W., Gerard, D.P., Magnusson, I., Rothman, D.L., and Shulman, G.I. 2001. Contribution of net hepatic glycogen synthesis to disposal of an oral glucose load in humans. *Metabolism* 50:598-601.

196. Holness, M.J., and Sugden, M.C. 1989. Pyruvate dehydrogenase activities during the fed-to-starved transition and on re-feeding after acute or prolonged starvation. *Biochem J* 258:529-533.

197. Abel, E.D. 2004. Glucose transport in the heart. *Front Biosci* 9:201-215.

198. Liu, B., Clanachan, A.S., Schulz, R., and Lopaschuk, G.D. 1996. Cardiac efficiency is improved after ischemia by altering both the source and fate of protons. *Circ Res* 79:940-948.

199. Korvald, C., Elvenes, O.P., and Myrmel, T. 2000. Myocardial substrate metabolism influences left ventricular energetics in vivo. *Am J Physiol Heart Circ Physiol* 278:H1345-1351.

200. Gollnick, P.D. 1977. Free fatty acid turnover and the availability of substrates as a limiting factor in prolonged exercise. *Ann N Y Acad Sci* 301:64-71.

201. Himwich, H.E., and Rose, M.I. 1927. The respiratory quotient of exercising muscle. *Am J Physiol* 81:485-486.

202. Taegtmeyer, H. 1994. Energy metabolism of the heart: from basic concepts to clinical applications. *Curr Probl Cardiol* 19:59-113.

203. Taegtmeyer, H. 2002. Switching metabolic genes to build a better heart. *Circulation* 106:2043-2045.

204. Girard, J., Ferre, P., Pegorier, J.P., and Duee, P.H. 1992. Adaptations of glucose and fatty acid metabolism during perinatal period and suckling-weaning transition. *Physiol Rev* 72:507-562.

205. Itoi, T., and Lopaschuk, G.D. 1993. The contribution of glycolysis, glucose oxidation, lactate oxidation, and fatty acid oxidation to ATP production in isolated biventricular working hearts from 2-week-old rabbits. *Pediatr Res* 34:735-741.

206. Jeffrey, F.M., Diczku, V., Sherry, A.D., and Malloy, C.R. 1995. Substrate selection in the isolated working rat heart: effects of reperfusion, afterload, and concentration. *Basic Res Cardiol* 90:388-396.

207. Gertz, E.W., Wisneski, J.A., Stanley, W.C., and Neese, R.A. 1988. Myocardial substrate utilization during exercise in humans. Dual carbon-labeled carbohydrate isotope experiments. *J Clin Invest* 82:2017-2025.

208. Wisneski, J.A., Stanley, W.C., Neese, R.A., and Gertz, E.W. 1990. Effects of acute hyperglycemia on myocardial glycolytic activity in humans. *J Clin Invest* 85:1648-1656.

209. Augustus, A.S., Kako, Y., Yagyu, H., and Goldberg, I.J. 2003. Routes of FA delivery to cardiac muscle: modulation of lipoprotein lipolysis alters uptake of TG-derived FA. *Am J Physiol Endocrinol Metab* 284:E331-339.

210. Moller, D.E. 2001. New drug targets for type 2 diabetes and the metabolic syndrome. *Nature* 414:821-827.

211. Gilde, A.J., and Van Bilsen, M. 2003. Peroxisome proliferator-activated receptors (PPARS): regulators of gene expression in heart and skeletal muscle. *Acta Physiol Scand* 178:425-434.

212. Depre, C., Rider, M.H., and Hue, L. 1998. Mechanisms of control of heart glycolysis. *Eur J Biochem* 258:277-290.

213. Belke, D.D., Larsen, T.S., Gibbs, E.M., and Severson, D.L. 2001. Glucose metabolism in perfused mouse hearts overexpressing human GLUT-4 glucose transporter. *Am J Physiol Endocrinol Metab* 280:E420-427.

214. Lopaschuk, G.D. 2002. Metabolic abnormalities in the diabetic heart. *Heart Fail Rev* 7:149-159.

215. Luiken, J.J., Arumugam, Y., Dyck, D.J., Bell, R.C., Pelsers, M.M., Turcotte, L.P., Tandon, N.N., Glatz, J.F., and Bonen, A. 2001. Increased rates of fatty acid uptake and plasmalemmal fatty acid transporters in obese Zucker rats. *J Biol Chem* 276:40567-40573.

216. Carley, A.N., Atkinson, L.L., Bonen, A., Harper, M.E., Kunnathu, S., Lopaschuk, G.D., and Severson, D.L. 2007. Mechanisms responsible for enhanced fatty acid utilization by perfused hearts from type 2 diabetic db/db mice. *Arch Physiol Biochem* 113:65-75.

217. Bonen, A., Parolin, M.L., Steinberg, G.R., Calles-Escandon, J., Tandon, N.N., Glatz, J.F., Luiken, J.J., Heigenhauser, G.J., and Dyck, D.J. 2004. Triacylglycerol accumulation in human obesity and type 2 diabetes is associated with increased rates of skeletal muscle fatty acid transport and increased sarcolemmal FAT/CD36. *FASEB J* 18:1144-1146.

218. Zurlo, F., Lillioja, S., Esposito-Del Puente, A., Nyomba, B.L., Raz, I., Saad, M.F., Swinburn, B.A., Knowler, W.C., Bogardus, C., and Ravussin, E. 1990. Low ratio of fat to carbohydrate oxidation as predictor of weight gain: study of 24-h RQ. *Am J Physiol* 259:E650-657.

219. Pehleman, T.L., Peters, S.J., Heigenhauser, G.J., and Spriet, L.L. 2005. Enzymatic regulation of glucose disposal in human skeletal muscle after a high-fat, low-carbohydrate diet. *J Appl Physiol* 98:100-107.

220. Finck, B.N., Lehman, J.J., Leone, T.C., Welch, M.J., Bennett, M.J., Kovacs, A., Han, X., Gross, R.W., Kozak, R., Lopaschuk, G.D., et al. 2002. The cardiac phenotype induced by PPARalpha overexpression mimics that caused by diabetes mellitus. *J Clin Invest* 109:121-130.

221. Finck, B.N., Bernal-Mizrachi, C., Han, D.H., Coleman, T., Sambandam, N., LaRiviere, L.L., Holloszy, J.O., Semenkovich, C.F., and Kelly, D.P. 2005. A potential link between muscle peroxisome proliferator- activated receptor-alpha signaling and obesity-related diabetes. *Cell Metab* 1:133-144.

222. Majer, M., Popov, K.M., Harris, R.A., Bogardus, C., and Prochazka, M. 1998. Insulin downregulates pyruvate dehydrogenase kinase (PDK) mRNA: potential mechanism contributing to increased lipid oxidation in insulin-resistant subjects. *Mol Genet Metab* 65:181-186.

223. Mandarino, L.J., Printz, R.L., Cusi, K.A., Kinchington, P., O'Doherty, R.M., Osawa, H., Sewell, C., Consoli, A., Granner, D.K., and DeFronzo, R.A. 1995. Regulation of hexokinase II and glycogen synthase mRNA, protein, and activity in human muscle. *Am J Physiol* 269:E701-708.

224. Buck, M.J., Squire, T.L., and Andrews, M.T. 2002. Coordinate expression of the PDK4 gene: a means of regulating fuel selection in a hibernating mammal. *Physiol Genomics* 8:5-13.

225. Goodwin, G.W., Taylor, C.S., and Taegtmeyer, H. 1998. Regulation of energy metabolism of the heart during acute increase in heart work. *J Biol Chem* 273:29530-29539.

226. Sidhu, S., Gangasani, A., Korotchkina, L.G., Suzuki, G., Fallavollita, J.A., Canty, J.M., Jr., and Patel, M.S. 2008. Tissue-specific pyruvate dehydrogenase complex deficiency causes cardiac hypertrophy and sudden death of weaned male mice. *Am J Physiol Heart Circ Physiol* 295:H946-H952.

227. Jenkins, A.B., Storlien, L.H., Chisholm, D.J., and Kraegen, E.W. 1988. Effects of nonesterified fatty acid availability on tissue-specific glucose utilization in rats in vivo. *J Clin Invest* 82:293-299.

228. Kim, J.K., Wi, J.K., and Youn, J.H. 1996. Plasma free fatty acids decrease insulin-stimulated skeletal muscle glucose uptake by suppressing glycolysis in conscious rats. *Diabetes* 45:446-453.

229. Nolte, L.A., Galuska, D., Martin, I.K., Zierath, J.R., and Wallberg-Henriksson, H. 1994. Elevated free fatty acid levels inhibit glucose phosphorylation in slow-twitch rat skeletal muscle. *Acta Physiol Scand* 151:51-59.

230. Goodman, M.N., Berger, M., and Ruderman, N.B. 1974. Glucose metabolism in rat skeletal muscle at rest. Effect of starvation, diabetes, ketone bodies and free fatty acids. *Diabetes* 23:881-888.

231. Berger, M., Hagg, S.A., Goodman, M.N., and Ruderman, N.B. 1976. Glucose metabolism in perfused skeletal muscle. Effects of starvation, diabetes, fatty acids, acetoacetate, insulin and exercise on glucose uptake and disposition. *Biochem J* 158:191-202.

232. Walker, M., Fulcher, G.R., Sum, C.F., Orskov, H., and Alberti, K.G. 1991. Effect of glycemia and nonesterified fatty acids on forearm glucose uptake in normal humans. *Am J Physiol* 261:E304-311.

233. Yki-Jarvinen, H., Puhakainen, I., and Koivisto, V.A. 1991. Effect of free fatty acids on glucose uptake and nonoxidative glycolysis across human forearm tissues in the basal state and during insulin stimulation. *J Clin Endocrinol Metab* 72:1268-1277.

234. Wolfe, B.M., Klein, S., Peters, E.J., Schmidt, B.F., and Wolfe, R.R. 1988. Effect of elevated free fatty acids on glucose oxidation in normal humans. *Metabolism* 37:323-329.

235. Boden, G., Jadali, F., White, J., Liang, Y., Mozzoli, M., Chen, X., Coleman, E., and Smith, C. 1991. Effects of fat on insulin-stimulated carbohydrate metabolism in normal men. *J Clin Invest* 88:960-966.

236. Saloranta, C., Koivisto, V., Widen, E., Falholt, K., DeFronzo, R.A., Harkonen, M., and Groop, L. 1993. Contribution of muscle and liver to glucose-fatty acid cycle in humans. *Am J Physiol* 264:E599-605.

237. Jucker, B.M., Rennings, A.J., Cline, G.W., and Shulman, G.I. 1997. ^{13}C and ^{31}P NMR studies on the effects of increased plasma free fatty acids on intramuscular glucose metabolism in the awake rat. *J Biol Chem* 272:10464-10473.

238. Bouzakri, K., Austin, R., Rune, A., Lassman, M.E., Garcia-Roves, P.M., Berger, J.P., Krook, A., Chibalin, A.V., Zhang, B.B., and Zierath, J.R. 2008. Malonyl CoenzymeA decarboxylase regulates lipid and glucose metabolism in human skeletal muscle. *Diabetes* 57:1508-1516.

239. Ussher, J.R., Koves, T.R., Jaswal, J.S., Zhang, L., Ilkayeva, O., Dyck, J.R., Muoio, D.M., and Lopaschuk, G.D. 2009. Insulin-stimulated cardiac glucose oxidation is increased in high-fat diet-induced obese mice lacking malonyl CoA decarboxylase. *Diabetes* 58:1766-1775.